HEAT TRANSFER AND AIR FLOW IN BUILDINGS.

by

Jeremy Paul Cockroft, B.Sc.

Ph.D. Thesis

UNIVERSITY OF GLASGOW

BUILDING SERVICES RESEARCH UNIT

MARCH 1979

CONTENTS

CONTENTS (Cont'd)

CONTENTS (Cont'd)

CONTENTS (Cont'd)

LIST OF TABLES

LIST OF FIGURES

LIST OF FIGURES (Cont'd)

ACKNOWLEDGEMENTS

The following individuals and organisations were instrumental to the successful completion of the work described in this thesis and their co-operation and assistance is gratefully acknowledged by the author.

Professor R.S. Silver - James Watt Professor of Mechanical Engineering, University of Glasgow.

Mr. W. Carson - Leader of the Building Services Research Unit.

Mr. P. Robertson - Mechanical Engineer - Building Services Research Unit.

Mr. J. Siviour - Electricity Council Research Centre

Mrs. A. Calderwood - Building Research Establishment, Scottish Laboratory.

Dr. C. Dodds - Department of Mechanical Engineering, University of Glasgow.

Dr. M. Titterington - Department of Statistics, University of Glasgow.

East Kilbride Development Corporation.

DECLARATION

The material presented in Section 3 of Chapter 6 describes work that was part of a study carried out jointly with P. Robertson of the Building Services Research Unit, University of Glasgow. The results of the Study were published in Building and Environment, 11, pp. 29-35. The sections of that study reported in this thesis represent the Author's contribution to that study. Mr. Robertson's agreement to the inclusion of this material in this thesis is gratefully acknowledged.

The remainder of the thesis is entirely the author's own, unaided work, and has not been previously published elsewhere.

SUMMARY

The development of design techniques for calculating heat transfer and air flows in buildings indicates the advantage of more realistic assessments of the behaviour of real buildings by modelling more parameters in greater detail. Considerable problems remain to be solved, particularly in calculating ventilation and infiltration. A balanced approach is required which will retain the essential advantages of computerised techniques without adopting excessively complex calculation procedures. A program which adopts such an approach is described in detail.

In order to validate the computer predictions a series of measurements in an unoccupied test house is described. These are compared with predictions, and discrepancies between the two sets of data are discussed. Further comparisons with manual calculations demonstrate the value of the detailed simulation approach whilst indicating scope for simplification in some of the calculation procedures.

To provide additional illustration of the value of computerised methods, test house model results are described in which the single glazed windows are compared with double glazed windows. The simulations are extended to include summer and winter periods, and the results show the relative contributions of solar gains and ventilation for the two glazing types.

The difficulties of estimating ventilation are further discussed and the effects of occupancy and turbulent wind are described in detail.

It is concluded that further work on several aspects of heat transfer and air flows in buildings is required, but that the approach described in the thesis represents a considerable advance on previously available techniques, particularly in relation to the integration of air flow calculations with heat transfer calculations. Applications for the developed model are described which extend beyond the replacement of current building and services design methods.

NOMENCLATURE

Symbols used on an *ad hoc* basis as local constants or coefficients are not included in this list.

a	absorption coefficient
A	area
C	cloud cover, thermal conductance, specific heat, concentration
d	wind direction
D	diffuse solar radiation intensity
f	function, ratio
F	angle factor
g	gravitational acceleration
G	global solar radiation intensity
h	height, heat quantity, convection coefficient
H	height, radiation exchange, heat flow rate
i	angle of incidence
I	direct solar radiation intensity
k	absorbtion coefficient, thermal conductivity, wavenumber
l	length
L	length
m	relative air mass, mixing ratio, mass
n	exponent, number of hours sunshine
N	number of hours
p	thermal diffusivity, pressure
P	pressure, perimeter
q	heat quantity, air flow rate
Q	heat flow rate
r	dimension, ratio
R	radius, gas constant, reflected solar radiation intensity, dimension, resistance
s	specific heat
t	temperature, time
T	temperature, time constant

NOMENCLATURE (Cont'd)

u	velocity
v	atmospheric vapour pressure
V	wind speed
w	water content, dimension
x	dimension
z	solar zenith angle
α	absorption coefficient
γ	solar altitude
Δ	difference
ϵ	angle of inclination, emissivity
ρ	density
σ	Stefan-Boltzmann constant
τ	transmission coefficient
ω	radian frequency
λ	wavelength

CHAPTER 1

AN APPROACH TO THE ESTIMATION OF BUILDING THERMAL PERFORMANCE

1.1 INTRODUCTION

In the past, design of environmental systems for buildings was largely a matter of experience. Those arrangements found to have worked in one building would be installed, with minor modifications, in another, and gradually become established as standard solutions for practical design. These systems were considered adequate in the buildings for which they were designed - thermally massive with small openable windows. For example, on a domestic scale, open grate fires would induce sufficient ventilation to overcome condensation problems and, to a large extent, low temperatures in hallways and bedrooms would be tolerated. There was little incentive to increase the efficiency of the heating device when fossil fuel was cheap and plentiful. Gradually we have moved towards light-weight construction, larger windows, and an increasing demand for improved environmental conditions. We have also created more demanding loads for systems to cope with. Hospitals, computer rooms, industrial clean areas, all require more complex and responsive systems to meet their needs.

As larger and larger systems are developed the need for more rigorous design calculations has been met by the introduction of more complex manual heat transfer calculations, with due allowance being made for solar radiation and thermal storage effects.

With rapidly increasing energy costs, and buildings consuming between 40% and 50% (1) of the nation's primary energy supply there is an overwhelming need for new and

reliable ways of assessing the energy demands of buildings. Only then can one confidently justify the high capital costs of improved insulation standards and the installation of expensive energy recovery systems to reclaim waste heat from building heating and cooling systems. Even on a domestic scale, the consequences of gross oversizing of heating systems are less likely to be tolerated in future.

1.2 EXISTING DESIGN METHODS

The current established methods for building energy systems design in the U.K. are those recommended by the Institution of Heating and Ventilating Engineers (now the Chartered Institution of Building Services) in the 1970 and later editions of their guide (2). These are based on the concept of "environmental" temperature or "index" temperature developed by Danter (3), being that room temperature at which both radiant and convective heat exchanges may be considered to take place at room surfaces. A series of approximating assumptions leads to a definition of this temperature as being the weighted average of air and room surface temperatures, appropriate weights being one-third and two-thirds respectively. This corresponds in some way to a comfort index, hence the label "environmental" temperature.

A development of earlier work by Danter, (4) the "admittance" procedure builds on the environmental temperature concept and enables the effects of heat storage in

building materials to be assessed. Milbank et al (5) consider simple sinusoidal temperature and energy variations, which are assumed to complete one cycle every 24 hours over a number of days. Various gross properties - admittance, decrement factor and surface factor - can be assigned to a section of building fabric, and enable its thermal response to be predicted.

Design in accordance with these principles is still basically a manual process. The main achievement of the I.H.V.E. in establishing this procedure is to have improved on the approximating assumptions inherent in any manual design process which can only consider a few of the variables affecting the behaviour of real buildings.

When the assessment of the thermal performance of a building, in terms of energy loads and consumptions, is required, this type of design procedure is of limited value. The basic concepts assume simple variations in internal and external conditions which are rarely encountered in practice. Although one may further extend the simplification process and assume that the various surface factors can be applied in more complex situations, the validity of such an approach must be in considerable doubt. A more complex synthesis of building components and external conditions is required and it is at this point that we seek recourse to computer models.

1.3 COMPUTER MODELLING

1.3.1 Response Factor Method

Realising the need to account for the real variations of weather conditions with time, Stephenson and Mitalas (6) utilised a basic dynamic characteristic of constant parameter linear systems. In this context, a building consists of several such systems. For example, an external wall is a system with external solar heat gain as a time dependent input, x(t), and the resultant room heat gain as the output y(t). A weighting function for such a system $h(\tau)$ can be defined as the output of the system at any time to a unit impulse applied a time τ before. For any arbitrary input x(t) the system output y(t) is given by the convolution integral

$$y(t) = \int_0^\infty h(\tau)\, x(t-\tau)\, d\tau \qquad 1.1$$

thus, the value of the output y(t) is given as a weighted sum over the entire history of the input x(t). In practice only a limited history of x(t) is required, since

$$h(\tau) \rightarrow 0 \quad as \quad \tau \rightarrow \infty \qquad 1.2$$

By taking discrete values of τ (e.g. at hourly intervals) a finite set of weighting factors can be defined for each system, e.g. room surface heat transfer, or heat gain/cooling load. It is these weighting factors that are referred to as response factors in the various computerised heating/cooling load calculation routines that utilise this technique. The American Society of Heating Refrigeration and Air-Conditioning Engineers (ASHRAE) has developed a set of

subroutines (7) which use the response factor technique and several programs have been produced based on the use of these subroutines, e.g. NBSLD (8).

1.3.2 Finite Difference Techniques

A more fundamental approach to building thermal behaviour can be obtained by modelling the heat transfer within and through building elements directly. These techniques generally subdivide sections of building fabric, e.g. a roof, into finite parallel layers within a slab. By calculating heat flows and temperature changes in each layer at successive time steps, the thermal performance can be simulated in great detail, though at the expense of computer processing time. The behaviour of air cavities can be included with greater precision than with the response factor method, and non-linear relationships can be easily incorporated, whereas the validity of the response factor technique is challenged when non-linear processes have to be approximated. Brown (9) was one of the first to seriously apply finite difference calculations to buildings, and he also included angle factor calculations to model internal radiation, and non-linear surface convection coefficients. Other finite difference programs have been developed e.g. by Basnett (10) but none has been applied commercially to the same extent as those based on the ASHRAE subroutines.

1.3.3 Characteristics of Computerised Techniques

The capability which computer programs have to model more closely the actual heat transfers as they occur in buildings is obvious. The real advantages of modern computers, however,lie to a large extent in their ability to process much larger amounts of data, and to draw on more extensive secondary input than is possible using manual methods.

For example, climatological data is readily available on magnetic tape for many stations throughout the world, often in the form of hourly data. This can be accessed directly and many programs make use of this type of input.

Danger lies in developing excessively sophisticated programs which are difficult to validate, require huge amounts of input data, and are more complex than is required in any practical situation. Yet the degree of sophistication required has largely to be determined by comparative tests which eliminate unnecessary calculation sequences but retain those which can be shown to improve the quality of assessments resulting from the program.

1.4 VENTILATION

1.4.1 Analytical Problems

In spite of the increasing complexity and detail of modelling of the thermal interactions in buildings, no program has been able to treat ventilation in the same depth. There are a number of reasons for this. Firstly, the building surface pressures require to be known. This in turn

requires both a knowledge of wind conditions at a building site, and the pressures developed at different points on each building surface for every wind direction. Secondly, the actual magnitudes of the flows through gaps in the building fabric depend on the sizes of these gaps, and these sizes are subject to large variations and uncertainties, and are difficult to measure. In a naturally ventilated building, the gaps include openings whose magnitudes are controlled by the occupants. Thirdly, the equations which relate air flow to the pressure difference across a given opening are non-linear and many such equations exist for all the gaps and openings in the external fabric and between internal spaces within a building. Temperature variations further complicate the system, causing density variations and convective or "stack" effects within a building. The complete system of equations must be solved for each set of external pressures. These three problems will now be dealt with in reverse order.

1.4.2 Airflow Calculations

Early attempts by Dick (11) to quantify ventilation rates in terms of the various causative factors for simple cases were succeeded by more complex network analyses, each with a different approach or application in mind. Tamura and Wilson (12), Barrett and Locklin (13) and Jackman (14) developed digital computer programs to deal with multi-storey offices. Den Ouden (15) used an analogue computer for his analysis. Bilsborrow (16) was particularly concerned with natural ventilation problems.

Tamura (17) and Wakamatsu (18) developed programs for computing the movement of smoke through tall buildings in the event of fire, and stack effect calculations are of major importance here.

The few comparisons with full scale measurements, e.g. Bilsborrow (19) tend to show that measured ventilation rates turn out to be higher than computed ventilation rates. The reasons for this will be discussed in more detail in Chapter 6. The development of a suitable algorithm for computing network airflows which does not require excessive computer processing time, but which will converge on solutions for a wide variety of problems, presents major difficulties.

1.4.3 Leakage Areas in Buildings

Several attempts have been made to measure the gaps, cracks and various openings in the building fabric through which air may flow.

Dick (11) computed equivalent areas for various building components such as window cracks, air bricks, timber floors, etc. These areas represent the areas of square-edged circular orifices that would pass the same quantity of air when subjected to the same pressure differences assuming a square law relationship. Several other workers, e.g. Shaw et al (20) and Tamura (21), have since produced data on the gross leakage characteristics of buildings whilst others, e.g. Sasaki and Wilson (22) have concentrated on individual components such as windows, often

with a view to specifying standards of weather tightness, rather than prediction of ventilation rates.

Advancing beyond the assumption of a square law relationship between flow and pressure difference, studies have been carried out to determine the actual behaviour of idealised cracks. The resultant relationships turn out to be complex. Hopkins and Hansford (23) for example, developed a variable coefficient of discharge, whereas Honma (24) developed an empirical relationship which included the effects of the transition between laminar and turbulent flow at low pressure differences across cracks.

One common factor revealed by these studies is the huge variation that exists between different samples of components.

1.4.4 Building Surface Pressures

Although several attempts at full scale measurements of wind pressure on buildings have been made, the potential value of wind tunnel studies has long been realised. In 1895 Irminger (25) studied wind pressures on elementary building forms, using a gasworks chimney as a source of suction to draw air through a small rectangular wind tunnel. Later studies such as that of Dryden and Hill who compared model and full scale measurements on the Empire State Building (26), demonstrated the difficulties of carrying out full-scale measurements, and the importance of correctly modelling the vertical wind velocity profile. Jensen (27) was one of the first to study this in detail and

he proposed logorithmic profiles based on surface roughness parameters, supported by comparison between full-scale and model tests on houses, e.g.

$$\frac{V(Z)}{V^*} = \frac{1}{x} \log_e \frac{Z - Z_o}{Z_o} \qquad 1.3$$

where V(Z) is the velocity at height Z

V* is the friction velocity

X = 0.4, Karman's constant

Z_o= roughness parameter.

This work is more fully reported by Jensen and Franck (28). Baines (29) and Ning et al (30) also noted the differences in pressure distributions that are obtained in a boundary layer flow, as opposed to flow with a uniform velocity distribution. Although Jensen proposed a logarithmic velocity profile, later workers (31) have preferred a power law,

$$\frac{V(Z)}{V^*} = \left(\frac{Z}{Z^*}\right)^k \qquad 1.4$$

where k is constant varying between 0.16 for open terrain, and 0.4 for city centres.

Jensen and Franck preferred to generate their velocity profile naturally by providing a long "fetch" of roughness elements in their wind tunnel. There have been many attempts, e.g. Armitt and Counihan (32) and Lloyd (33), to generate the required profile and turbulent characteristics within a shorter length of tunnel by installing grids, prisms, bars or other obstructions upstream of the working section.

1.4.5 Requirements for Ventilation Design

From the foregoing it would appear that there is sufficient data available to enable reasonable estimation of building surface pressures for the calculation of ventilating airflows for simple building shapes in exposed conditions. In more complex situations wind tunnel modelling may be desirable, depending on the relative magnitude of ventilation heat loss in relation to other losses or gains. This has been done in specific instances on large projects, such as hospitals, for example, by Jackman and Potter (34), but there remain specific modelling problems which will be discussed in Chapter 6.

1.5 AN INTEGRATED APPROACH

A comprehensive model of a building, the air contained within it, the services installed, and the external climate could, in theory be simulated very closely, using very much more sophisticated techniques than have been suggested here. However, although the computing power required for such an exercise is possibly available, for practical purposes we must select those physical processes that are most relevant, and model these to a degree of exactness commensurate with our expected final predictions. These will always be influenced to a greater or lesser extent by human activity which no computer can, or probably ever will be able to model with much precision. The

construction and integration of algorithms to describe these various processes to produce a balanced thermal performance assessment computer program has been a major aim of the present work.

A description of this program follows in Chapter 2. An essential prerequisite to the evaluation of such a model is a comparison with full-scale measurements in a real building. This is reported in Chapters 3 and 4.

Some of the more important aspects of a model simulation approach are demonstrated in Chapter 5, by extending the comparisons to consider double glazing installed in the test house, and to examine seasonal variations in energy consumption with and without the double glazing.

Chapter 6 expands some of the problems of predicting ventilation in buildings. Since building occupancy has its least predictable effects in naturally-ventilated buildings, further discussion of this topic is included in Chapter 6.

Chapter 7 summarises all the major findings and presents overall conclusions to the work described in this thesis.

Summary of Chapter 1

The historical development of computerised calculations of heat transfer and airflows in buildings is outlined. The clear advantage of being able to simulate more realistically the behaviour of a real building due to the ability to model more parameters in greater detail is explained. Considerable problems remain to be solved, particularly in calculating ventilation and infiltration. A balanced approach is required which will retain the essential advantages of computerised techniques without adopting excessively complex calculation procedures.

CHAPTER 2

A DESCRIPTION OF THE COMPUTER MODEL

2.1 INTRODUCTION

This chapter describes the digital computer program AIRNET which was used to carry out the simulations described in Chapters 4 and 5.

The program was to be developed initially with airflow calculations as a priority, and heat transfer calculations were therefore incorporated within the network concept adopted for the airflow calculations. This means that there is only one possible representation for any building component, either as a node or as a branch within a network. It will be seen that this convention is very convenient, as it simplifies the structure of what would otherwise become a very complicated system of routines and data files.

After describing the overall framework of the program AIRNET, the methods used to carry out the physical calculations embodied in the program will be described in detail. The extent of input data required, the geometrical limitations imposed on the input by the program, and the method of operation are described in Appendix I.

2.2 OVERALL FRAMEWORK OF COMPUTER PROGRAM

A five minute time step is employed in a series of finite difference calculations of air flows, heat flows and temperature within and through each part of a building's fabric. The computer model can be perceived as a network of branches communicating between various nodes. (Figure 2.1). Each node represents a building space, such as a room,

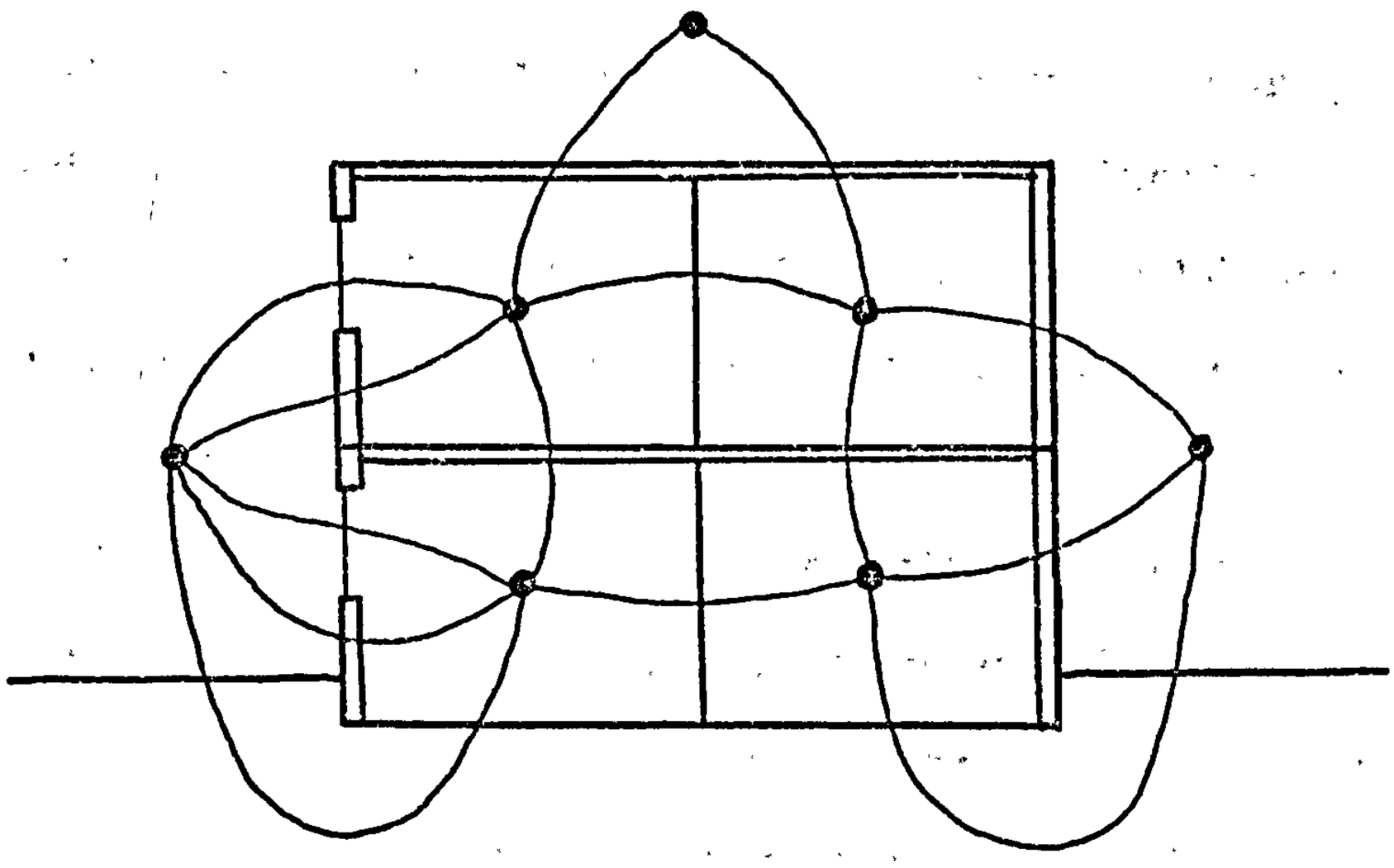

FIGURE 2.1

Node/Branch Network Representation of a Building

corridor, or stairwell. The branches represent the interconnecting partitions between spaces; for example, walls, floors, ceiling, windows and doors. Branches to the outside air connect an internal space to an external surface. This representation of the external environment conveniently enables different conditions at different outside surfaces to be accommodated.

Each interconnection can be assigned a number of physical properties. In particular, they are normally subdivided into several parallel layers, for finite difference heat conduction calculations. They may also be permeable to air flow, and possess individual surface heat transfer characteristics.

Spaces, represented by the network nodes, are considered to be cuboid shaped. More complex shapes may either be approximated by a cuboid, or represented by two or more adjacent cuboids. Each cuboid shaped space is bounded by six main surfaces. These main surfaces bound interconnections which may have co-planar partitions contained within them, e.g. windows and doors. These are separately defined interconnections and require the same structural description as other interconnections. The surface of such a co-planar partition is referred to as a sub-surface.

An interconnection may be bounded by a main surface on one side and a sub-surface on the other. This enables a fairly complex juxtaposition of cuboid spaces to be assembled to form the computer model.

Initially the temperature in each space and within each layer of each partition is set to a starting value. The basic input data which supplies the simulation model with external conditions is contained in the climatological data file. This file includes hourly values of dry bulb temperatures, vapour pressure, sea level atmospheric pressure, total cloud amount, duration of bright sunshine, wind speed and wind direction. These values are interpolated when necessary to obtain data relating to the five-minute time-steps of the program.

The calculation sequence proceeds by first determining all the internal and external heat fluxes due to air and fabric temperatures, air flows, and climatological data. These are then used to estimate new temperatures at the end of one time-step.

Solar radiation falling on each external surface is computed at the start of the first time-step, and the same values are reused for the following five time-steps. Therefore, solar radiation is re-calculated for every half-hour.

The surface heat transfer due to absorbed solar radiation at each external surface is calculated, and to this is added, algebraically, the longwave component of radiation and the convective heat transfer. Solar radiation transmitted through and absorbed by windows is also calculated, and the amounts absorbed by different internal surfaces are assigned to their respective surface heat flows.

The radiation between all internal surfaces is then computed , utilising pre-calculated angle (form) factors. The calculation of convective heat transfer at each internal surface completes this section of the program, at the end of which there exists a complete set of space temperatures, surface temperatures, surface heat flows and internal heat inputs to layers within the building structure. These internal heat inputs may be due to absorption of solar radiation by window glass or the heat input to a heating element, either as part of an ordinary interconnection, e.g. a radiant ceiling panel, or as the core of a separately defined heater. The construction of such a heater can be defined in the same way as the construction of all other interconnections, with the requirement that a "space" must be defined at the centre of the heater. Airflows through permeable interconnections are re-calculated every half-hour. With the foregoing calculations complete, the consequences of a five-minute time-step are then determined. All surface and interlayer temperatures are re-calculated using a forward differencing technique and, knowing the airflows into each space, and the capacity of the air in each space, the new space temperatures are obtained.

This completes the calculations for one time-step. The program outputs the major variables to a data file for later analysis, and repeats the entire process for the next interval.

A number of secondary calculations take place during the execution of the above procedure. At each time interval,

numbers of persons moving between spaces are estimated. This affects airflows through doorways, and hence ventilation rates. Calculation of moisture contents, air densities, and mean radiant temperatures proceeds in parallel with the main computations. These are required for use in assessing comfort conditions, which in turn affect window opening behaviour. The mean radiant temperatures are also used in conjunction with air temperatures to calculate thermostat temperatures, which control heaters in their respective zones, along with pre-defined "time-switch" settings.

2.3 SOLAR RADIATION

Since the U.K. Meteorological Office collects solar radiation measurements at only a few stations, the program was developed to compute solar radiation using the standard Meteorological Office data - particularly cloud cover and sunshine hours - as input.

The rate of energy emission from the sun is constant for all practical purposes. However, the rate at which it falls on a plane at the earth's surface depends on a large number of factors, some of which are geometrical, others which depend on the constitution and properties of the atmosphere through which the sun's rays must pass. The geometrical factors are easily determined by trigonometric consideration of relative sun-earth motions. These have been well documented elsewhere, for example in the Astronomical Ephemeris (35). Since most of the atmospheric effects are dependent on the wavelength of the radiation, it

is necessary to consider the solar radiation spectrum, and to treat each factor as a function of wavelength.

2.3.1 The Solar Constant

The "solar constant" is defined as the amount of energy per unit time falling on a unit area of plane normal to the sun's rays at the mean sun-earth distance, outside the earth's atmosphere. This has been distributed into twenty-two wavebands for convenience in Table 2.1. Due to the slightly elliptical orbit of the earth, the amount actually reaching the outside of the earth's atmosphere varies by about ±3%. This is taken into account very simply by applying a seasonal correction factor to the values of $I_{C\lambda}$, the radiation intensity contribution to the solar constant at mid-band frequency λ, such that

$$I_{o\lambda} = I_{C\lambda} \left(1 + .0335 \cos \frac{2\pi \text{ days}}{365}\right) \qquad 2.1$$

where days is the number of days in the current year to date.

2.3.2 Relative Air Mass

In order to compute the direct solar radiation at the earth's surface one must first determine the attenuating effect of the earth's atmosphere. This will largely depend on the actual path to be traversed by the sun's rays. The relative air mass at a point on the earth's surface is the ratio of the mass of air of unit cross-sectional area traversed by the sun's rays, to the mass of air of the same cross-sectional area normal to the earth's surface at this point. The relative air mass would therefore be unity with

	λ	$\bar{\lambda}$	H_λ	$d\lambda$	$I_{c\lambda}=H_\lambda d\lambda$	α
wave band nos.	wave band, microns	mid-band wave length microns	Solar radiation intensity W/cm^2 micron	band width microns	Total radiation in band W/cm^2	Ozone absorbtion coefficient cm^{-1}
1	.22-.29	.255	.0149	.07	.00105	8.
2	.29-.36	.325	.0934	.07	.00654	.018
3	.36-.41	.385	.1631	.05	.00681	0.
4	.41-.44	.425	.1886	.03	.00566	0.
5	.44-.47	.455	.216	.03	.00647	.0002
6	.47-.50	.485	.208	.03	.00625	.001
7	.50-.53	.515	.193	.03	.00579	.002
8	.53-.56	.545	.195	.03	.00586	.0034
9	.56-.59	.575	.187	.03	.00561	.005
10	.59-.63	.61	.177	.04	.00709	.0052
11	.63-.67	.65	.162	.04	.00650	.0023
12	.67-.72	.695	.146	.05	.00730	.001
13	.72-.76	.74	.131	.04	.00524	.0003
14	.76-.80	.78	.118	.04	.00472	0.
15	.80-.90	.85	.1007	.1	.01007	0.
16	.9-1.	.95	.0807	.1	.00807	0.
17	1.-1.25	1.125	.0588	.25	.01470	0.
18	1.25-1.5	1.375	.0347	.25	.00868	0.
19	1.5-2.0	1.75	.0174	.5	.00870	0.
20	2.0-3.0	2.5	.00563	1.	.00563	0.
21	3.0-5.0	4.0	.00113	2.	.00226	0.
22	5.0-7.0	6.0	.00024	2.	.00048	0.

Table 2.1

Solar Radiation Intensity in Wavebands

the sun directly overhead and would increase with increasing zenith angle Z. Sec(Z) gives a fair approximation to the relative air mass, but neglects to allow for the effect of the curvature of the earth's surface, which becomes significant at low sun altitude. The following formula expresses the relative air mass of a homogenous spherical atmosphere and gives values in good agreement with observed values (36, p.51).

$$m_{gr} = \left[\left(\frac{R}{H}\right)^2 \cos^2 Z + 2\frac{R}{H} + 1\right]^{\frac{1}{2}} - \frac{R}{H}\cos Z \qquad 2.2$$

where $H = \frac{P_o}{g\rho_o}$,

R = radius of the earth,

P_o = sea level atmospheric pressure,

ρ_o = sea level air density.

At elevated sites the air mass may vary considerably from that at sea level, and therefore m_r is calculated from

$$m_r = m_{gr}\frac{P}{P_o} \qquad 2.3$$

where P is the site barometric pressure.

2.3.3 Effect of the Earth's Atmosphere

The various radiation attenuating factors are most easily expressed as transmission coefficients, such that the direct component of radiation reaching the earth's surface is given by the sum for all wavebands of

$$I_\lambda = \tau_a \tau_w \tau_d \tau_{wa} \tau_{oz} I_{o\lambda} \qquad 2.4$$

where τ_a = transmission coefficient to account for Mie scattering (dry air),

τ_w = transmission coefficient for scattering by water vapour,

τ_d = transmission coefficient for scattering by dust,

τ_{wa} = transmission coefficient for absorption by water vapour, carbon dioxide and oxygen,

τ_{oz} = transmission coefficient for absorption by ozone.

Mie scattering

The amount of radiation scattering due to air molecules depends on the number of molecules in the path of the solar beam. The Rayleigh extinction coefficient, which includes corrections for refraction and anisotropy of the air molecules, is given by

$$a_A = .00386\ \lambda^{-4.05} \qquad 2.5$$

and therefore

$$\tau_a = 10^{-.00386(\lambda^{-4.05})m_r\left(\frac{P}{1000}\right)} \qquad 2.6$$

Water Vapour scattering

Similarly, the transmission coefficient for scattering by water vapour is given by

$$\tau_w = 10^{-.0075(\lambda^{-2})\frac{w}{.02}\ m_r} \qquad 2.7$$

where w = the water content of the atmosphere expressed as metres of precipitable water.

w cannot be determined explicitly but may be estimated by extrapolation from the atmospheric moisture content mixing ratio m_o (kg/kg) at sea level.

If atmospheric pressure is assumed to follow the relationship

$$P_h = P_o e^{-\frac{gh}{Rt}} \qquad 2.8$$

where P_h is the atmospheric pressure at height h,

t is the sea level air temperature,

then we can use the theory of Benoy (37) that a parabolic relation exists between moisture content and atmospheric pressure, i.e.

$$\frac{m_h}{m_o} = \left(\frac{P_h - P_m}{P_o - P_m}\right)^2 \qquad 2.9$$

where P_m is atmospheric pressure at height H

where m reduces to zero.

m_h is moisture content at height h.

It can be shown that

$$W_o = \frac{P_o m_o}{3 \rho_w g}\left[1 - \exp\left(\frac{-gH}{Rt}\right)\right] \qquad 2.10$$

where ρ_w is the density of water

g is the gravitational acceleration

R is the gas constant.

Using suitable average values, we end up with the formula

$$w = .0034\ P_o m_o \left[1 - \exp(-312.6/t_o)\right] \qquad 2.11$$

Dust particle scattering

Baxter (38) carried out a survey of dust particle concentrations in a city environment. His results are applied in the following formula due to Moon (39) for determining the transmission coefficient due to scattering by dust.

$$\tau_d = 10^{-.0353\left(\lambda^{-.75}\left(e^{-.0005h}\right)\frac{d}{800}\right)m_r} \qquad 2.12$$

where d is the dust particle concentration ($\mu g/m^3$)

This assumes that dust is concentrated in the lower atmospheric regions, and the factor $e^{-.0005h}$ where h is the site elevation (m), is a correction factor to allow for this effect.

d is assumed to vary seasonally, and, by fitting a sine curve to Baxter's data, the dust concentration is given by

$$d = 96 + 62 \cos\left(\frac{\text{month} - .5}{6}\pi\right) \qquad 2.13$$

where month varies from 1 to 12.

This value is then scaled up or down depending on site conditions, to allow for atmospheric dust concentrations not typical of a city environment.

Water vapour absorption

No explicit formulae exist for the absorption of radiation by water vapour and the less important carbon dioxide and oxygen. The empirical results of Fowle are adapted from Robinson (36, p.114) in Table 2.2. The transmission coefficient is given by

Waveband, microns	precipitable water depth, $m_{r.w}$, cm										
	.1	.2	.4	.7	1.0	2.0	4.0	7.0	10.0	20.0	30.0
.72-.76	.0005	.001	.002	.005	.008	.017	.033	.056	.072	.12	.14
.76-.80	.002	.003	.0056	.01	.015	.027	.045	.076	.095	.15	.18
.80-.90	.005	.008	.015	.021	.027	.043	.064	.105	.13	.18	.22
.90-1.00	.01	.0135	.022	.031	.040	.060	.092	.125	.16	.22	.26
1.00-1.25	.017	.023	.033	.047	.058	.087	.129	.177	.21	.272	.315
1.25-1.5	.097	.143	.203	.260	.302	.388	.483	.567	.62	.720	.780
1.5-2.0	.066	.092	.120	.144	.160	.191	.223	.249	.266	.295	.315
2.0-3.0	.190	.256	.328	.402	.435	.566	.683	.786	.863	1.00	1.09
3.0-5.0	.21	.285	.365	.465	.52	.67	.81	.98	1.1	1.25	1.35
5.0-7.0	.23	.300	.39	.49	.56	.70	.88	1.05	1.18	1.38	1.50

Table 2.2

Water vapour absorption coefficients (a_w)

$$\tau_{aw} = 10^{-a_w} \qquad 2.14$$

where the total amount of water vapour traversed by the solar beam expressed as a depth of precipitable water $w.m_r$, is entered into Table 2.2 to determine a_w .

Ozone absorption

Again empirical data must be used. Robinson (36, p.114) gives the seasonal variations of atmospheric ozone, expressed as a depth x, in cm at NTP (Table 2.3). The transmission coefficient is then obtained as

$$\tau_{oz} = 10^{-\alpha x m_r} \qquad 2.15$$

where the ozone absorption coefficient α is as given in Table 2.1 .

2.3.4 Diffuse Radiation at the Earth's Surface

The diffuse radiation falling on the Earth's surface consists of a portion of the radiation scattered into the atmosphere by air, water vapour molecules, and dust particles. If we denote the radiation reaching the surface of the earth depleted by absorption alone as $I_{a,\gamma}$ at solar altitude γ ,

$$I_{a,\gamma} = \int_{\lambda} \tau_{wa}\, \tau_{oz}\, I_{o\lambda}\, d\lambda \qquad 2.16$$

and the radiation scattered into the atmosphere is therefore

$I_{a,\gamma} - I_{\gamma}$,

where $I_{\gamma} = \int_{\lambda} I_{o\lambda}\, d\lambda$ at solar altitude γ .

Latitude	Month											
	Jan.	Feb.	Mar.	Apr.	May	June	July	Aug.	Sep.	Oct.	Nov.	Dec.
90°N	0.33	0.39	0.46	0.42	0.39	0.34	0.32	0.30	0.27	0.26	0.28	0.30
80°N	0.34	0.40	0.46	0.43	0.40	0.36	0.33	0.30	0.28	0.27	0.29	0.31
70°N	0.34	0.40	0.45	0.42	0.40	0.36	0.34	0.31	0.29	0.28	0.29	0.31
60°N	0.33	0.39	0.42	0.40	0.39	0.36	0.34	0.32	0.30	0.28	0.30	0.31
50°N	0.32	0.36	0.38	0.38	0.37	0.35	0.33	0.31	0.30	0.28	0.29	0.30
40°N	0.30	0.32	0.33	0.34	0.34	0.33	0.31	0.30	0.28	0.27	0.28	0.29
30°N	0.27	0.28	0.29	0.30	0.30	0.30	0.29	0.28	0.27	0.26	0.26	0.27
20°N	0.24	0.26	0.27	0.28	0.27	0.26	0.26	0.26	0.26	0.25	0.25	0.25
10°N	0.23	0.24	0.24	0.25	0.26	0.25	0.25	0.24	0.24	0.23	0.23	0.23
0°N	0.22	0.22	0.23	0.23	0.24	0.24	0.24	0.23	0.23	0.22	0.22	0.22
10°S	0.23	0.24	0.24	0.24	0.24	0.24	0.24	0.24	0.24	0.24	0.24	0.23
20°S	0.24	0.25	0.24	0.25	0.25	0.25	0.25	0.26	0.26	0.26	0.26	0.25
30°S	0.27	0.28	0.26	0.27	0.28	0.28	0.29	0.31	0.32	0.32	0.29	0.29
40°S	0.30	0.29	0.28	0.29	0.31	0.33	0.35	0.37	0.38	0.37	0.34	0.32
50°S	0.31	0.30	0.29	0.30	0.32	0.36	0.39	0.40	0.40	0.39	0.37	0.35
60°S	0.32	0.31	0.30	0.30	0.33	0.38	0.41	0.42	0.42	0.40	0.39	0.35
70°S	0.32	0.31	0.31	0.29	0.34	0.39	0.43	0.45	0.43	0.40	0.38	0.34
80°S	0.31	0.31	0.31	0.28	0.35	0.40	0.44	0.46	0.42	0.38	0.36	0.32
90°S	0.31	0.30	0.30	0.27	0.34	0.38	0.43	0.45	0.41	0.37	0.34	0.31

Table 2.3

Seasonal variation of atmospheric ozone in cm NTP (Robinson)

The diffuse radiation on a horizontal plane is then given by

$$D_\gamma = k_\gamma (I_{a,\gamma} - I_\gamma) \sin \gamma \qquad 2.17$$

K_γ is a factor, which can be expressed empirically (Robinson,36, p.117) by

$$K_\gamma = 0.5 \sin^{1/3} \gamma \qquad 2.18$$

This was derived from data collected in the Congo where the ground surface reflectivity (often referred to as the albedo) is 0.25. K_γ is a function of ground reflectivity, A, but the variations are small within our range of interest (< 2% for .1 < A < .3) and equation 2.18 is therefore assumed to be universally applicable.

The global radiation falling on a horizontal surface is given by

$$G_\gamma = I_\gamma \sin \gamma + D_\gamma \qquad 2.19$$

where there is no cloud cover.

2.3.5 Radiation Falling on an Inclined Plane, in Cloudy Conditions

So far we have been concerned only with clear sky conditions and horizontal surfaces. The values of I_γ, D_γ and G_γ must now be modified to compute radiation falling on an inclined plane, with cloud cover and sunshine hours being incorporated into the analysis.

An important consideration at this point is the distribution of diffuse radiation over the global hemisphere.

Forward scattering of radiation as it passes through the Earth's atmosphere leads to a large proportion of diffuse radiation falling on the Earth's surface at angles of incidence very close to the direct solar beam. If we fail to account for this anisotropy in the distribution of diffuse solar radiation, then radiation falling on south facing surfaces will be underestimated, whilst that falling on north facing surfaces will be overestimated. A number of investigators have studied this problem but Robinson (36, p.123) suggests simply reducing the luminance of the clear sky fraction by 25% and adding the difference to the direct component so that the same global radiation G_γ is obtained.

$$\text{Thus} \quad I_{\gamma,\epsilon} = (I_\gamma + 0.25 \frac{D_\gamma}{\sin\gamma}) \sin i \qquad 2.20$$

for a surface inclined at an angle ϵ to the horizontal, where i is the angle of incidence of the solar beam on the surface. This is further modified by sunshine hours $\frac{n}{N}$ and cloud cover C. These two variables can be treated separately by assuming that the direct component of radiation is modified by sunshine hours (duration of bright sunshine) and that the diffuse component is dependent on cloud cover. The direct component now becomes

$$I_{\gamma,\epsilon,\frac{n}{N},C} = \left[\frac{n}{N} I_\gamma + 0.25(1-c)\frac{D_\gamma}{\sin\gamma}\right] \sin i \qquad 2.21$$

The diffuse radiation on a horizontal plane must now be separated into components emanating from the clear and cloudy portions of the sky. The clear component, as discussed above will be given by

$$D_{\gamma,blue} = 0.75\ (1-C)\ D_\gamma \qquad 2.22$$

whilst the cloudy component is given by

$$D_{\gamma,cloud} = G_{\gamma}\ f(c) \qquad 2.23$$

where f(c) is an empirical function of cloud cover and cloud type.

Robinson (36, p.127) lists values of a function $f(\frac{n}{N})$ which relates to daily sums of radiation at several sites. The program assumes $f(c) = f\ (1-\frac{n}{N})$ and that the data are applicable to the short-term sums which it computes. The Potsdam values (Table 2.4) are used as these are representative of low-level stations at middle latitudes. This is probably as detailed a description as is justified by the data available and the intended application. Therefore, combining equations 2.22 and 2.23 .

$$D_{\gamma,c} = 0.75\ (1-c)D_{\gamma} + G_{\gamma}\ f(c) \qquad 2.24$$

For an inclined surface a $\cos^2 \frac{\epsilon}{2}$ law is assumed to apply, and

$$D_{\gamma,\epsilon,c} = \left[0.75(1-c)D_{\gamma} + \cos\tfrac{\epsilon}{2}\ G_{\gamma}\ f(c)\right]\cos^2 \tfrac{\epsilon}{2} \qquad 2.25$$

An additional component of radiation reflected from the ground will now be included. This is assumed to be proportional to the global radiation falling on the horizontal ground in view of the receiving surface, now given by -

$$G_{\gamma,\frac{n}{N},c} = \frac{n}{N} I_{\gamma} \sin\gamma + (1-c)D_{\gamma} + G_{\gamma}\ f(c) \qquad 2.26$$

n/N	f(n/N) (Potsdam)
1.0	0.00
0.9	0.04
0.8	0.08
0.7	0.12
0.6	0.16
0.5	0.19
0.4	0.22
0.3	0.25
0.2	0.26
0.1	0.26
0.05	0.24
0	0.14

Table 2.4

Values of function f(n/N)
for different values of
sunshine hours fraction n/N.

The radiation reflected from the ground surface will depend on its reflectivity A and is given by

$$R_{\gamma,\epsilon,A,\frac{n}{N},c} = G_{\gamma,\frac{n}{N},c}\, A\, (1-\cos^2\frac{\epsilon}{2}) \qquad 2.27$$

The global radiation falling on an inclined plane is the sum of the individual components given by equations 2.21, 2.25 and 2.27 .

$$G_{\gamma,A,\epsilon,\frac{n}{N},c} = I_{\gamma,\epsilon,\frac{n}{N},c} + D_{\gamma,\epsilon,c} + R_{\gamma,\epsilon,A,\frac{n}{N},c} \qquad 2.28$$

2.4 TRANSMISSION OF RADIATION THROUGH WINDOWS

Of the total radiation falling on a window surface, after allowing for structural shading, some will be reflected at the glass/air surface, some will be absorbed in the window glass, and some will be transmitted into the building where it will be absorbed at the internal room surfaces.

2.4.1 Reflected radiation

The proportion of radiation reflected by a window depends on the angle of incidence of the solar beam, and the reflectivity of the glass surfaces. The reflectivity at a smooth air/surface interface of a dielectric medium is given by Ozisik (40) as

$$r_i = \frac{Ir}{Io} = \frac{\sin^2(i-i')}{2\sin^2(i+i')} + \frac{\tan^2(i-i')}{2\tan^2(i+i')} \qquad 2.29$$

where Io = intensity of incident beam

Ir = intensity of reflected beam

i = angle of incidence of incident beam

i' = angle of incidence of refracted beam.

This gives a reflectivity which is essentially constant for angles of incidence to the normal of up to 60^{o}, increasing to unity at grazing incidence. For real materials, unity reflectivity is not attained, and surface coatings could further modify the theoretical reflectivity. The reflectivity for normal incidence is supplied to the program for each window construction (single or multisheet) and is assumed constant for angles of incidence up to 60^{o}. Beyond 60^{o}, the reflectivity is assumed to increase linearly up to 0.8 at 90^{o}. This is believed to be sufficiently accurate for all practical purposes.

2.4.2 Glass Absorption

The transmission factor for each glass sheet is computed as

$$\tau_a = e^{-kL} \qquad 2.30$$

where L = path length = $L'/\cos i$

L' = glass thickness

k = glass absorption coefficient.

For the diffuse component of radiation L is assumed equal to L'. Shading devices are treated in the same way as glass sheets.

2.4.3 Room Surface Absorption

The radiation transmitted to a room consists of a direct component, if the direct solar beam falls on the window, and a diffuse component. To avoid the complex calculations involved in computing the lit area and consequent short-wave radiations (which would be necessary for daylighting calculations) all the direct component is assumed to fall on the room floor. Half the diffuse component of radiation transmitted to a room is assumed to fall on the floor, and one sixth on each of the side walls adjacent to the window wall, and on the wall directly opposite the window wall.

2.5 HEAT TRANSFER AT BUILDING SURFACES

2.5.1 Radiation at External Surfaces

In addition to the absorption of solar radiation, long-wave radiation occurs at all the external surfaces of a building. This consists of an outward radiated component, and an incoming atmospheric component. Ångström (41) gives an empirical relationship for the incoming component for a clear sky.

$$I\downarrow o = \epsilon \sigma T_o^4 (a_o - b_o 10^{-c_o v}) \qquad 2.31$$

where T_o is the air temperature, C,

v is the atmospheric vapour pressure, N/m^2

a_o, b_o and c_o are empirical constants,

ϵ is the surface emissivity,

σ is the Stefan-Boltzmann constant.

The effect of water vapour is thereby accounted for, being an important atmospheric constituent with absorption bands at long wavelengths. Geiger's equation (42) is used to account for the effect of clouds and modifies the radiation obtained using equation 2.31 .

$$I_{\downarrow} = I_{\downarrow o} (1+KC^2) \qquad 2.32$$

where C is the cloud amount, $0 < C < 1$

K is a constant obtained from observations.

Thus the "greenhouse" effect of nocturnal cloud cover is accounted for as is the high rate of outgoing radiation associated with a clear night sky.

A value of K = 0.2 is used in the above equation as this corresponds to the average cloud density and height obtained from U.K. observations. For vertical or inclined surfaces, radiation exchange also takes place with the ground surface. The assumption made is that the ground surface temperature is the same as the air temperature. Outgoing longwave radiation is simply obtained as

$$I_{\uparrow} = \epsilon \sigma T_s^4 \qquad 2.33$$

where T_s = surface temperature.

The sum of all components for both short- and long-wave effects make up the radiation balance for each external surface.

2.5.2 Convection at External Surfaces

The 1970 IHVE Guide (2) quotes the following equation for computing the convection coefficient of an external surface.

$$h_c = 5.2 + 4.1V \quad W/m^2C \qquad 2.34$$

where V is the wind speed in m/s

Ito et al (43) carried out a full scale study of the external convection coefficient of a building. Their tests were not exhaustive, but indicate the magnitude of the effects of wind on convection at external surfaces. They related the convection coefficient to the local air velocity over a surface, which was in turn related to the wind speed measured above the building. The following equation is derived from their results, based on a mid floor of a six storey building

$$h_c = 5.8 + 2.0V \quad W/m^2C \qquad 2.35$$

Equation 2.35 is used in preference to 2.34 as it is more soundly based on actual experimental data, although some improvement may be forthcoming in the future, which will allow for wind direction, turbulence and surface roughness effects.

2.5.3 Radiation at Internal Surfaces

Longwave radiation between a pair of internal surfaces can be computed knowing their surface temperatures and their geometrical relationship. Thus, assuming grey diffusely

emmitting surfaces only,

$$H_{r_{a \to b}} = \epsilon_a \epsilon_b \sigma F_{a \to b} A_a (T_a^4 - T_b^4) \qquad 2.36$$

where $H_{r_{a \to b}}$ is the net radiation between surface a and surface b

ϵ_a and ϵ_b are surface emmissivities of surfaces a and b

σ is the Stefan-Boltzmann constant,

A_a is the surface area of surface a,

T_a and T_b are surface temperatures of surfaces a and b

$F_{a \to b}$ is the angle factor for radiation from surface a to surface b, i.e. the proportion of radiation leaving a that reaches b.

The pre-calculated quantities supplied are the area weighted angle factors, which for equation 2.33 is $F_{a-b}A_a$. As

$$F_{a \to b} A_a = F_{b \to a} A_b \qquad 2.37$$

only one such product need be obtained for each pair of surfaces in common view. Various geometrical configurations are possible between pairs of surfaces in a building, but only two general relationships are used in the work to be described later and these will be stated here.

Parallel Rectangular Surfaces

The angle factor for radiation between a pair of identical opposite parallel surfaces (Figure 2.2) is given by Sparrow and Cess (44) and will not be repeated here. We will denote this by $F_{11}(a,b;c)$ for rectangular surfaces measuring axb separated by a distance C.

Simple rules for angle factor algebra enable the determination of the angle factors between any parallel rectangular surfaces by consideration of the sums of angle factors between up to 16 pairs of opposite surfaces, which are in turn determined from $F_{11}(a,b;c)$.

The calculation procedure is described in Appendix 2. There is no restriction on the relative dimensions of two surfaces in common view.

Perpendicular Rectangular Surfaces

A similar expression can be derived for rectangular surfaces at right angles to one another based on the angle factor $F_{\perp}(a,b,c)$ for surfaces with a common edge length C at right angles, and with radiation from a surface of breadth a to a surface of breadth b. Again the calculation can be carried out with any combination of relative dimensions for the two surfaces (Appendix 2).

A complete set of angle factors between pairs of surfaces in common view is calculated prior to execution of the main simulation program. "Cut-outs" are permissible, e.g. for a wall containing a window, separate angle factors

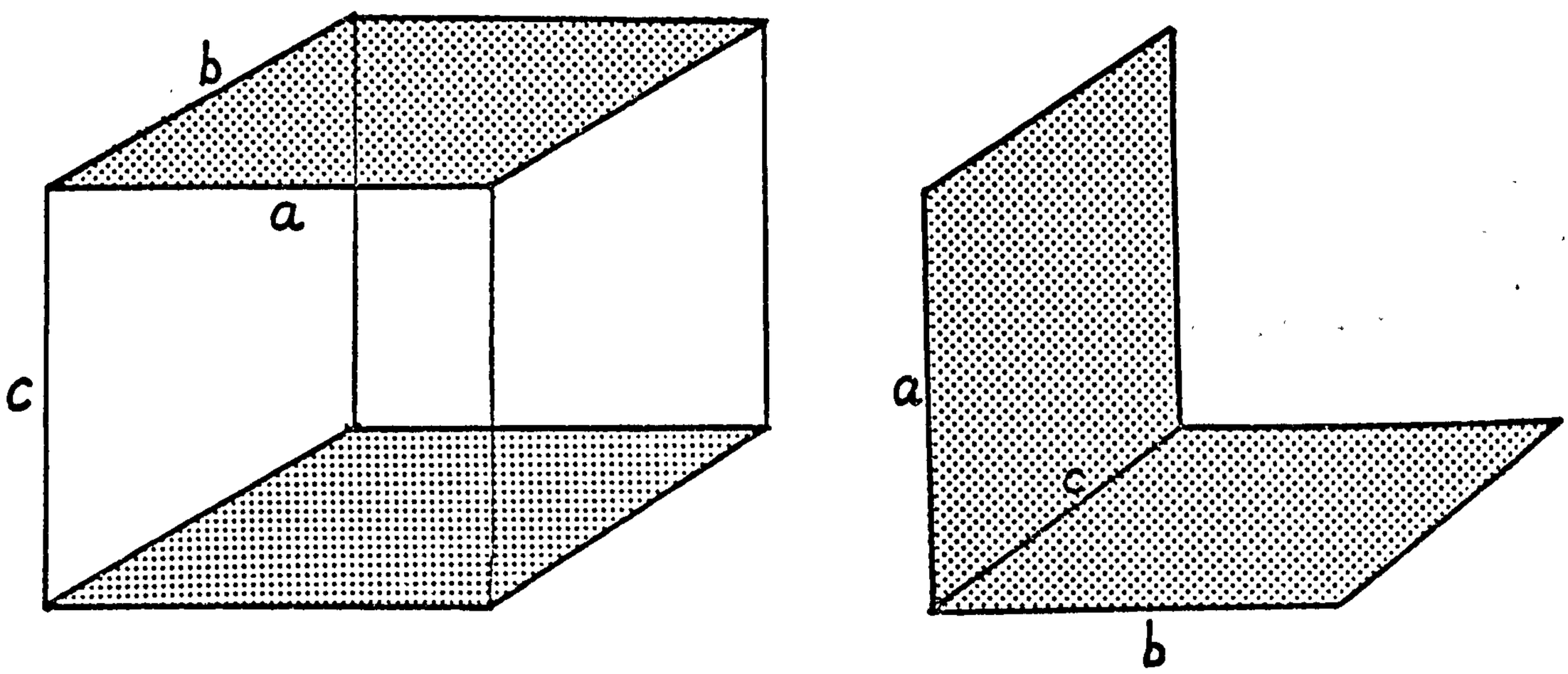

FIGURE 2.2

Pairs of Parallel and Perpendicular Surfaces

are determined for radiation exchange with the window surface, and with the wall surface omitting the area occupied by the window. The entire procedure is automatic, once the geometric data have been input.

2.5.4 Convection at internal surfaces

In order to model the different convective heat transfer coefficients that exist at walls, floors and ceilings, and to include the dependence on temperature difference, the results of Min et al were used. (45)

i) for heat flow at a vertical surface,

$$h_c = 1.87 \ \Delta t^{.32} l^{-.05} \qquad 2.38$$

where h_c is the convective heat transfer coefficient, W/m^2C

Δt is the temperature difference between the surface and room air, C

l is the height of the surface, m.

ii) for downward heat flow at a ceiling or floor,

$$h_c = 0.203 \ \Delta t^{.25} l^{-.24} \qquad 2.39$$

where l is the hydraulic diameter of the surface, m, given by

$$l = 4A/P \qquad 2.40$$

where A is the surface area, m^2

P is the surface perimeter, m.

iii) for upward heat flow at a floor or ceiling,

$$h_c = 2.42\ \Delta t^{.31} l^{-0.08} \qquad 2.41$$

where l is the hydraulic diameter, m.

In a heated space, some vertical temperature stratification usually exists. In unfavourable conditions in dwelling houses, this may be as great as 10 C temperature difference between floor and ceiling. The program makes some allowance for this by subtracting a given amount from the mean room temperature when calculating convection at the floor surface, and adding the same quantity for calculating at the ceiling surface.

The amount of stratification is input as data for each space, and the adjustment is made only when the heating in a space is switched on.

2.6 CONDUCTION

2.6.1 Conduction through building fabric

Interconnections between spaces usually consist of partitions which can be considered as several layers of material, including air gaps, within which thermal properties may be regarded as uniform. The procedure used in this program to compute successive sets of temperatures based on the heat flows existing at the surfaces of the outermost layers, is a modified version of the one described by Brown (9).

Consider two adjacent layers ABC and CDE in a multi-layer slab. (Figure 2.3). The temperatures at the interfaces between each layer are T_-, T and T_+. After a time interval Δt, the new temperatures will be T_-' , T' and T_+' .

We are interested in heat flows to and from the composite section BCD consisting of half of two adjacent layers ABC and CDE. The conduction heat from the left, q_c^-, in time Δt per unit area can be calculated as being dependent on the mean temperature difference between B and C,

$$q_c^- = \left[\frac{\frac{T_- + T}{2} + \frac{T_-' + T'}{2}}{2} - \frac{T + T'}{2} \right] \frac{k^- \Delta t}{w^-/2} \qquad 2.42$$

where k^- is the thermal conductivity of the material in ABC and w^- is the thickness of layer ABC.

$$\therefore\ q_c^- = (T_- - T + T_-' - T') \frac{k^- \Delta t}{2w^-} \qquad 2.43$$

Similarly, the heat flow from the right into section BCD is given by

$$q_c^+ = (T_+ - T + T_+' - T') \frac{k^+ \Delta t}{2w^+} \qquad 2.44$$

The heat stored in section BCD will change in the time interval Δt by amounts proportional to the changes in the mean temperatures of the sections. For section BC, the heat stored q_s^-, is given by

$$q_s^- = \left[\frac{\frac{T_-' + T'}{2} + T'}{2} - \frac{\frac{T_- + T}{2} + T}{2} \right] s^- \rho^- \frac{w^-}{2} \qquad 2.45$$

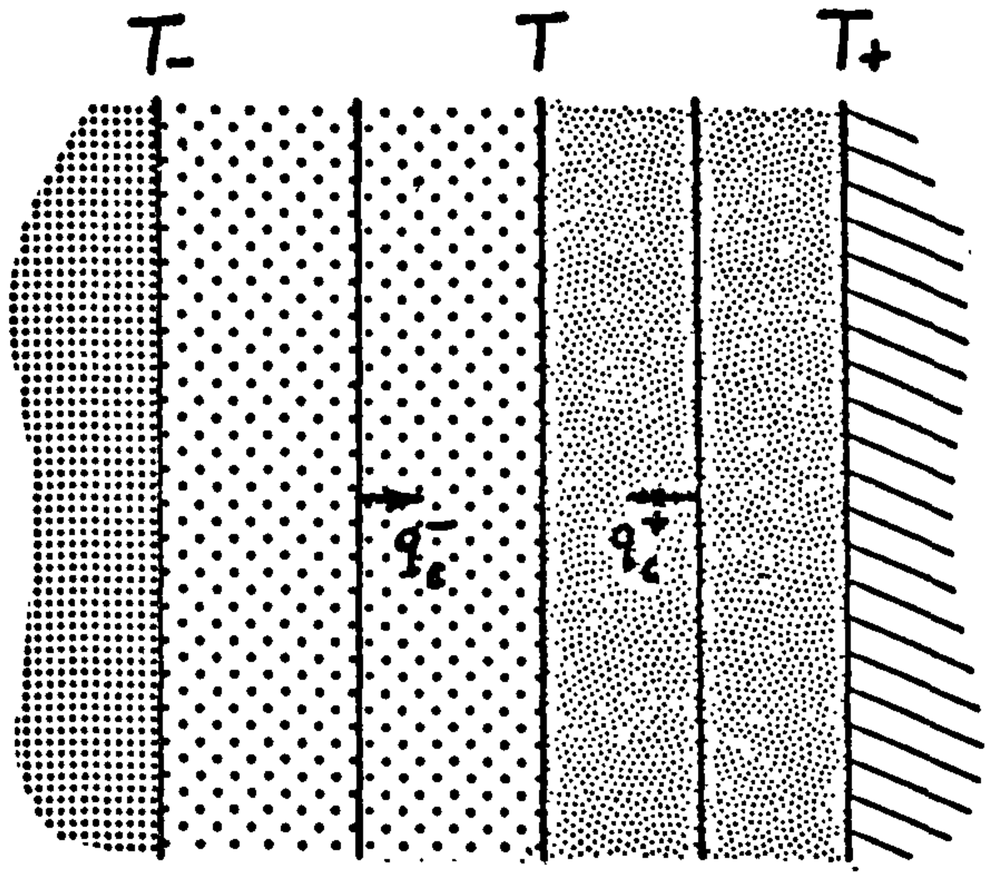

FIGURE 2.3 Heat Conduction within Multilayer Slabs

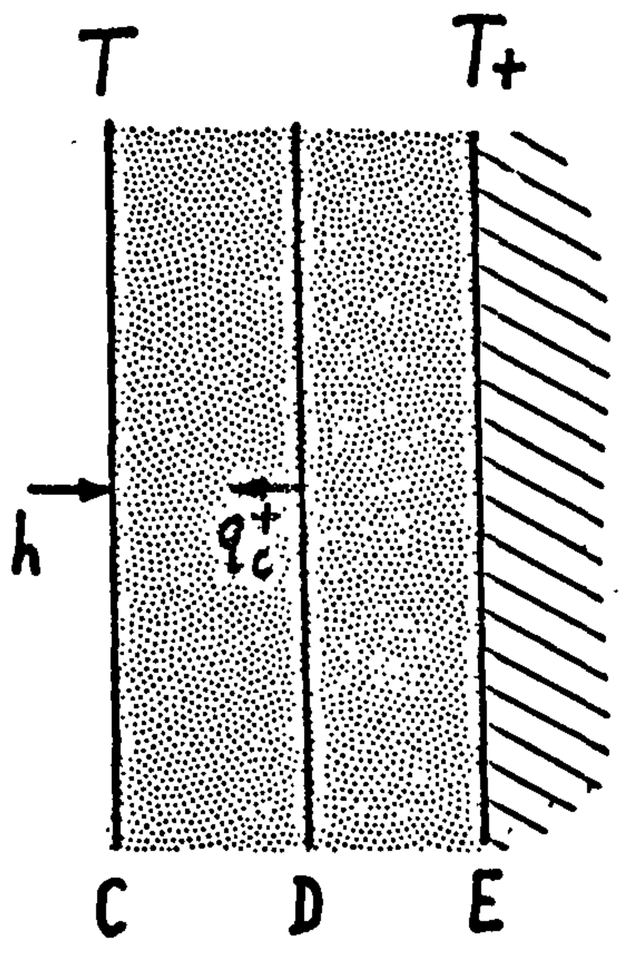

FIGURE 2.4 Heat transfer at "Left Hand" Surface of Multilayer Slab

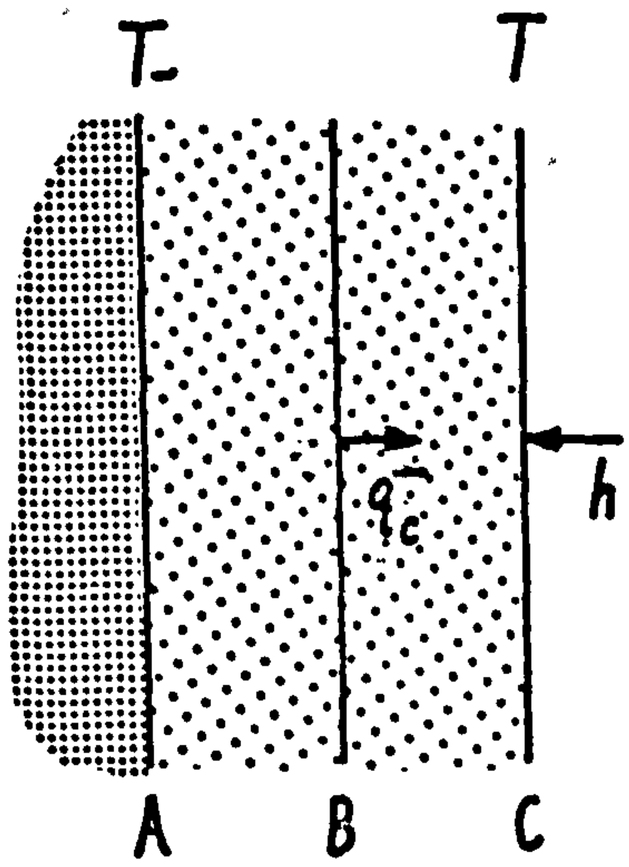

FIGURE 2.5 Heat Transfer at "Right Hand" Surface of Multilayer Slab

where s^- is the specific heat of layer ABC

ρ^- is the density of layer ABC.

Thus $q_s^- = \left(\frac{T^{-\prime} + 3T'}{4} - \frac{T- + 3T}{4}\right) \frac{s^- \rho^- w^-}{2}$ 2.46

Similarly, for section CD,

$$q_s^+ = \left(\frac{3T' + T+'}{4} - \frac{3T + T+}{4}\right) \frac{s^+ \rho^+ w^+}{2} \quad 2.47$$

There may in addition be external heat inputs to layers ABC and CDE of Q^- and Q^+ respectively. The external heat inputs to sections BC and CD in time Δt will therefore be

$$q_i^- = \frac{Q^-}{2} \Delta t \quad 2.48$$

and

$$q_i^+ = \frac{Q^+}{2} \Delta t \quad 2.49$$

The heat balance for section BCD can be written as

$$(q_c^- + q_c^+) + (q_i^- + q_i^+) = (q_s^- + q_s^+) \quad 2.50$$

If we set $C^- = \frac{k^-}{w^{-\prime}} C^+ + \frac{k^+}{w^+}$

$$a^- = \frac{k^-}{s^- \rho^{-\prime}} \qquad a^+ = \frac{k^+}{s^+ \rho^+}$$

$$p^- = \frac{w^-}{a^{-\prime}} \qquad p^+ = \frac{w^+}{a^+}$$

then the above equation becomes,

$$
\begin{aligned}
&T_{-}\left(1+\tfrac{1}{4}\cdot\frac{p^{-}}{\Delta t}\right)\\
&+T\left(-1-\frac{c^{+}}{c^{-}}+\tfrac{3}{4}\cdot\frac{p^{-}}{\Delta t}+\tfrac{3}{4}\cdot\frac{c^{+}}{c^{-}}\cdot\frac{p^{+}}{\Delta t}\right)\\
&+T_{+}\left(\frac{c^{+}}{c^{-}}+\tfrac{1}{4}\cdot\frac{c^{+}}{c^{-}}\cdot\frac{p^{+}}{\Delta t}\right)\\
&+T_{-}'\left(1-\tfrac{1}{4}\cdot\frac{p^{-}}{\Delta t}\right)\\
&+T'\left(-1-\frac{c^{+}}{c^{-}}-\tfrac{3}{4}\cdot\frac{p^{-}}{\Delta t}-\tfrac{3}{4}\cdot\frac{c^{+}}{c^{-}}\cdot\frac{p^{+}}{\Delta t}\right)\\
&+T_{+}'\left(\frac{c^{+}}{c^{-}}-\tfrac{1}{4}\cdot\frac{c^{+}}{c^{-}}\cdot\frac{p^{+}}{\Delta t}\right)\quad+\frac{q^{-}+q^{+}}{c^{-}}\quad=0.
\end{aligned}
\tag{2.51}
$$

At an external or room air/surface interface, a similar analysis can be applied. Referring to Figure 2.4,

$$q_c^{+}=\left(T_{+}-T+T_{+}'-T'\right)\frac{k^{+}\Delta t}{2w^{+}} \tag{2.52}$$

$$q_s^{+}=\left(\frac{3T'+T_{+}'}{4}-\frac{3T+T_{+}}{4}\right)\frac{s^{+}\rho^{+}w^{+}}{2} \tag{2.53}$$

$$q_i^{+}=\frac{Q^{+}}{2}\Delta t \tag{2.54}$$

These are identical to equations 2.44, 2.47 and 2.49 relating to the previous case considered. These heat flows are balanced by the heat input at the surface H, and

$$h=H\Delta t \tag{2.55}$$

The heat balance for section CD can be written as

$$q_c^{+}+q_i^{+}+h=q_s^{+} \tag{2.56}$$

and hence, using the previous terminology,

$$T\left(-1+\frac{3}{4}\cdot\frac{p^+}{\Delta t}\right)+T_+\left(1+\frac{1}{4}\cdot\frac{p^+}{\Delta t}\right)+T'\left(-1-\frac{3}{4}\cdot\frac{p^+}{\Delta t}\right)+T'_+\left(1-\frac{1}{4}\cdot\frac{p^+}{\Delta t}\right)+\frac{2h+q^+}{c^+}=0 \qquad 2.57$$

Similarly, for the other surface, (Figure 2.5)

$$T_-\left(1+\frac{1}{4}\cdot\frac{p^-}{\Delta t}\right)+T\left(-1+\frac{3}{4}\cdot\frac{p^-}{\Delta t}\right)+T'_-\left(1-\frac{1}{4}\cdot\frac{p^-}{\Delta t}\right)+T'\left(-1-\frac{3}{4}\cdot\frac{p^-}{\Delta t}\right)+\frac{2h+q^-}{c^-}=0 \qquad 2.58$$

The complete set of equations, one for each interface within the partition, form a simultaneous set which can be solved very easily by a simple process of diagonal elimination, each equation involving a maximum of three unknown temperatures (i.e. terms like T').

Equations 2.57 and 2.58 are valid provided the rate of change of temperature, and hence heat flux, at the surfaces is small. However, the above equations may have to be applied during rapid temperature fluctuations. To compensate for the dependence of heat flow on surface temperature, a modified heat flow is calculated by using the known previous and current time steps' surface heat

flows and temperatures. To estimate the next temperature, we require a forward estimate of the mean heat flow over the next time interval. To do this we assume a linear relationship between heat flow and temperature, (Figure 2.6).

$$h = kt+C \qquad 2.59$$

$$\text{i.e. } h_p = kt_p+C \qquad 2.60$$

$$\text{and } h_n = kt_n+C \qquad 2.61$$

where h_p and t_p are the previous time step's heat flow and temperature,

h_n and t_n are the current time step's heat flow and temperature.

$$k = \frac{h_n-h_p}{t_n-t_p} \qquad 2.62$$

$$C = h_n - t_n \frac{h_n-h_p}{t_n-t_p} \qquad 2.63$$

$$\text{so } h = h_n + \frac{h_n-h_p}{t_n-t_p}(t-t_n) \qquad 2.64$$

length/ breadth ratio	B
1:1	1.6
2:1	1.3
3:1	1.2
4:1	1.15
5:1	1.12
6:1	1.1
10:1	1.06

Table 2.5

Values of B for calculation of heat loss through the ground

We require a mean $\overline{h}$ such that

$$\overline{h} = \tfrac{1}{2}(h_n + h_f) \qquad 2.65$$

where h_f = next time step's heat flow.

$$\therefore \overline{h} = h_n + \tfrac{1}{2}t_f\left(\frac{h_n - h_p}{t_n - t_p}\right) - \tfrac{1}{2}t_n\left(\frac{h_n - h_p}{t_n - t_p}\right) \qquad 2.66$$

Substituting $\overline{h}$ for h in equation 2.57 and 2.58 yields additional coefficients of T_+' and T_-' respectively corresponding to the coefficient of t_f above. The subsurface equations are unaffected by this amendment.

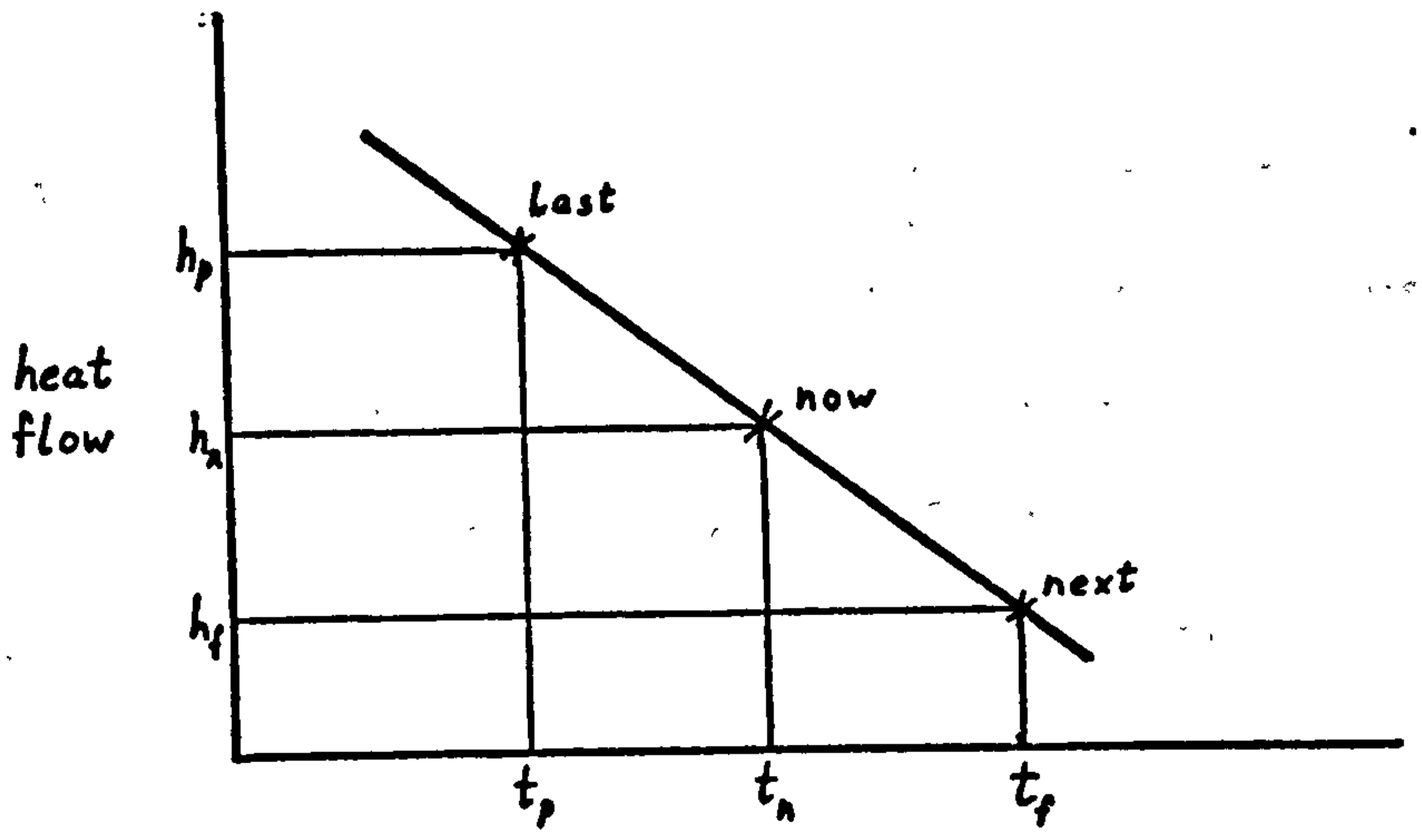

FIGURE 2.6 Algorithms for Determining Forward Estimate of Mean Heat Flow

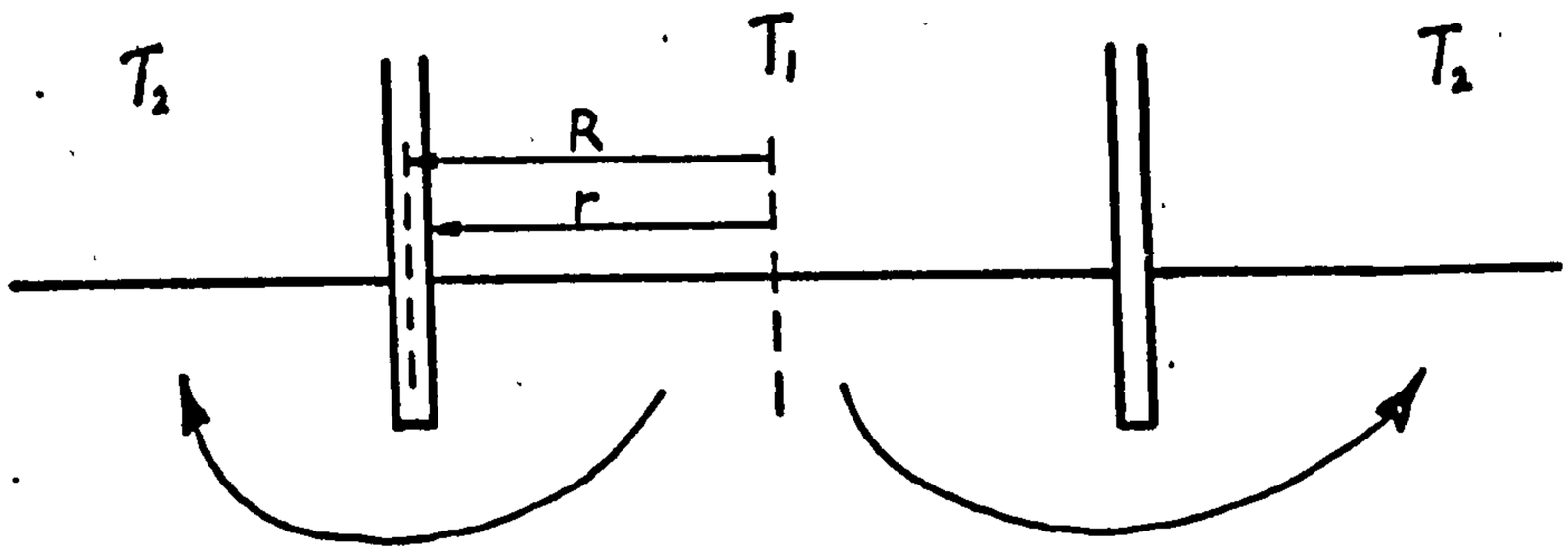

FIGURE 2.7 Heat Loss Through Ground Floor

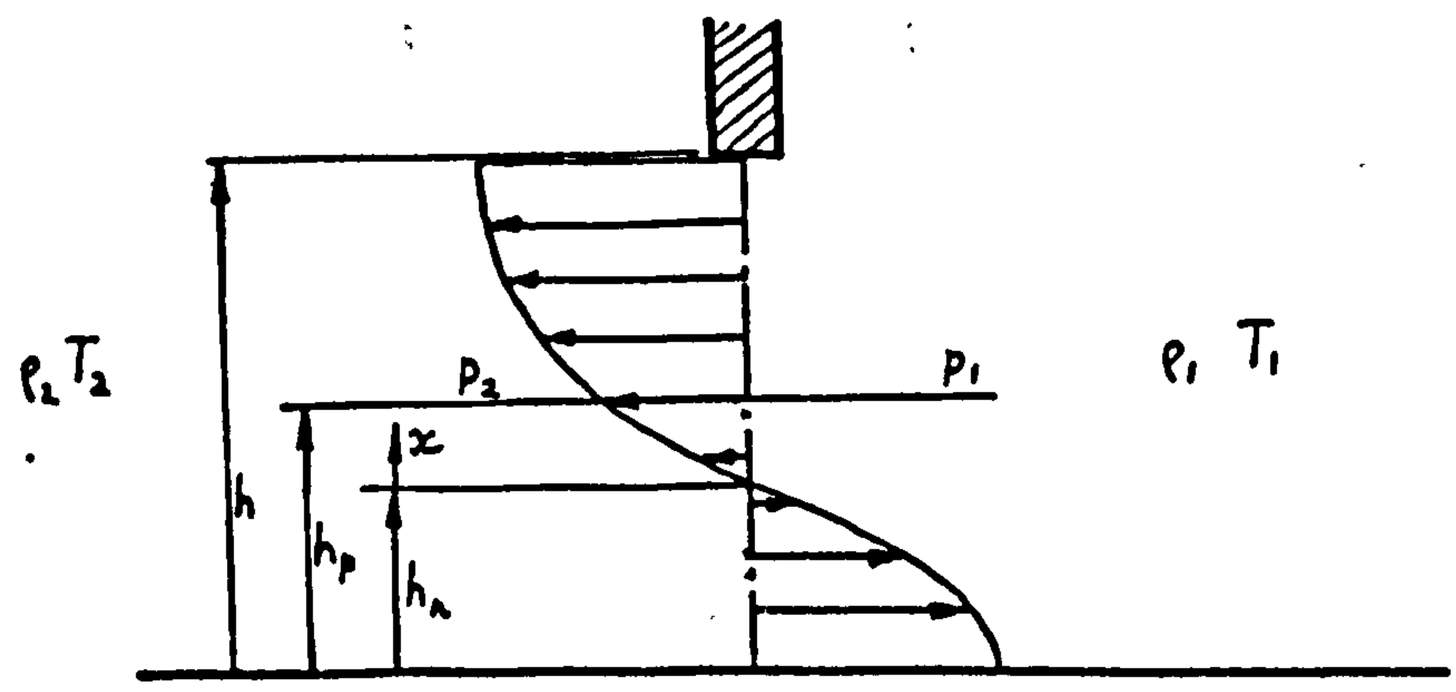

FIGURE 2.8 Bi-directional Airflow Through a Doorway

At an air gap within the structure of a partition, the direction of heat flow is determined before assigning a value to the thermal conductivity of the air layer. Thus the thermal resistance of a horizontal floor containing an air space will be higher for downward heat flow than for upward heat flow.

2.6.2 Conduction Through the Ground

Heat transfer from the space immediately above the ground must have a component of conduction from the ground surface into the bulk of earth below the building, and to the external ground surface. Macey (46), who was concerned with heat loss from brick kilns, derived the following relationships for heat loss per unit length of floor (Figure 2.7).

$$Q = \frac{4kB(t_1-t_2)}{\pi} \tanh^{-1}\frac{r}{R} \qquad 2.67$$

where t_1-t_2 is the inside/outside temperature difference,

r = half the breadth of the space between outside walls.

R = r + half the wall thickness

k is the thermal conductivity of the ground

B is a tabulated function which depends on the length/breadth ratio of the plan area. (Table 2.5)

If we set $T = \frac{\pi r}{2B\tanh^{-1}\frac{r}{R}}$

then $Q = 2rk\frac{t_1 - t_2}{T}$ 2.68

i.e. T is an equivalent thickness for the ground under the building, and can be subdivided into layers and treated as any other partition in the building.

2.7 AIR FLOW CALCULATION

2.7.1 External Surface Pressure Distribution

Before air flow calculations can proceed, the external air pressure distribution on the building surfaces must be determined. Relatively few full scale measurements have been carried out due partly to problems of dealing with rapidly fluctuating wind speeds and direction, and partly due to the expense of large scale monitoring operations. Realisation of the importance of the ground surface roughness on the formation of the atmospheric boundary layer near the ground (28) has led to an increased understanding of the effects of wind on buildings. Wind tunnels are usually used as a means of arriving at pressure distribution data (29). In most cases, the data is expressed as a set of pressure coefficients, one set for each wind direction, such that, at any point i,

$$C_i = \frac{p_i'}{\frac{1}{2}\rho V^2} \qquad 2.69$$

where p_i' is the mean surface wind pressure at that point at the mean wind speed V. The coefficients may reflect any local wind shielding for particular wind directions. The surface pressure used in the program is corrected to account for height, i.e.

$$p_i = p_i' - \rho_o g\, h_i \qquad 2.70$$

where h_i is the height above a reference level.

In this way, all external pressures at interconnections on the external surfaces of the building are evaluated.

Restriction		k	n	a
Cracks	.1	.001	1	
width	.5	.1	.95	crack
mm	2.5	1	.72	length
	5	2	.61	m
	10	8.4	.5	
Openings		.84	.5	opening area m^2

Table 2.6

Value of k and n for equation 2.71

2.7.2 Iterative Relaxation Procedure

Arbitrary initial pressures are assigned to the internal spaces, giving a complete set of pressures for every node in the network of building spaces and interconnections. Iterative adjustment of these pressures is then carried out until the calculated flows through the interconnections balance one another to within $\pm$ .002 m^3/s maximum error for the sums of flows into each space. This adjustment procedure is not carried out using variational calculus techniques, as might seem appropriate.

This type of method produced serious convergence problems and was ultimately abandoned for a more empirical "learning" type of algorithm. The spaces are assigned "boost" factors which are increased or decreased as the sensitivity of flows to pressure variations in each space is determined. The boost factor multiplied by the flow residual becomes the pressure change applied to a space during a cycle of the iterative procedure, when the magnitude of the residual for that space is the maximum of all space residuals. This technique converges rapidly even when combinations of very large and very small air flow resistances occur in close proximity in the air flow network.

2.7.3 Simple Openings

Flows are calculated using equations of the form

$$q = k.a.\ \Delta p^{n} \qquad 2.71$$

where q is the flow rate

k is an empirical coefficient

n is an empirical exponent

Δp is the pressure difference

a is the flow area or crack length.

The values of k and n may not necessarily be fixed. For example Honma (24) developed an empirical equation designed to cover a range of pressure differences across cracks in window components, and including the effect of the transition from laminar to turbulent flow:

$$q = \propto . \ell . \Delta p^{1/\beta} \qquad 2.72$$

where α is an empirical constant,

$$\beta = 2 - exp(-5\alpha\Delta p)$$

Where precise information on crack dimensions is available, and particularly precise flow estimates are required, this equation can be used in place of equation 2.71. However, to reduce the amount of computation for ordinary ventilation problems, the values in Table 2.6 are normally used in equation 2.71.

2.7.4 Large Vertical Openings

If a temperature difference exists across a large vertical opening such as a doorway, flows of air can occur in both directions through the doorway due to the action of small density variations over the height of the doorway. (Figure 2.8).

Shaw (47) studied this phenomena in relation to the isolation of contamination in hospital intensive care rooms, with and without forced air flow through the doorway. His theory was not sufficiently developed for use in a general application and a more universal procedure is required.

We assume that at any height, the flow through the doorway is proportional to the square root of the pressure difference, i.e.

$$dq = C_d\, w\, dx \sqrt{\frac{2\Delta p_x}{\rho}} \qquad 2.73$$

where C_d is a coefficient of discharge

w is the door width

$\Delta p_x = p_1 - p_2$ = the pressure difference at height x

ρ is the mean air density.

If we take x = 0 at the neutral height, i.e. where the pressure difference is zero, then

$$P_1 = P_2 = P_n \quad \text{when } x = 0 \text{ and,}$$

$$P_1 = P_n - \rho_1 g x$$

$$P_2 = P_n - \rho_2 g x \qquad 2.74$$

where ρ_1 and ρ_2 are air densities,

g is the gravitational constant.

Now;

$$\rho_1 = \frac{P}{RT_1} \qquad \rho_2 = \frac{P}{RT_2} \qquad 2.75$$

where p is mean atmospheric pressure

T_1 and T_2 are absolute air temperatures,

R is the gas constant,

$$\text{so, } \Delta p_x = \frac{g P x}{R}\left(\frac{1}{T_2} - \frac{1}{T_1}\right) \qquad 2.76$$

Now, if we assume the pressures at height h_p are known to be $p_1 = P_1$ $p_2 = P_2$

then at this height, i.e. $x = h_p - h_n$,

$$\Delta p_x = P_1 - P_2$$

$$= \frac{g P(h_p - h_n)}{R}\left(\frac{1}{T_2} - \frac{1}{T_1}\right)$$

$$\text{so } h_n = h_p - \frac{P_1 - P_2}{\frac{gP}{R}\left(\frac{1}{T_2} - \frac{1}{T_1}\right)} \qquad 2.77$$

Now, if we define $r_n = \frac{h_n}{h}$, $r_p = \frac{h_p}{h}$

and $C_t = \frac{gPh}{R}\left(\frac{1}{T_2} - \frac{1}{T_1}\right)$

then $r_n = r_p - \frac{P_1 - P_2}{C_t}$ 2.78

This equation allows the neutral height to be explicitly determined, and is used when substituting the limits of integration to obtain the flows through the opening above and below the neutral height.

Thus, from equation 2.73

$$q = \int_{-h_n}^{h-h_n} B\, w \sqrt{\frac{gPx}{R}\left(\frac{1}{T_2} - \frac{1}{T_1}\right)}\, dx \qquad 2.79$$

where $B = C_D\sqrt{\frac{2}{\rho}}$

$$\therefore\ q = \frac{2}{3} B\, w \sqrt{C_t}\left[(h-h_n)^{\frac{3}{2}} - (-h_n)^{\frac{3}{2}}\right]$$

$$= \frac{2}{3} B\, w\, h \sqrt{C_t}\left\{\left[\frac{(1-r_p)C_t + (P_1-P_2)}{C_t}\right]^{\frac{3}{2}} - \left[\frac{(P_1-P_2) - r_p C_t}{C_t}\right]^{\frac{3}{2}}\right.$$

$$= \frac{2}{3} B\, A \left(C_a^{\frac{3}{2}} - C_b^{\frac{3}{2}}\right)/C_t \qquad 2.80$$

where A = door opening area,

$$C_a = (1 - r_p)\, C_t + (P_1 - P_2)$$

$$C_b = (P_1 - P_2) - r_p C_t$$

On evaluation this equation yields a sum of real and imaginary parts. Real parts indicate the flow in the positive direction (from 1 to 2). Imaginary parts represent the flow in the negative direction (from 2 to 1).

If C_t is near zero, an approximate equation is used to avoid division by C_t

$$q = BA(P_1-P_2)^{\frac{1}{2}}\left[1+\frac{1}{4}\cdot\frac{C_t}{(P_1-P_2)}\cdot(1-2r_p)\right] \qquad 2.81$$

This is either real or imaginary, depending on the sign of (P_1-P_2), with the same consequence as above.

2.8 SPACE TEMPERATURE CALCULATIONS

Having determined all room surface heat flows and air flows, the net space heat flows and hence temperatures can be determined. The net space heat flow for a space is the algebraic sum of the surface heat flows to that space, plus the heat content of the air entering the space, less the heat content of the air leaving the space. The total quantity of air in the space is heated (or cooled) by this amount, and the resultant temperature increase (or decrease) is readily computed. Unfortunately, due to the relatively low heat capacity of air, oscillations may result during periods of high heat inputs. To avoid this risk, and to some extent allow for the variations in surface heat flows as room air temperature changes, a modified heat flow is used in the calculation of new space temperatures. This procedure is similar to the one which calculated a modified surface heat flow for the interconnection heat flow calculations.

A linear relationship between net space heat flow and air temperature is assumed, and Figure 2.6 can be used again. Therefore,

$$\frac{t_f - t_n}{h_f - h_n} = \frac{t_n - t_p}{h_n - h_p} \qquad 2.82$$

Also,

$$C_p m (t_f - t_n) = \frac{h_n - h_f}{2} \Delta t \qquad 2.83$$

where C_p is the specific heat of air

m is the mass of air in the space

Δt is the time interval.

Equation 2.83 states that the temperature rise $t_f - t_n$ is determined by the mean heat flow $\frac{h_n + h_f}{2}$

So

$$\frac{h_f + h_n}{h_f - h_n} \cdot \frac{\Delta t}{m C_p} = 2 \frac{t_n - t_p}{h_n - h_p} \qquad 2.84$$

Now if $k_1 = \frac{\Delta t}{m C_p}$ and $k_2 = 2 \frac{t_n - t_p}{h_n - h_p}$

then $$t_f = t_n + h_n \left(\frac{k_1 k_2}{k_2 - k_1} \right) \qquad 2.85$$

If $t_p = t_n$ then $k_2 = 0$, so h_n is set constant, and

$$t_f = t_n + \frac{\Delta t \, h_n}{m C_p} \qquad 2.86$$

If $h_p = h_n$, k_2 is infinite, but t_f tends to become $(t_n + h_n k_1)$ which is the same as equation 2.86.

Mean radiant temperatures for each space are calculated as the fourth root of the area weighted mean of the fourth power of the surface temperatures. A thermostat response temperature is calculated as

$$t_r = 0.85t_a + 0.15t_m \qquad 2.87$$

where t_r is the response temperature

t_a is the room air temperature

t_m is the room mean radiant temperature.

These figures resulted from tests carried out by Baxter and Longworth on room air thermostats (48). This temperature is then used in the following time step to determine the switching of heaters controlled by air thermostats.

Summary of Chapter 2

The entire chapter is a description of the algorithms and procedures used to calculate air temperatures, fabric temperatures, heat flows and air flows in a building, and the methods used to link these calculations to enable step by step simulation of the behaviour of a building. Although all the physical processes that determine building performance have been included, the effects of building occupancy have been omitted. These are discussed in Chapter 6.

CHAPTER 3

MEASUREMENTS AT THE TEST HOUSE

3.1 DESCRIPTION OF THE HOUSE

The house in which measurements were taken to assess thermal performance was situated at St. Leonard's, East Kilbride. This house was a staggered terrace type on two levels, (Fig. 3.1). There are a living room and separate kitchen downstairs, opening on to a common hall which runs the full depth of the house, with both front and back doors opening onto it. Upstairs there are three bedrooms and a bathroom. The front and back wall construction consists of timber framing with plasterboard mounted internally, 25mm glass fibre insulation in the cavity, and external claddings of asbestos sheeting downstairs and cedar boarding upstairs. Dry lining partitions separate the internal spaces, and the party walls between houses are of cavity brick construction. The roof space is insulated with 50mm of glass fibre between rafters. Figure 3.2 and Table 3.1 detail the actual construction.

Wall mounted direct electric convector heaters are installed in the rooms with outputs as given in Table 3.2. One time switch controlled the downstairs heaters, and was set to switch on at 7.00 hours, and off at 23.00 hours. A thermostat in the living room controlled all the downstairs heaters and was set at 20^{o}C nominally. Another time switch controlled the upstairs heaters, and was set to switch on at 22.00 hours, and off at 8.00 hours. The upstairs heaters each had an output control of the "simmerstat" type.

The house was unoccupied for the duration of the tests.

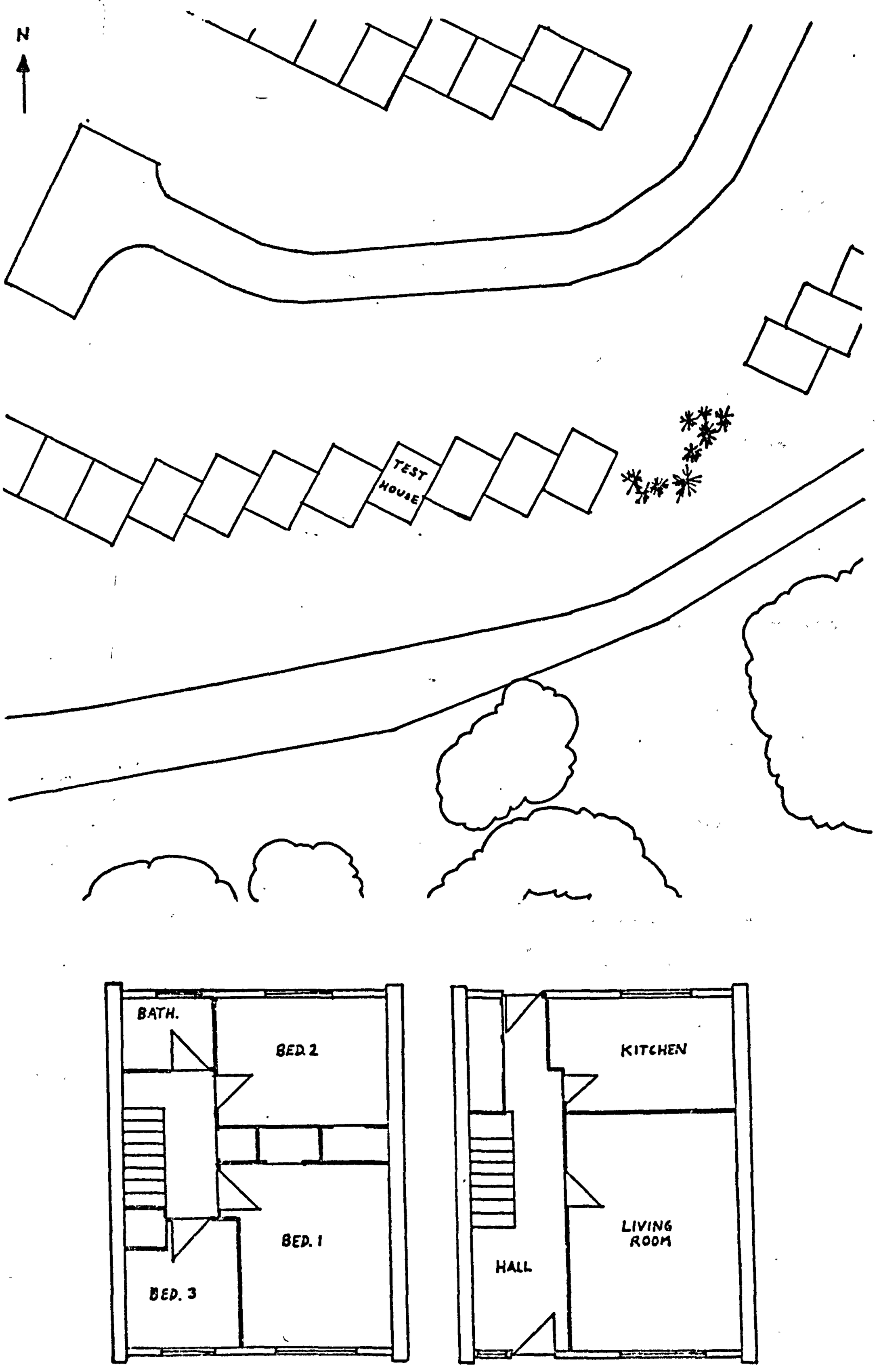

FIGURE 3.1 Site Layout and Lower and Upper Floor Plans of Test House

Figure 3.2: Test House Construction Details.

Roof

Selected concrete tiles on
1½" x 1½" battens on
untearable roofing felt on
1½" x ¾" counter battens on
30 lb roofing felt on
⅜" gyproc sarking.
Roof truss formed with 4 x 1½" rafters -
4 x 1½" struts and ties
4 x 1½" ceiling joists
2" x 2" ceiling binders
truss members connected by
patent toothed metal plates each side
2" fibre glass insulation
½" taper jointed plaster board

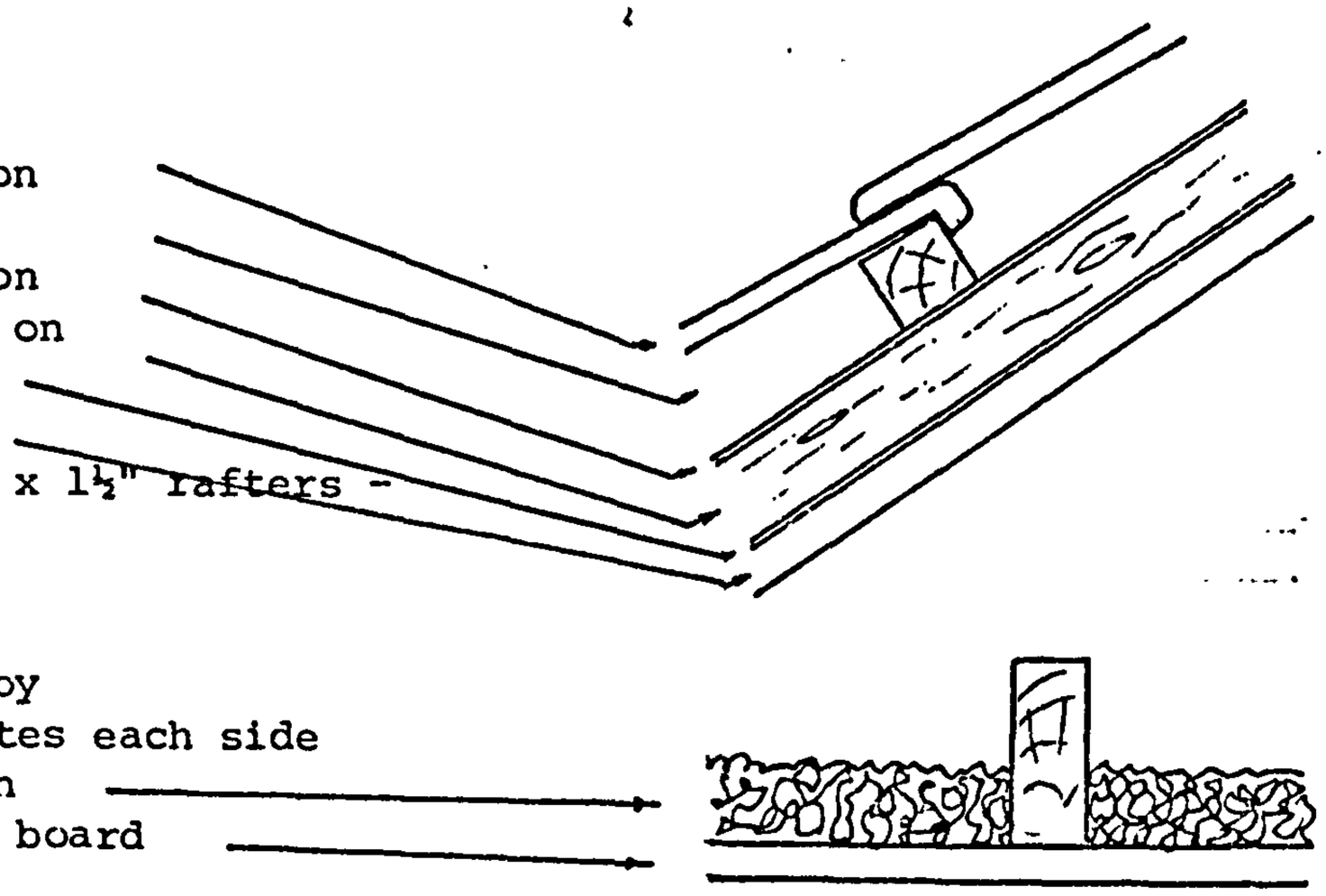

Mid Floor

13/16" t. & g. flooring on
8" x 2" joists at 18" centres
⅜" taper jointed plaster board

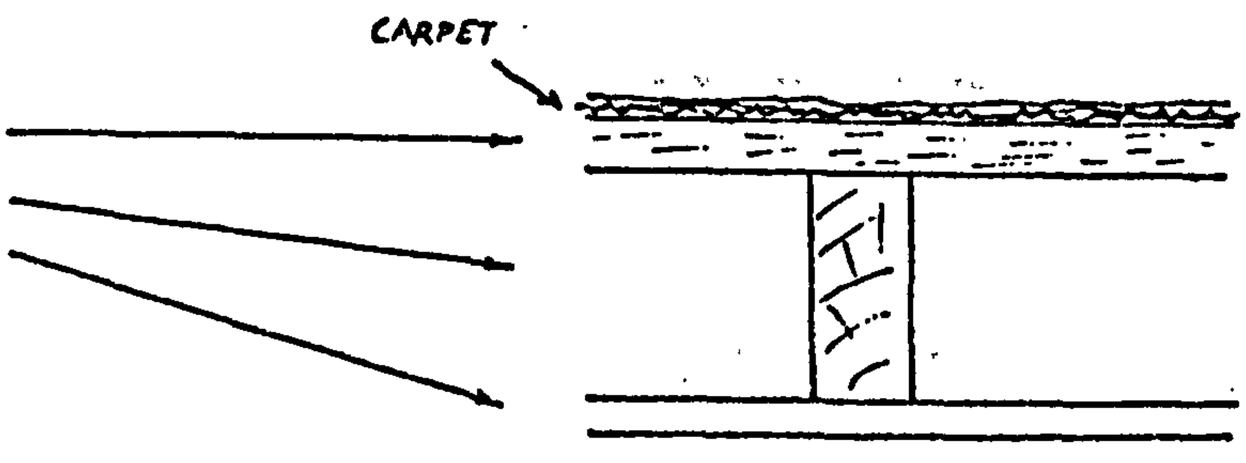

Ground Floor

13/16" t. & g. flooring on
4" x 2" joists at 18" centres
4" x ¾" wall plates on DPC on
4½" brick sleeper walls

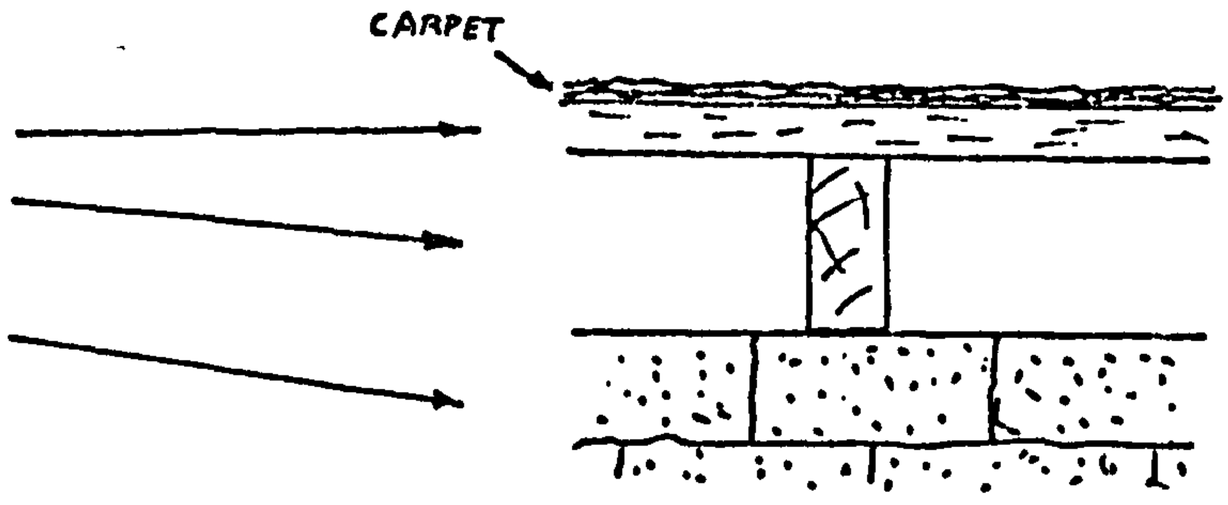

Solum Finish

½" asphalt on 3" ashes

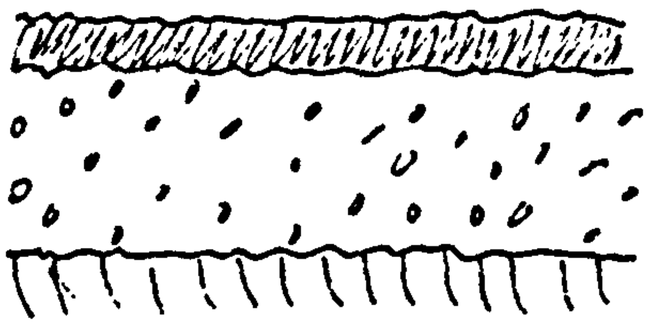

Gable Walls

11" cavity brick with outer leaf
selected facing brick.

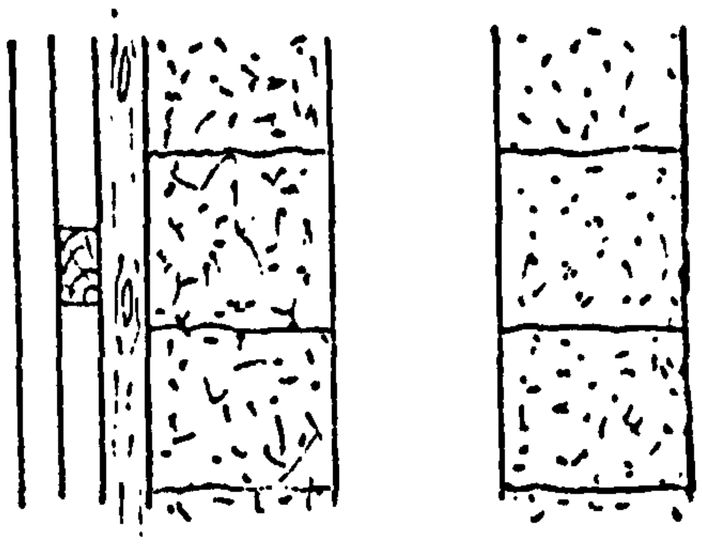

Party Walls

11" cavity brick
Internal finish to gable and party walls:-
⅛" Taper jointed plaster board on
1½" x ¾" vertical battens at 16" centres on
1" x ¼" horizontal battens at 16" centres,
Dooked to brick work

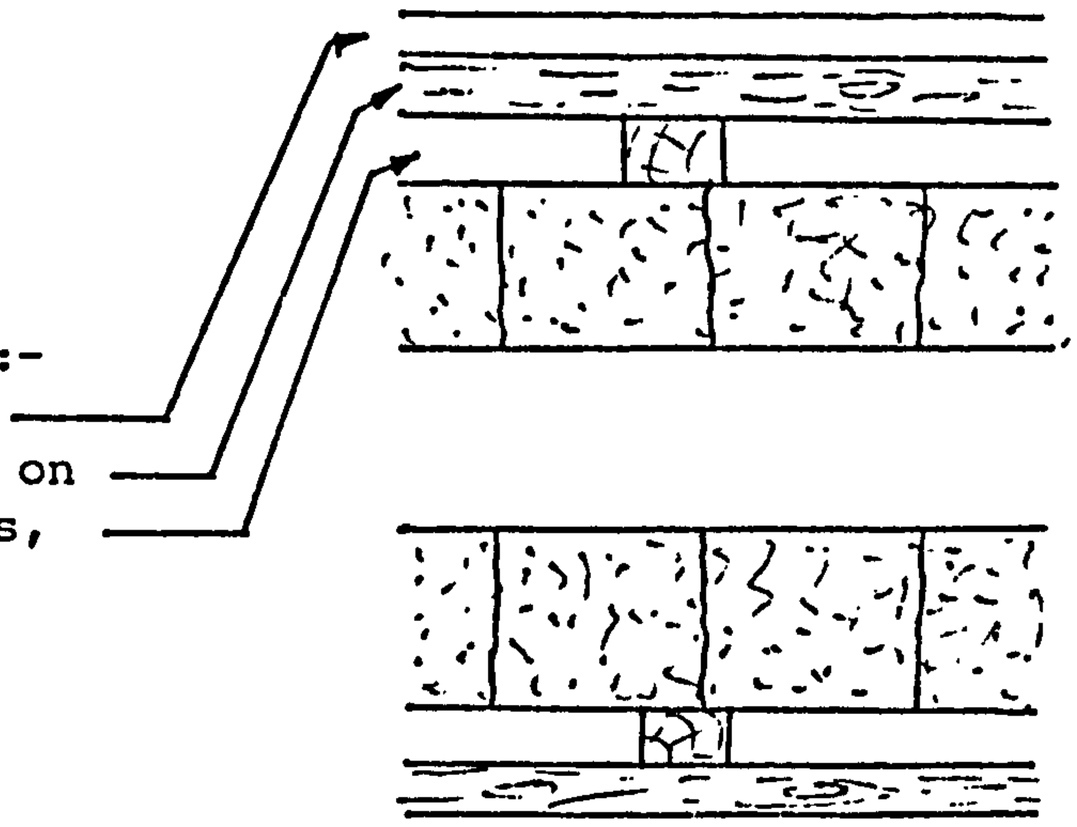

External walls, upper floor

7/8" V-jointed cedar boarding on
1" x ¾" counter battens on
"Ibeco" craft breather type building paper No. 80
3" x 2" framing with 1" fibre glass insulation
polythene vapour barrier
½" taper jointed plaster board

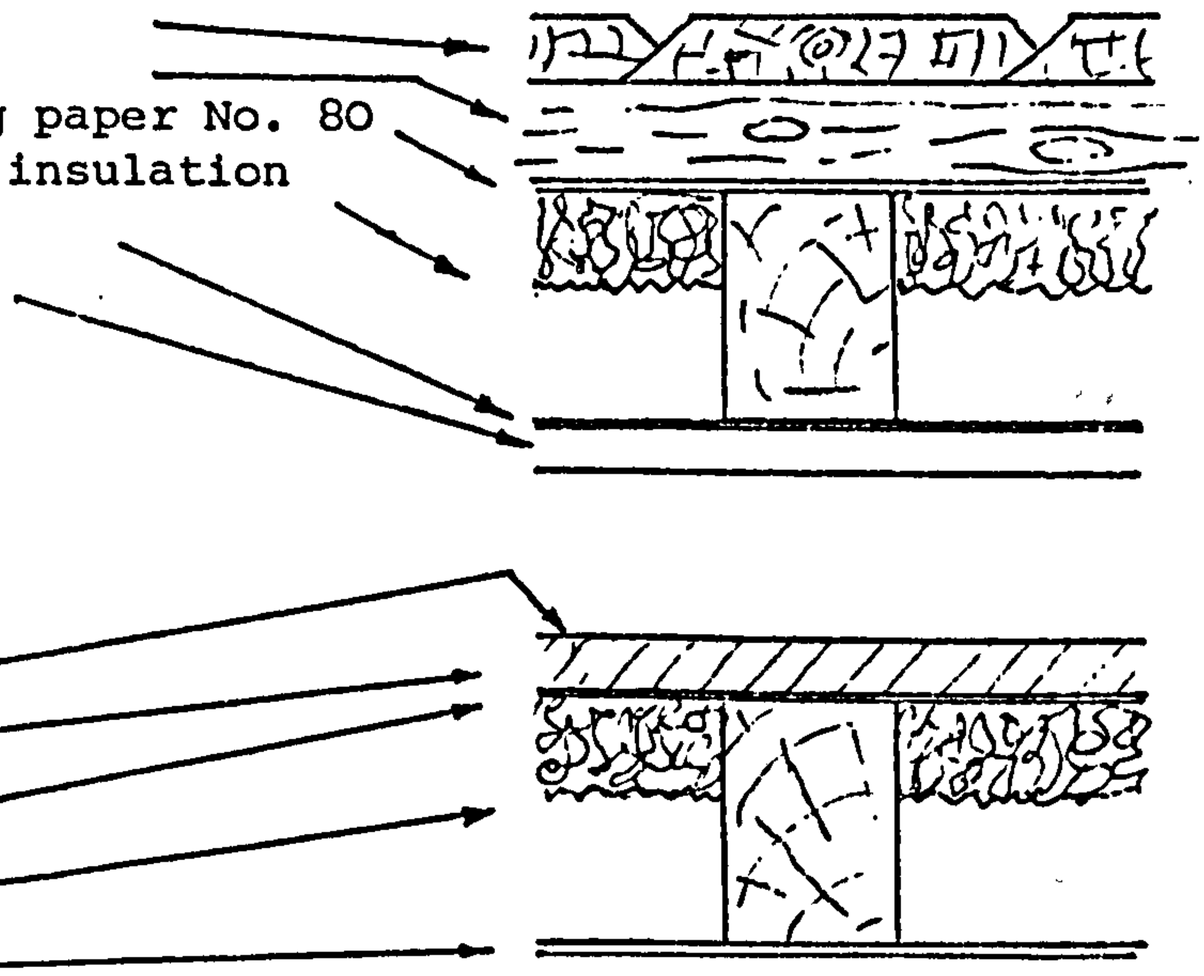

External walls, Lower floor

2 coats heavy duty "co-seal" on
¼" Asbestos sheeting on
0.001 polythene D.P.C. membrane on
3" x 2" framing with
1" fibre glass insulation
polythene vapour barrier
⅛" taper jointed plaster board.

	Thickness mm	Thermal Conductivity W/mC	Density kg/m^3	Specific Heat kJ/kgC	Resistance m^{2}C/W
Roof					
Concrete tiles	12	1.4	2100	.65	.01
Airspace	39	-	-	-	.06
Roofing felt	.5	.19	960	-	.003
Airspace	19	-	-	-	.09
Roofing felt	.5	.19	960	-	.003
Gyproc sarking	10	.19	1600	.84	.05
Ceiling					
Glass fibre insulation	50	.04	25	.66	1.25
Plasterboard	13	.19	1600	.84	.07
Mid Floor					
Carpet	13	.045	55	2.0	.30
Floor boards	21	.14	600	3.3	.15
Airspace	102	-	-	-	.03
Plasterboard	10	.19	1600	.84	.05
Ground Floor					
Carpet	13	.045	55	2.0	.29
Floor boards	21	.14	600	3.3	.15
Solum					
Asphalt	13	.5	1700	1.7	.03
Ashes	76	.07	700	.84	1.1
Soil	2870	.7	1300	.84	4.2
Gable Wall					
Plasterboard	10	.19	1600	.84	.05
Airspace	38	-	-	-	.19
Brickwork	114	.62	2600	.84	.18
Airspace	50	-	-	-	.10
Brickwork	114	.96	2000	.84	.12
Party Wall					
Plasterboard	10	.19	1600	.84	.05
Airspace	38	-	-	-	.19
Brickwork	114	.62	2600	.84	.18
Airspace	50	-	-	-	.18
Brickwork	114	.62	2600	.84	.18
Airspace	38	-	-	-	.19
Plasterboard	10	.19	1600	.84	.05
External Wall, Upper Floor					
Plasterboard	10	.19	1600	.84	.05
Airspace	39	-	-	-	.14
Fibreglass	25	.04	25	.66	1.6
Airspace	19	-	-	-	.18
Cedar boarding	22	.14	600	3.3	.16
External Wall, Lower Floor					
Plasterboard	10	.19	1600	.84	.05
Airspace	39	-	-	-	.14
Fibreglass	25	.04	25	.66	1.6
Asbestos sheeting	6	.16	2500	1.05	.04

Table 3.1
Thermal Properties of Test House Construction

Room	Rated Output kw	Actual Output kw
Living Room	3.5	3.10
Kitchen	1.0	0.89
Hall	2.0	1.77
Bedroom A	1.0	0.98
Bedroom B	1.0	0.92
Bedroom C	1.0	0.85

Table 3.2

Electric Convector Heater Measured Outputs

3.2 THE MEASURING SYSTEM

3.2.1 Air Temperatures

Air temperature measurements were taken at the geometric centre of each room or space using copper-constantan calibrated thermocouples connected to a twenty channel potentiometric chart recorder with built in cold junction compensation. Two measuring points were fixed at each end of the hall and one at the upstairs landing. In addition one thermocouple was installed externally on the roof, in a position shaded from direct solar radiation.

A reference temperature was provided by an automatic $0^{o}C$ cold cell, connected to one channel of the recorder. More detailed temperature measurements were carried out in the living room. (Figure 3.3). Nine thermocouples were deployed here to obtain a complete cross-section of temperatures in this room.

Each internal thermocouple was shielded from radiation effects by a 15cm. diameter cylinder of aluminium foil (Figure 3.4) and additional shielding was provided for those thermocouples likely to be exposed to direct solar radiation.

Complete scans of the thermocouple inputs were initiated every ten minutes. Each scan was completed in twenty seconds and recorded by the chart recorder. Accuracy of temperature measurements was better than $\pm$ 0.5 C.

3.2.2 Electrical Consumptions

Current consumptions of the heaters were measured using Ferranti clip-on current transformers, and their outputs were recorded on chart recorders. The ammeter

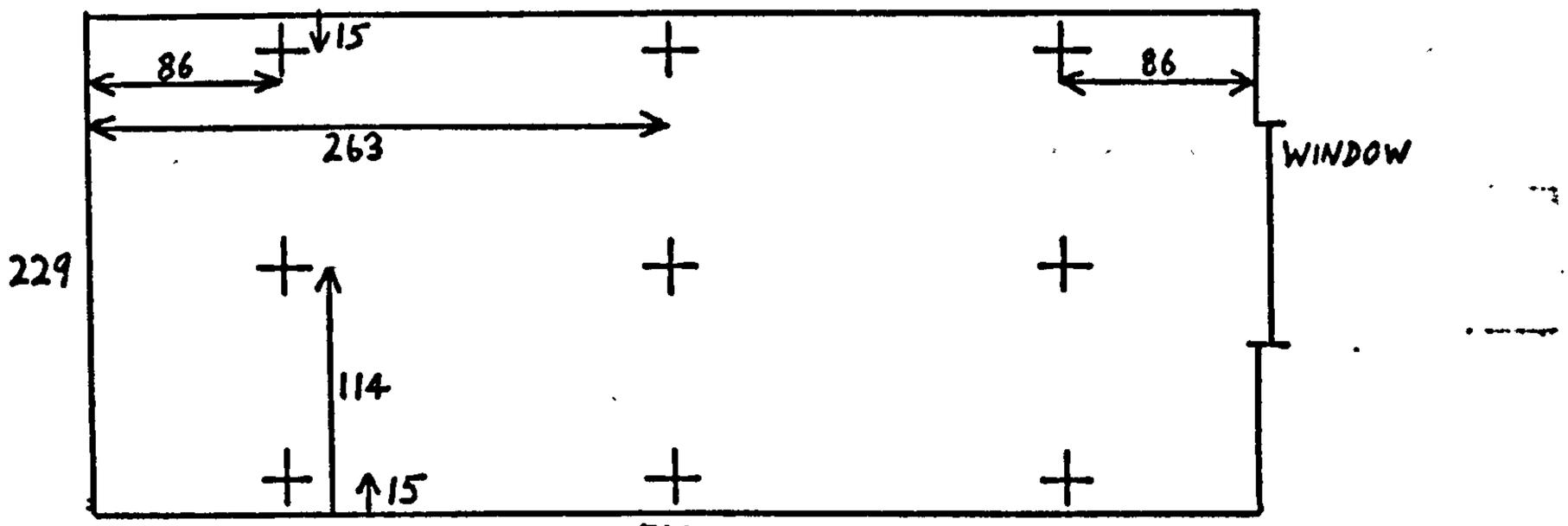

514

FIGURE 3.3 Vertical Cross-Section Through Living Room Showing Thermocouple Positions

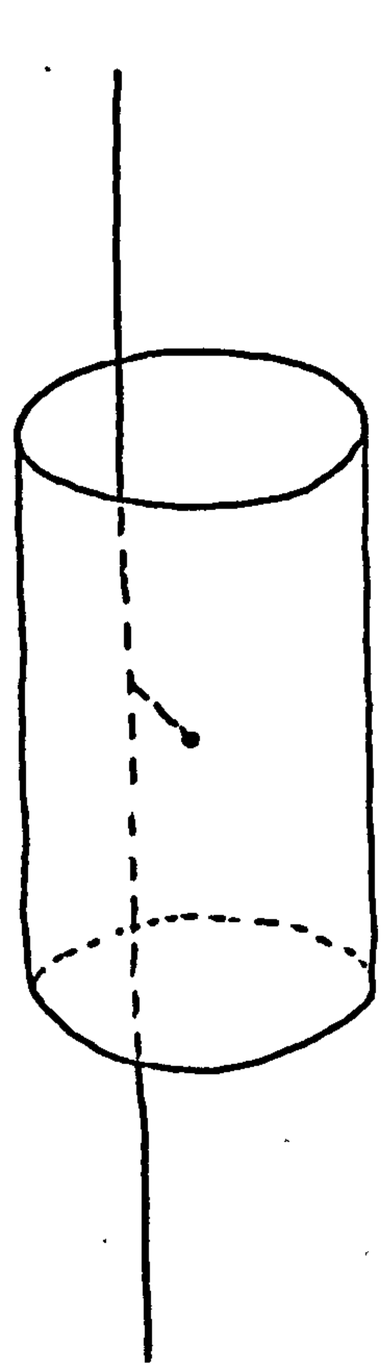

FIGURE 3.4 Thermocouple Radiation Shield

readings were not particularly accurate, but knowing the heater ratings, and the supply voltage, which did not vary appreciably from 240V, the heater consumptions could be estimated to within $\pm$ 5%.

3.2.3 Solar Radiation

Solar radiation was measured using a Moll-Gorczynski solarimeter, mounted above roof height in a horizontal plane. This was connected to a potentiometric chart recorder which provided a continuous record of solar radiation falling on a horizontal surface. The solarimeter was calibrated at the Electricity Council Research Centre, at Capenhurst, and its estimated accuracy is about $\pm$ 5% at solar altitudes above 15^{o}.

3.2.4 Ventilation

Ventilation rates in the various rooms in the house could not be monitored continuously, and a separate programme of manual measurements was organised to obtain some data on ventilation. From previous experience the tracer gas decay method was chosen for carrying out these measurements. A small quantity of nitrous oxide gas is released into the space under test, and is thoroughly mixed with the room air. This is not difficult in an empty room devoid of furniture and fittings. A pump draws air continuously through an infra-red gas analyser which measures the concentration of gas in the air. Mixing of the room air continues for the duration of the tests. An exponential decay of gas concentration is obtained, from which the fresh air ventilation

rate may be determined, i.e.

$$C_t = C_o e^{-\frac{t}{T}} \qquad 3.1$$

where C = gas concentration at time t

C_o = initial gas concentration

T = decay rate time constant, the time for one complete fresh air change

and "ventilation rate" = $\frac{q}{V} = \frac{1}{T}$ 3.2

where q is the rate of addition of fresh air

V is the room volume.

3.2.5 Meteorological Data

In order to provide input for the computer model, data on wind speed and direction was required. Fortunately this was readily available from the Building Research Establishment, Scottish Laboratory, which was situated about 1 mile from the test house.

3.3 RESULTS OF MEASUREMENTS

From the available data a period of four days from the 12th to 15th March was chosen for the comparison with the computer model. Of this period, only the last day was considered in detail. This ensures that all transient effects due to the previous three days conditions are modelled, and eliminates residual effects due to the arbitrary starting conditions. Data could only be collected for a few months, and therefore additional comparisons at different seasons were not possible. Appendix 3 is a record of the temperatures measured at each measuring point for the 15th March. Only one vertical set of living room points is included, as the horizontal variations in temperature were very small. Figure 3.5 presents this data graphically for selected measuring points. On the same graph, the electricity consumptions are shown, and Table 3.3 gives hourly totals of electricity consumptions. Solar radiation measurements are also plotted on Figure 3.5. A check on the external temperature measurements over the four-day period was carried out by comparing these with hourly thermograph measurements at the B.R.E. station nearby. (Figure 3.6). These show good agreement, considering the difference in instruments and sitings.

It is worthwhile pointing out some major features of the performance of this house and associated heating system. It can be seen that considerable variations in internal temperature take place while the heating is switched on, especially in the living room. The temperature here cycles with a typical period of 15 minutes. This is due to the excessive heat output from the electric heaters. The living

TEXT BOUND INTO

THE SPINE

Figure 3.5 One Day's Measurements in Test House - 15.3.76

Hour	Living Room kwh	Kitchen kwh	Hall kwh	Bedrooms kwh	
0				.7	
1				.8	
2				.6	
3				.6	
4				.8	
5				.8	
6				.8	
7	2.8	.8	1.6	.9	
8	1.8	.5	1.0	.1	
9	1.8	.5	1.0		
10	1.2	.4	.7		
11	1.2	.3	.7		
12	1.3	.4	.7		
13	1.2	.4	.7		
14	1.2	.3	.7		
15	1.2	.3	.7		
16	1.2	.4	.7		
17	1.2	.4	.7		
18	1.2	.3	.7		
19	1.2	.4	.7		
20	1.2	.3	.7		
21	1.2	.4	.7	.1	
22	1.3	.4	.7	.8	
23	0.1		.1	.6	
					Total
Total	22.3	6.5	12.8	7.6	49.2

Table 3.3

Hourly Electricity Consumptions in the Test House - 15.3.76

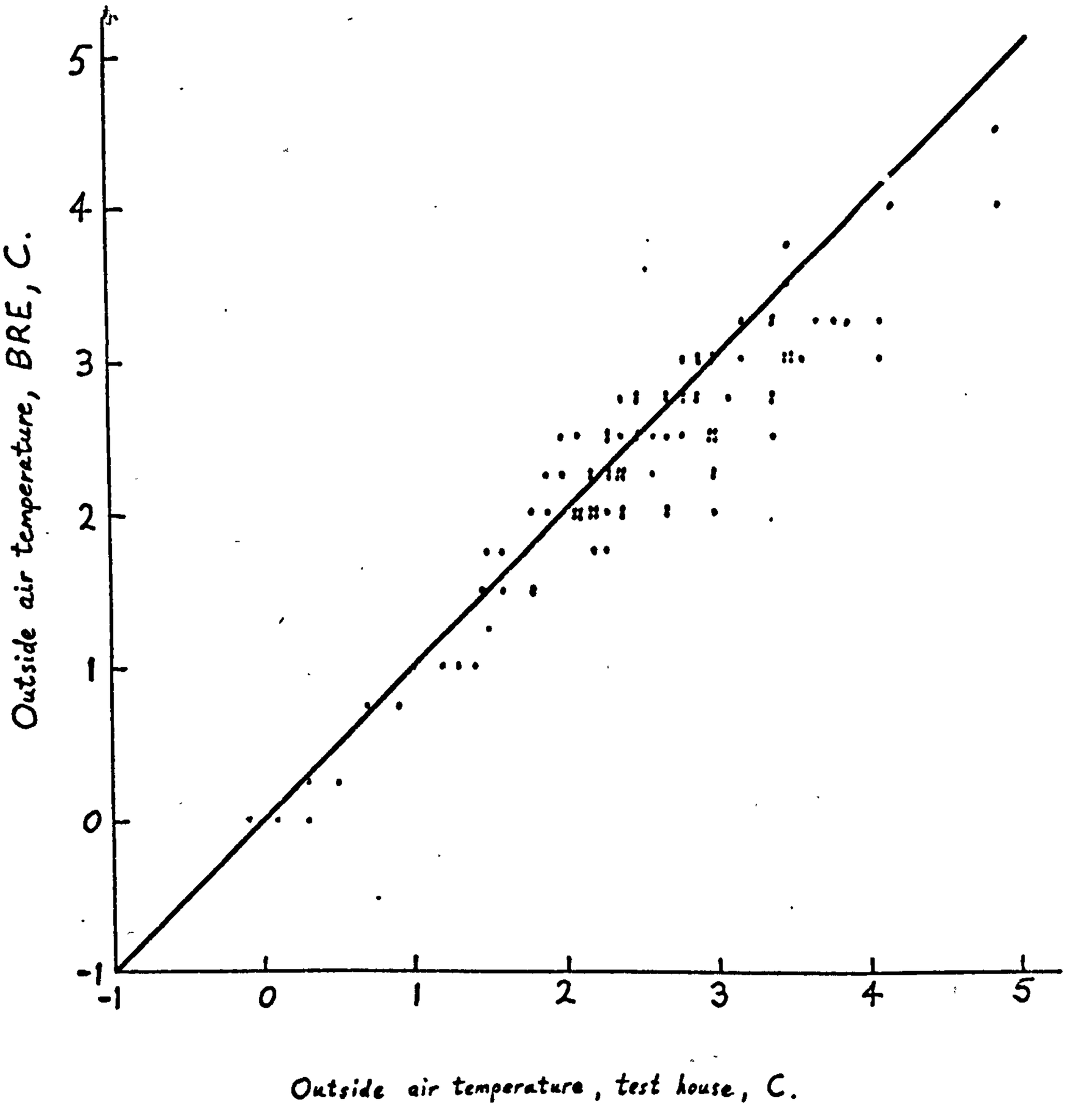

FIGURE 3.6 Comparison Between Site and B.R.E. Outside Temperature Measurements

room thermostat provides only on/off control and cannot respond quickly enough to the rapid rise in air temperature caused by the instant direct heat input. The thermal stratification caused by the high temperature leaving these heaters leads to very high ceiling temperatures accompanied by low floor temperatures. A maximum difference in temperature over the height of the room of 10 C is typical.

The ventilation measurements are detailed in Table 3.4.

Attempts to correlate wind with ventilation rate are only meaningful in the living room and hall, where sufficient data was obtained. The living room ventilation rates did not correlate with wind speed or direction in any obvious manner. This room was well sealed against infiltration, the mean ventilation rate being only ½ air change per hour. The windows were normally kept closed but were opened for short periods during the ventilation tests to disperse residual tracer gas prior to a further release and decay rate measurement of tracer gas in the house. This may have altered the window air-tightness between measurements and this could have contributed significantly to the variations in infiltration in this room. Temperature effects would also cause variations due to stack effect in the house.

The hall ventilation rates were much more likely to be wind induced, due to the situation of two doors at either end of the hall. To test this hypothesis, ventilation rates in the hall were plotted (Figure 3.7) against a combined wind speed/direction function,

$$f = V \times \frac{\cos 2d + 2}{3} \qquad 3.3$$

where V is the wind speed
d is the wind direction.

		Ventilation rate air ch./hour	Wind Speed knots	Wind Direction degrees fr. N
Living Room		.13	5	190
		.28	10	220
		.31	0	-
mean	.46	.35	9	210
s.d.	.19	.36	9	210
		.36	5	270
		.45	15	300
		.56	5	50
		.65	7	270
		.65	8	260
		.70	8	230
		.74 .76	6 13	60 90
Kitchen		.94	5	300
		1.09	7	260
mean	1.89	1.74	14	270
Hall		.76	7	260
		1.09	7	260
mean	2.03	1.20	9	260
s.d.	.95	1.62	7	220
		1.68	13	260
		2.03	8	190
		2.31	15	300
		2.71	5	120
		3.13	9	200
		3.74	28	240
Bedroom A		.55	9	270
		.66	7	260
mean	.69	.85	14	150

Table 3.4

Measured Ventilation Rates
in Test House

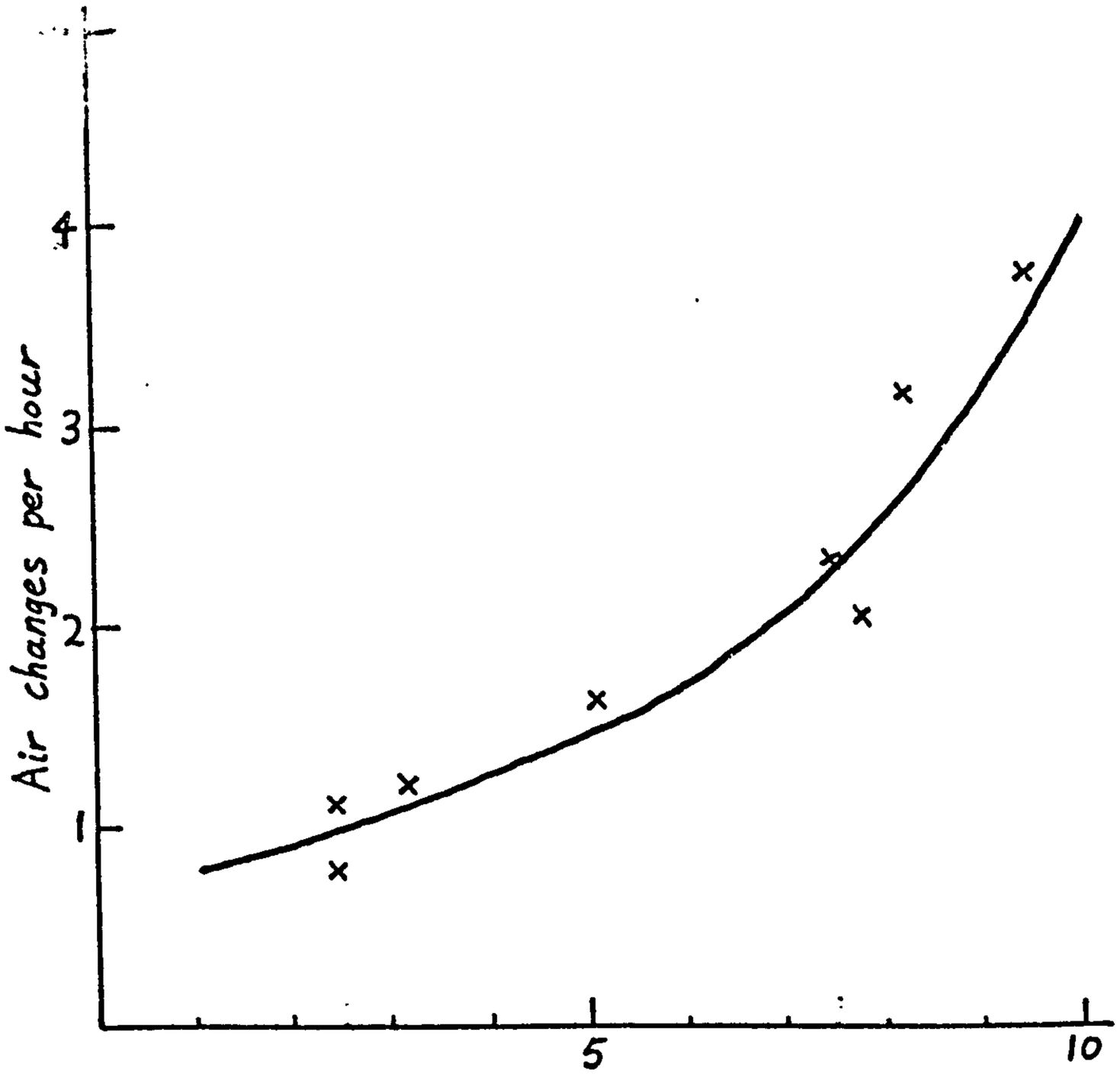

FIGURE 3.7 Hall Ventilation Rate, as a Function of Wind Speed and Direction

The wind speed multiplying factor is unity when the wind blows normal to the line of staggered terraced houses, i.e. when maximum pressure difference occurs, and has a minimum value of one third when the wind is parallel to the line of houses. It can be seen from the figure that a definite relationship exists between wind and ventilation rate, but again, other factors are clearly at work.

Summary of Chapter 3

Measurements of temperatures, electricity consumption, solar radiation and ventilation rate were made at an unoccupied test house. Measurements of wind speed and direction were obtained from a nearby meteorological station. Detailed measurements are presented for the day of the 15th of March 1976.

CHAPTER 4

THE PERFORMANCE OF THE COMPUTER MODEL

4.1 MODEL OF TEST HOUSE

In order to obtain a detailed comparison between the computer calculations and the actual building, a fairly detailed model of the test house described in the previous chapter was set up. Figure 4.1 shows the geometry of the model and the composition of the building. Table 3.1 gives details of the thermal properties of each fabric component. The complete air flow network is shown diagrammatically in Figure 4.2 and the various crack widths and lengths assumed for air permeable interconnections are given in Table 4.1. To reduce the size of the network, the several leakage paths through a facade are agglomerated into one representative crack, and where deliberate openings are provided that swamp the effect of the cracks, those other cracks are neglected. The complete set of input data is listed in Appendix 4. This is input to a pre-processing program which abstracts the constructional details represented in Figure 3.2 from component data files, and also pre-calculates the angle factors. The secondary input data thus generated is also listed in Appendix 4.

The heater outputs used are in fact less than those installed at the test house. The reason for this reduction was because the computer program could not cope with the very high heat input to the room air, with the existing five minute time step. This will be discussed more fully later.

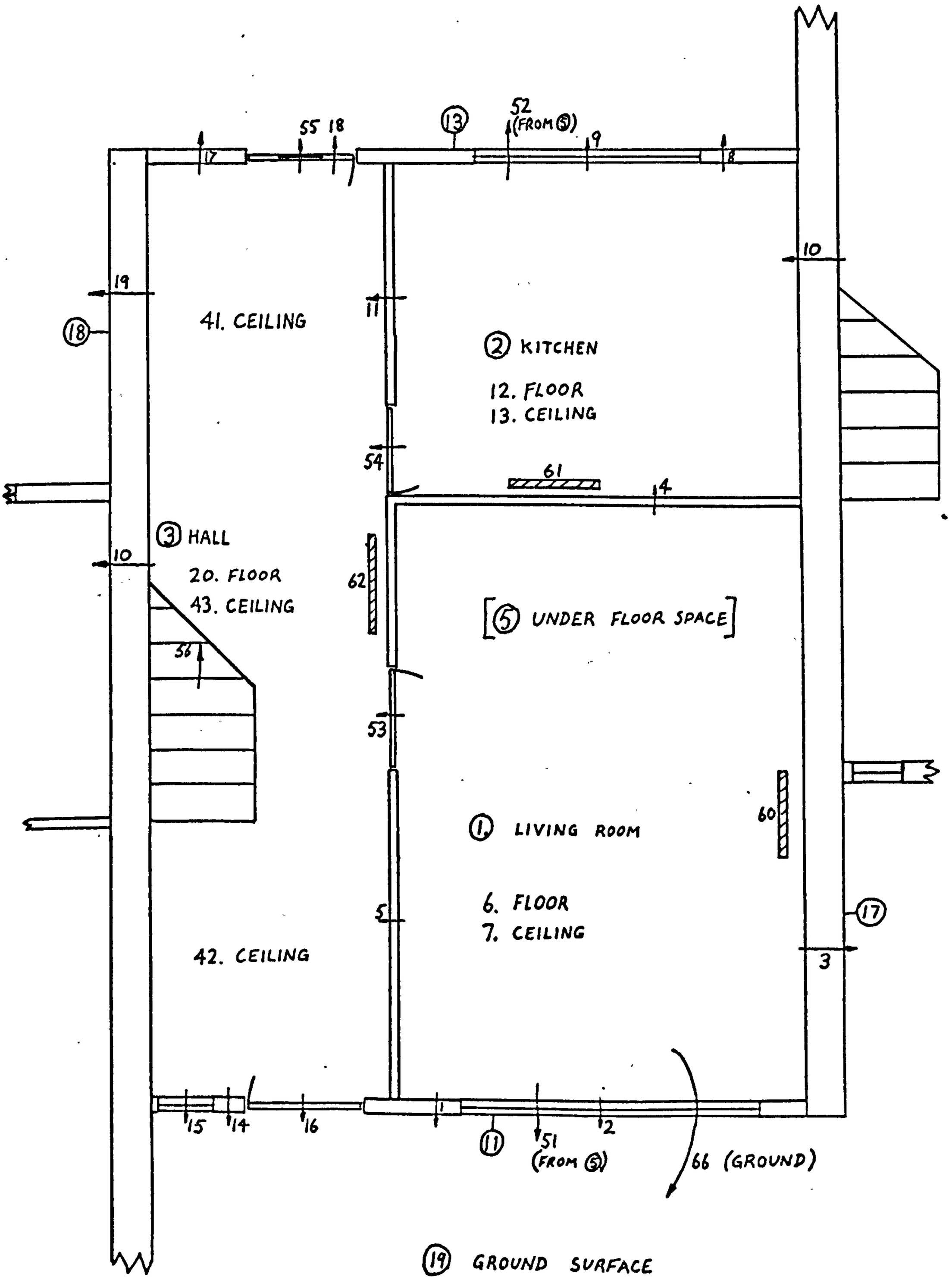

FIGURE 4.1 Model of Test House

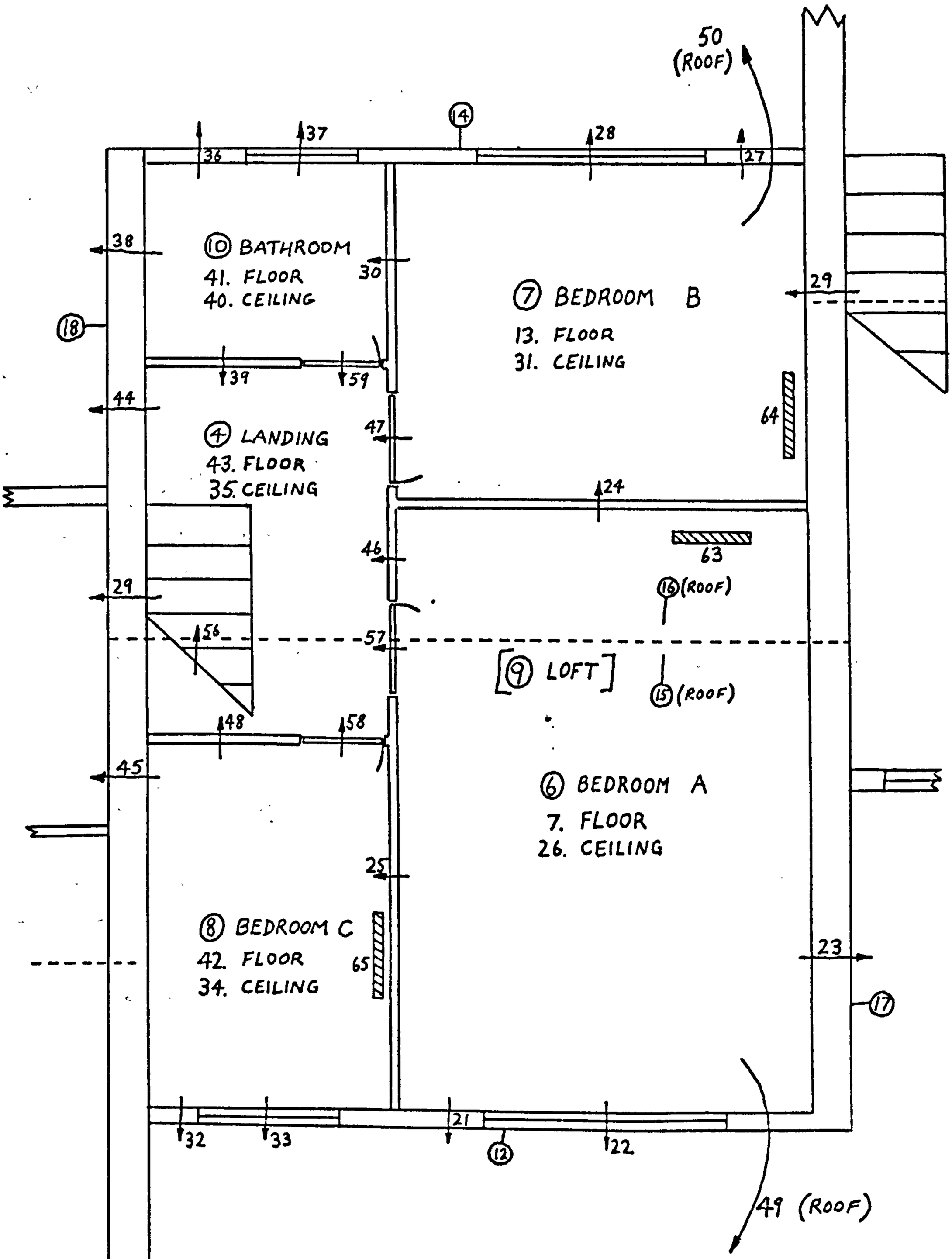

FIGURE 4.1 (contd.)

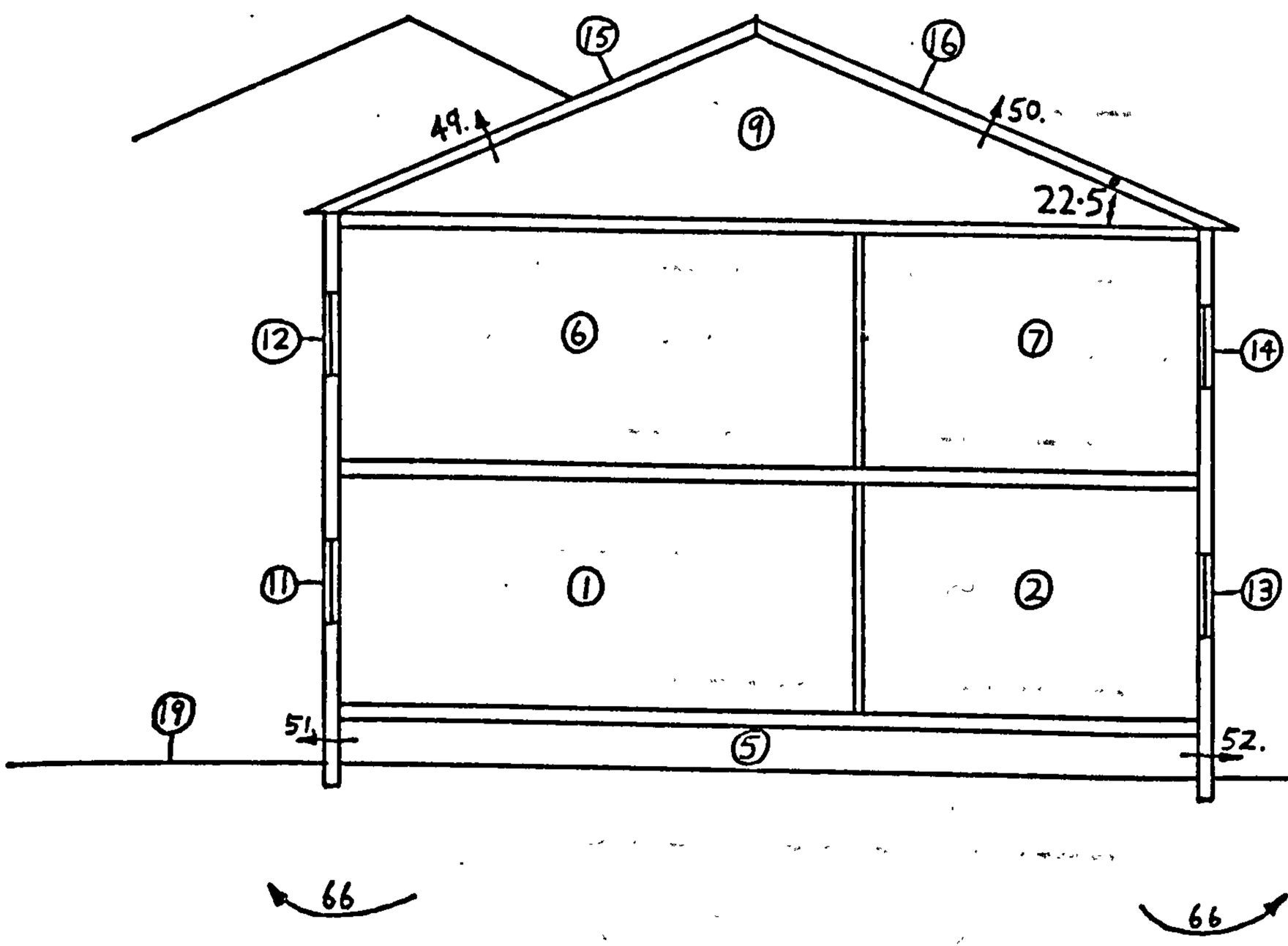

FIGURE 4.1 (contd.)

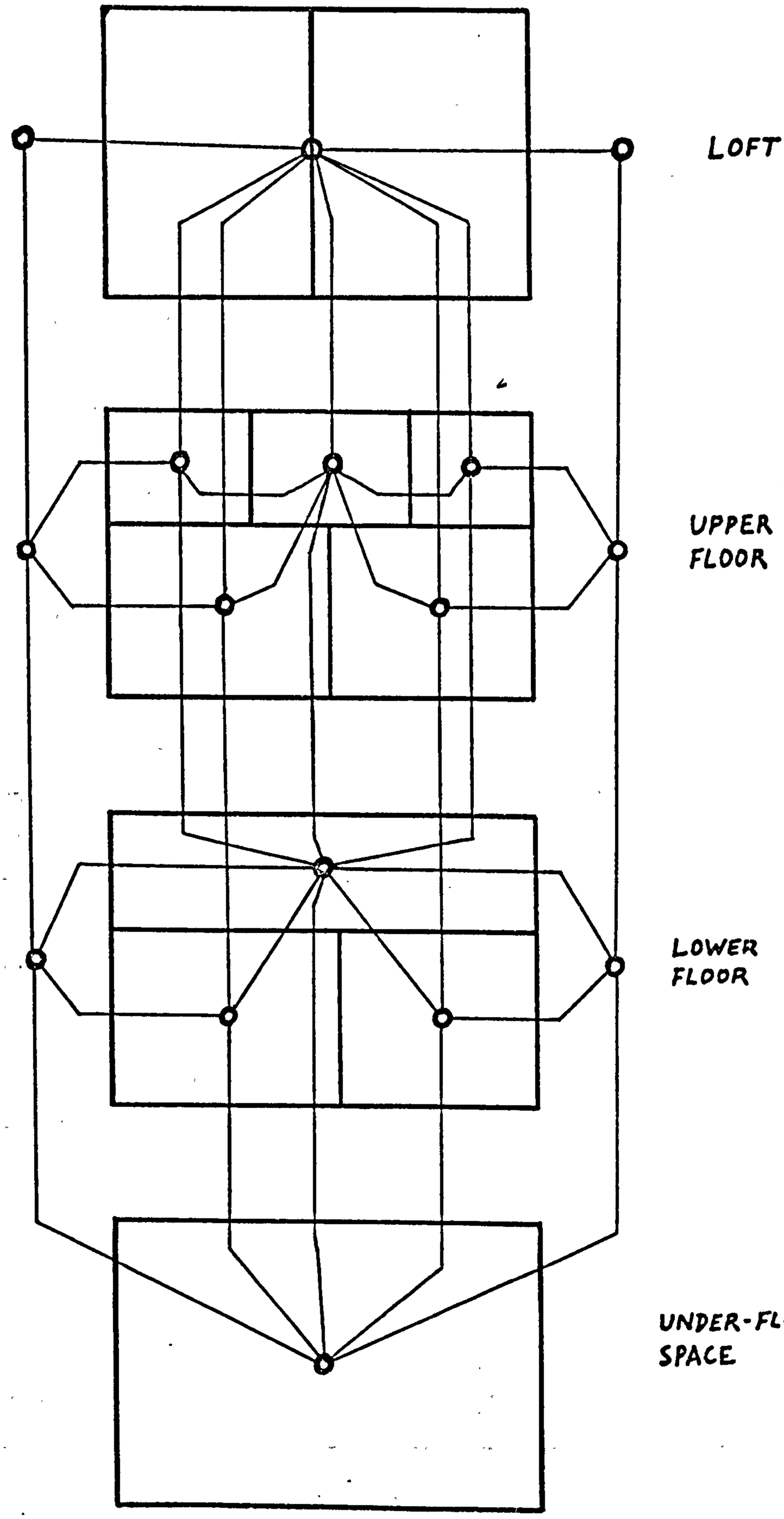

FIGURE 4.2 The Airflow Network

		Crack width mm	Crack length m
	Living room window	.5	10
	Living room floor	.5	100
*	Living room door	10	.74
	Kitchen window	2.5	10
	Kitchen floor	.5	60
	Kitchen door	5	5.38
	Bedroom A window	.5	15
	Bedroom A floor	.5	18
*	Bedroom A door	10	.66
	Bedroom B window	.5	15
	Bedroom B floor	.5	10
*	Bedroom B door	10	.66
	Bedroom C window	.5	10
	Bedroom C floor	.5	4
*	Bedroom C door	10	.66
*	Bathroom window	2.5	2
	Bathroom floor	.5	4
	Bathroom door	5	5.23
	Access hatch to left (from hall)	.5	2.6
	Front roof (eave)	2.5	5.64
	Back roof (eave)	2.5	5.64
*	Front air bricks in underfloor space	10	1.02
*	Back air bricks in underfloor space	10	1.02
	Hall front door	2	8
	Hall back door	2.5	8
	Hall floor	.5	75

Table 4.1

Crack Widths and Lengths
in Test House

* Deliberate ventilation opening

4.2 WEATHER DATA

Since cloud cover and sunshine hours were not recorded at the test site, values of these quantities were estimated to produce the same values of computed solar radiation on a horizontal plane as were recorded at the test site. Otherwise the recorded site data and BRE station data were used directly. The wind speeds expected at the house site would be less than were measured at BRE and an attenuation factor of 0.3 was applied to the measured values to obtain values applicable to the more sheltered test house. The building surface pressure co-efficients shown in Figure 4.3 were based on the available literature, and assume maximum pressure development with the wind normal to the row of terraced houses.

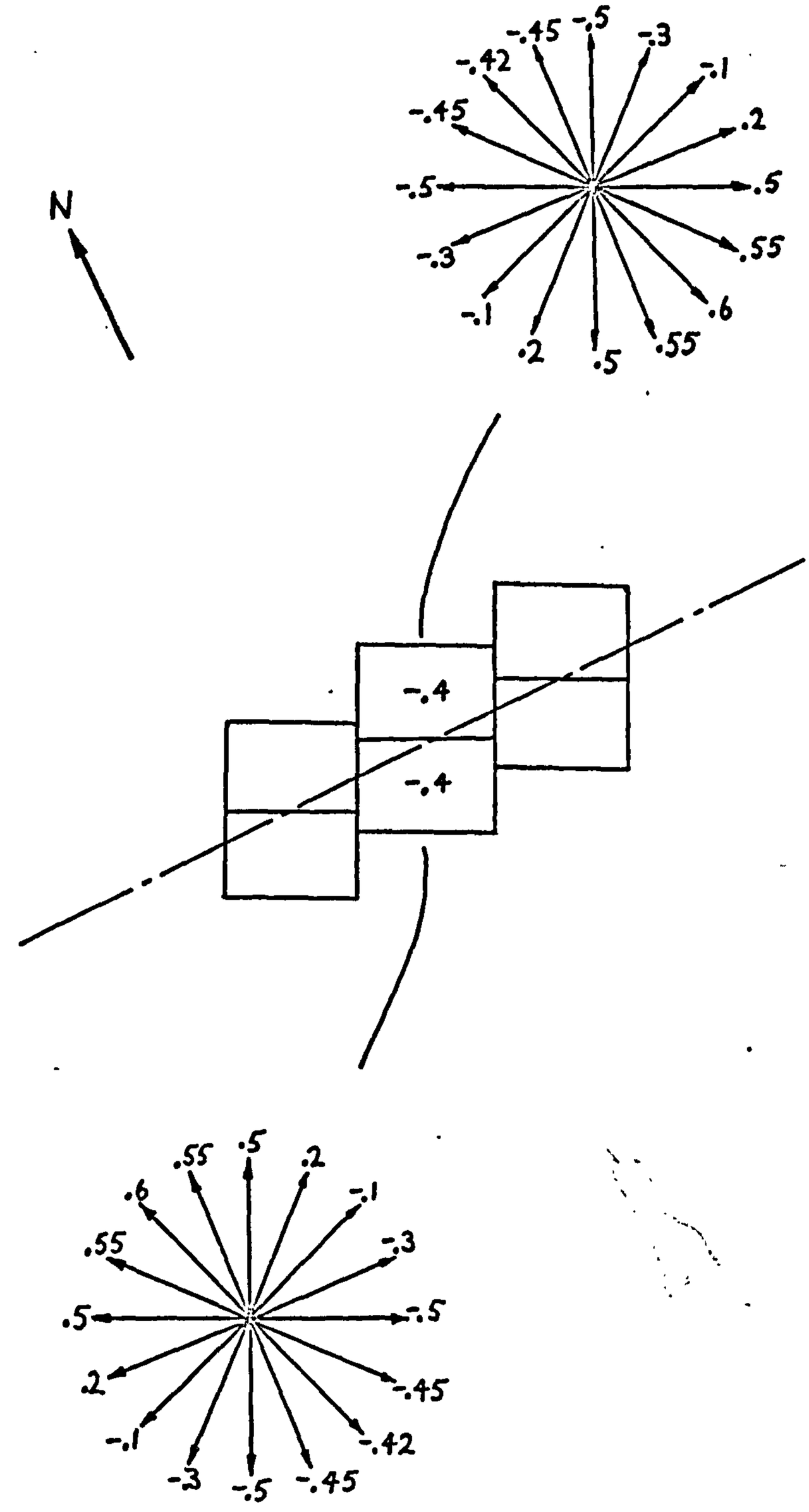

FIGURE 4.3 Building Surface Pressure Coefficients for Test House

4.3 MODEL SIMULATION RESULTS

4.3.1 Comparisons with Measured Temperatures

Living Room

Figure 4.4 shows the temperatures obtained in the living room superimposed on the measured values, for every time step over 24 hours.

The rate of overnight cooling is modelled very closely, with the measured value of temperature falling between the computed air and mean radiant temperatures. The measured temperature should be fairly close to air temperature but will be affected to some small extent, perhaps by about 10%, by the mean radiant temperature. Agreement between measured and computed data here is encouraging as the rate of cooling is directly dependent on the reducing heat loss from the room as the temperature drops.

When the heaters start up at 7.00 hours there is a rapid build-up of air temperature, with the mean radiant temperature rising much more slowly. The agreement between measured and computed data is poorer here, with the thermostat cutting off after only half-an-hour in the measured case. This is due to the modelled heat input being less than the actual heater rating. At the full heater rating input, and with a five-minute time step, the computer model had to assume that the heater was either on or off for the entire time interval. This led to overshooting of the room temperature on several

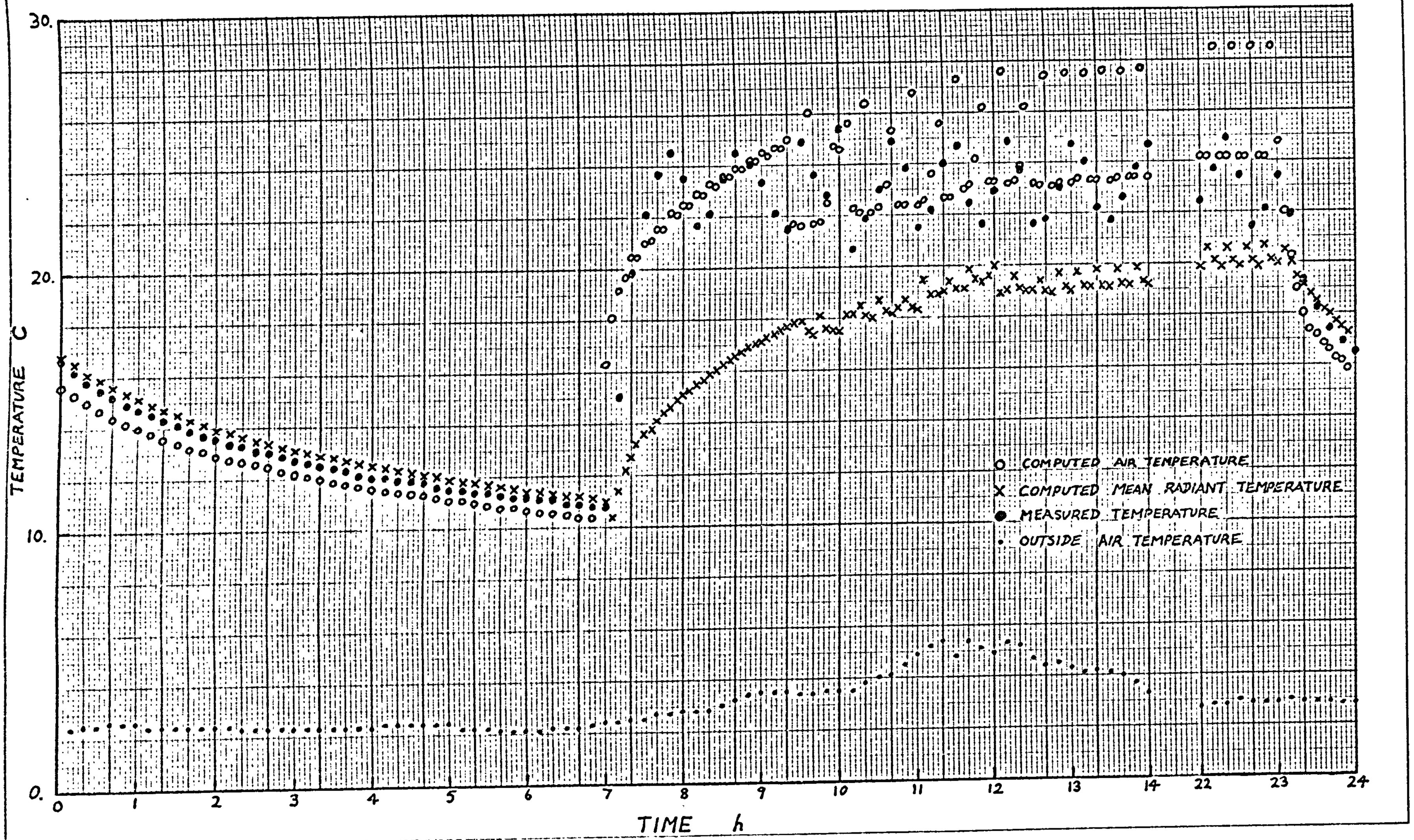

FIGURE 4.4 Measured and Computed Temperatures in Living Room - 15.3.76

occasions throughout the day. The actual "on" portion of the thermostat cycle could be as little as five minutes. Therefore if, in reality, a 5.5 minute heat input were demanded, the model would assume 10 minutes. Only by reducing heater input could overshooting be avoided, but at the expense of not modelling the warm up period correctly.

A stable cyclic condition is reached after the warm up period and this is modelled fairly well. Figure 4.5 shows in greater detail a comparison between the two sets of data. Again the measured data falls between the computed air and mean radiant temperatures. The measured data cycles more rapidly due to the higher heat input.

Kitchen

Figure 4.6 shows the measured and computed temperatures in the kitchen. Again excellent agreement is obtained overnight. Surprisingly, the warm up temperatures after 7.00 hours also agree well, although the modelled values do not start to cycle until the model living room thermostat cuts out.

The rating of the kitchen heater was less than that of the living room heater, and therefore a more uniform warm up of the room would have been obtained. This uniform heating corresponds more closely to the model's behaviour, and could account for the better agreement here than in the living room.

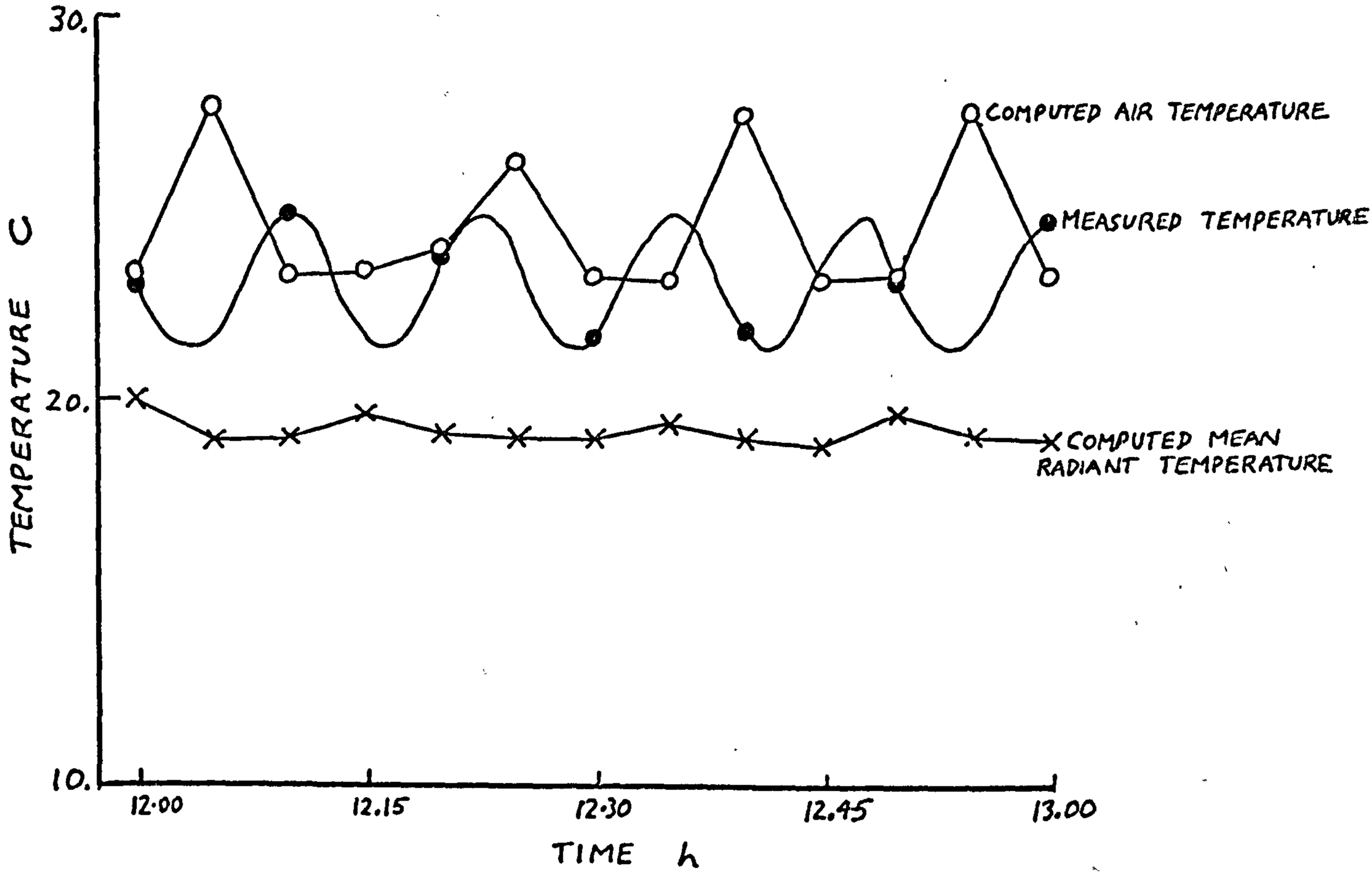

FIGURE 4.5 Measured and Computed Temperatures in Living Room - Cyclic Variations

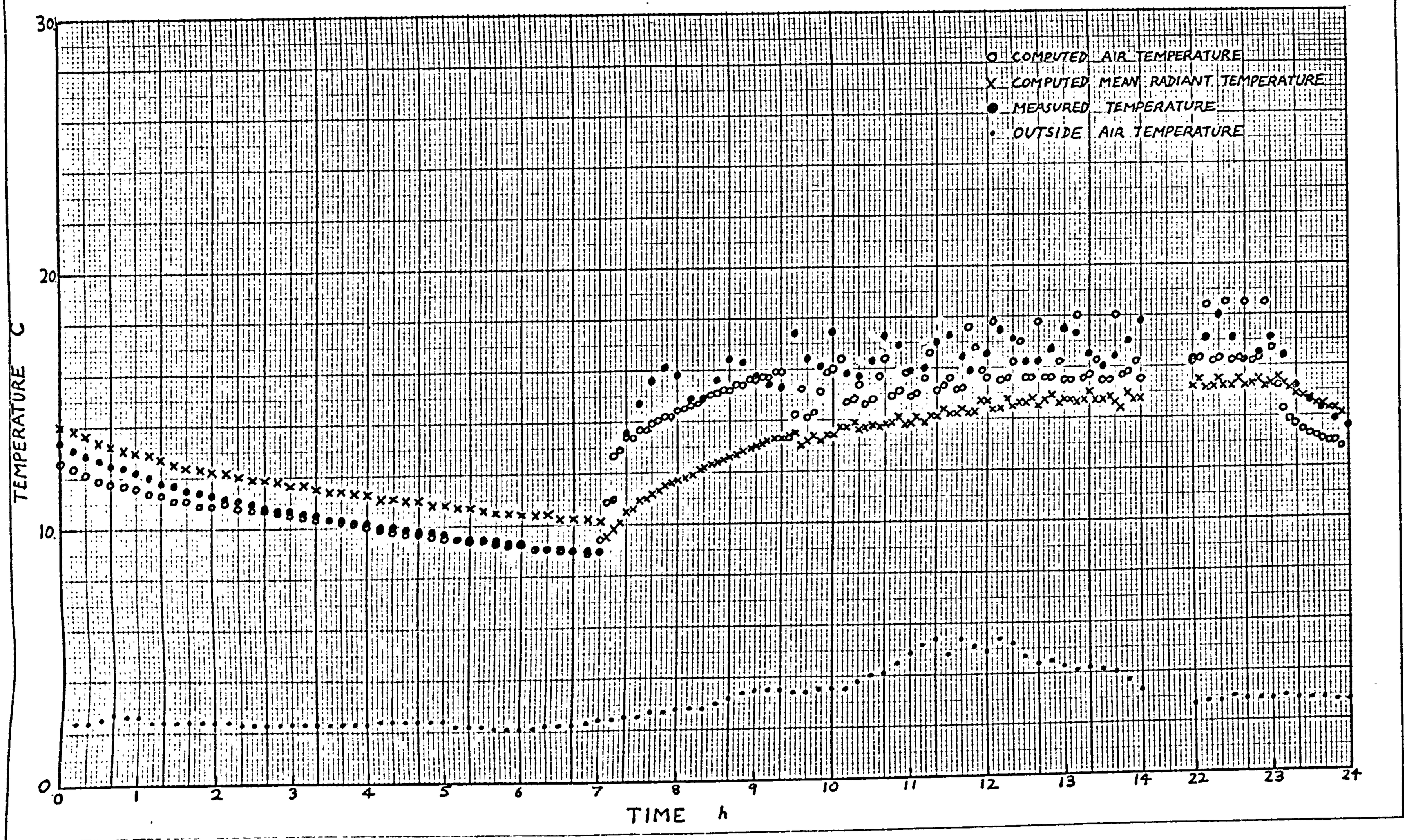

Figure 4.6 Measured and Computed Temperatures in Kitchen - 15.3.76

Hall

Figure 4.7 gives temperatures in the hall. The modelled night time cooling temperature is about 1 degree Centrigade less than the measured value, possibly due to the hall ventilation rate being too high. The day time values show good agreement although the model shows signs of over-estimating the range of temperature fluctuations to a greater extent here than in the other downstairs rooms.

Bedroom A

Figure 4.8 shows the temperatures in bedroom A.

Again, due to reduced model heat inputs, the cyclic control variations are not accurately modelled. Although the day time air temperatures are about 1 degree Centrigade too low, the variations are faithfully reproduced. Note in particular the slight rise in temperature caused by some direct solar gain at around noon. This is mirrored exactly by the model.

Bedroom B

Bedroom B's day time temperatures(Figure 4.9)are very much higher than the model predicts; 3 deg.C higher at 22.00 hours. This is due to the fact that bedroom B was used to house the recording instruments which monitored the temperatures and solar radiation. The heat gain from this equipment amounted to about 50W, and this would account for almost all of this difference. The night time fluctuations are modelled very accurately in this room.

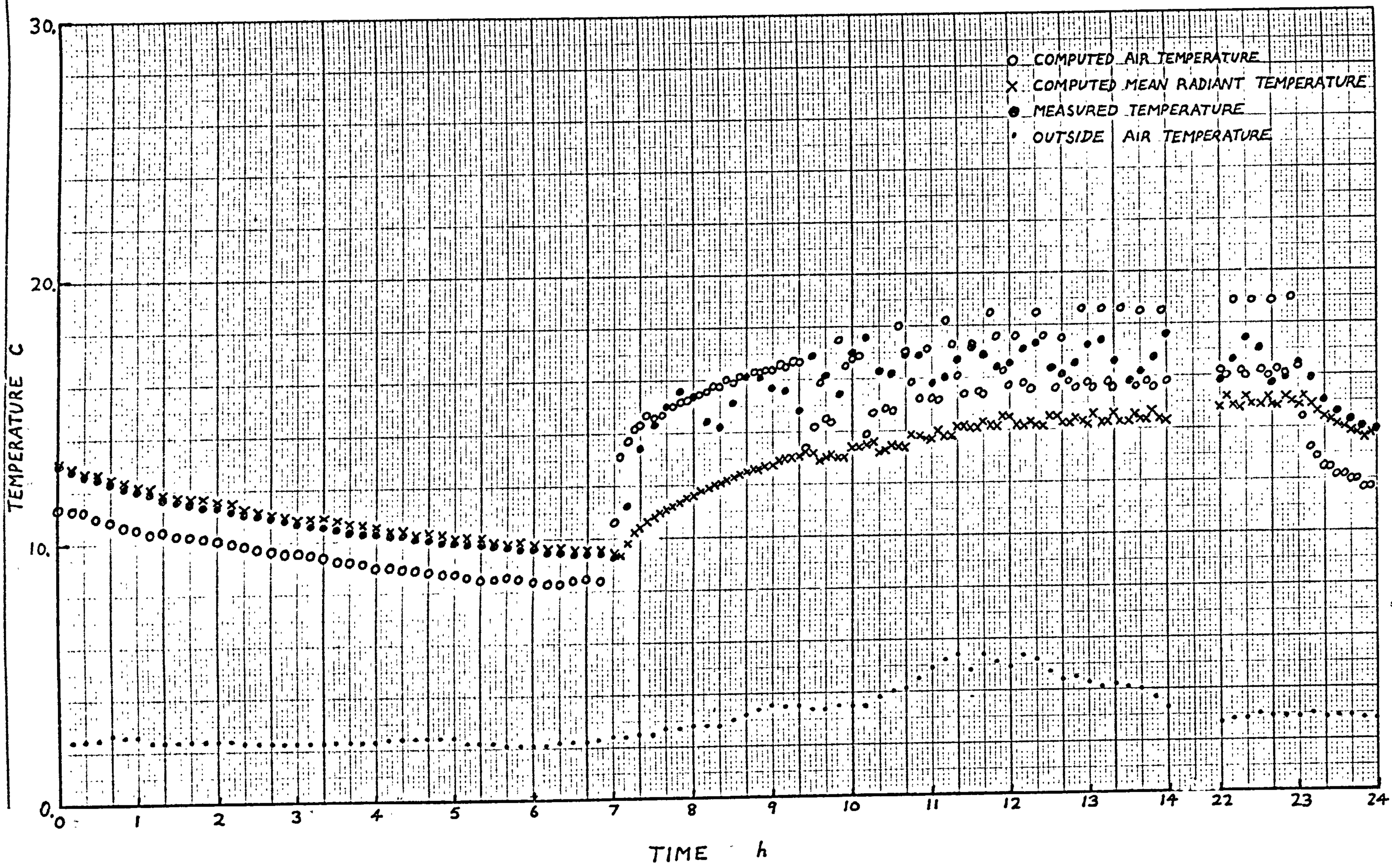

Figure 4.7 Measured and Computed Temperatures in Hall - 15.3.76

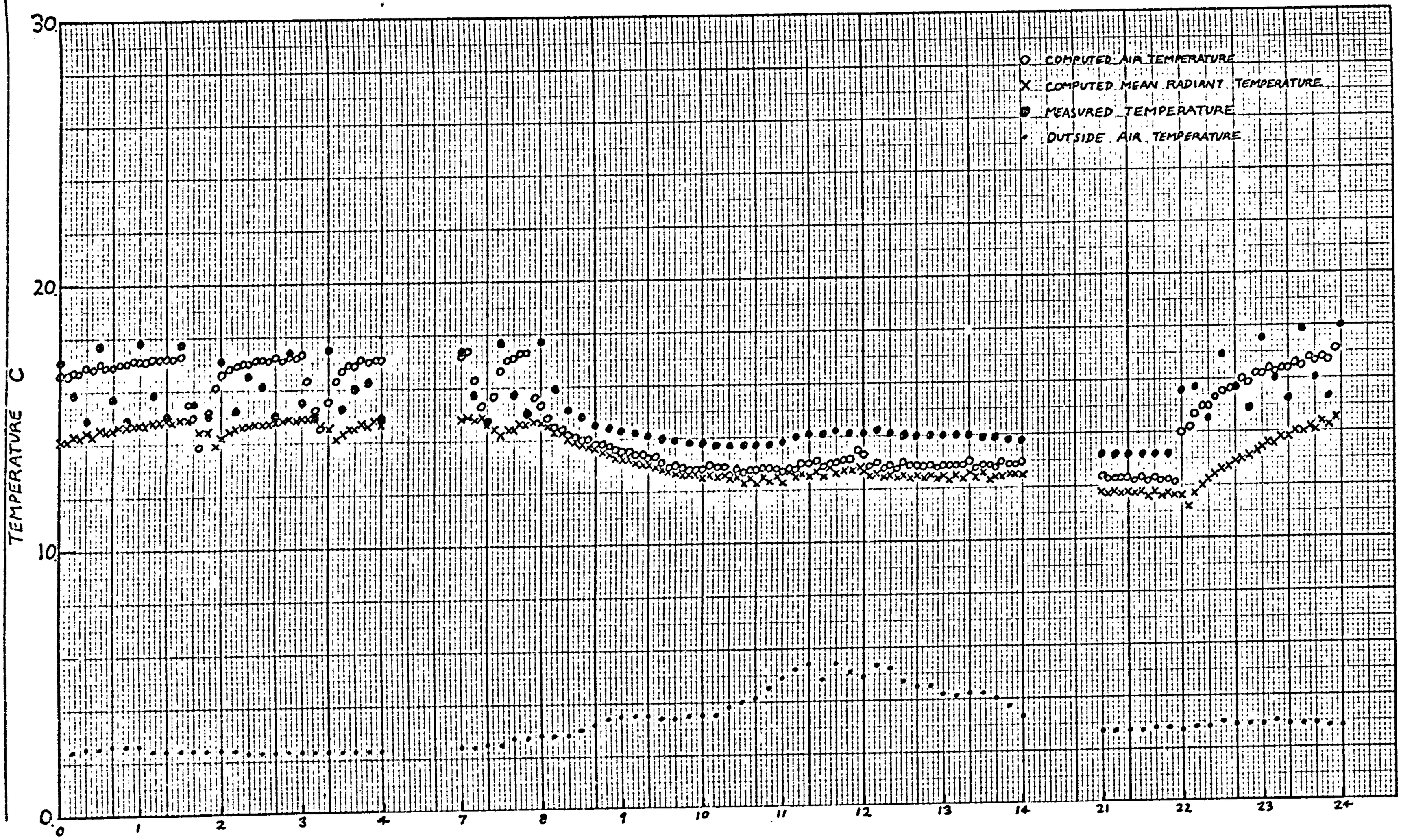

Figure 4.8 Measured and Computed Temperatures in Bedroom A - 15.3.76

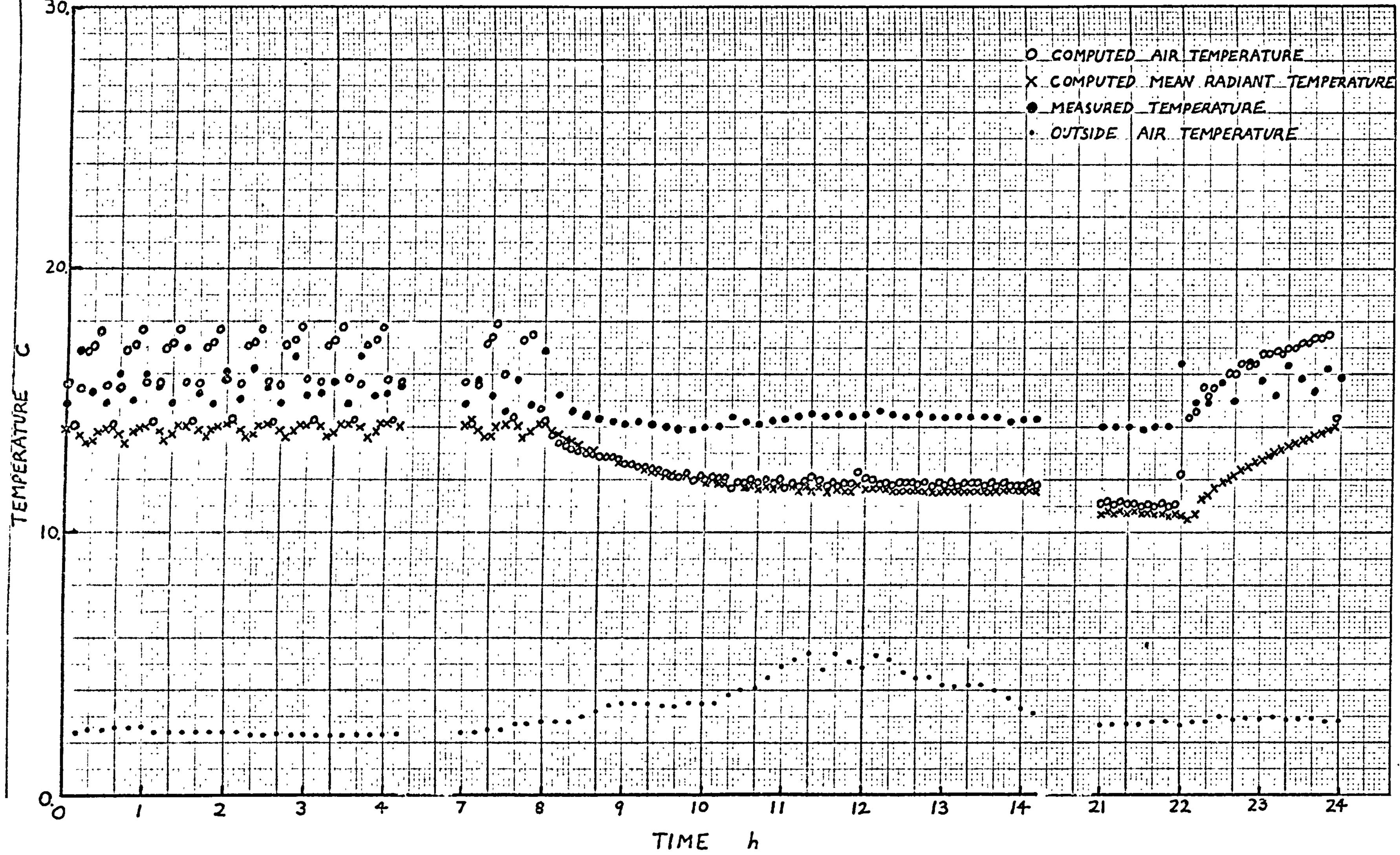

Figure 4.9 Measured and Computed Temperatures in Bedroom B - 15.3.76

Bedroom C

In bedroom C (Figure 4.10) there is again a low predicted temperature, although again, the slight increase at around mid-day, due to solar gain, is accurately reproduced.

4.3.2 Energy Consumptions

The total measured and computed energy consumptions for the day 15.3.76 in each space are shown in Table 4.2 . Only total energy consumption for all the bedrooms was measured.

	Measured kwh	Computed kwh
Living room	22.3	20.4
Kitchen	6.5	5.8
Hall	12.8	11.6
Bedroom A	)	5.3
Bedroom B	7.6)	4.3
Bedroom C	)	2.8
Total	49.2	50.2

Table 4.2

Measured and Computed Energy Consumptions

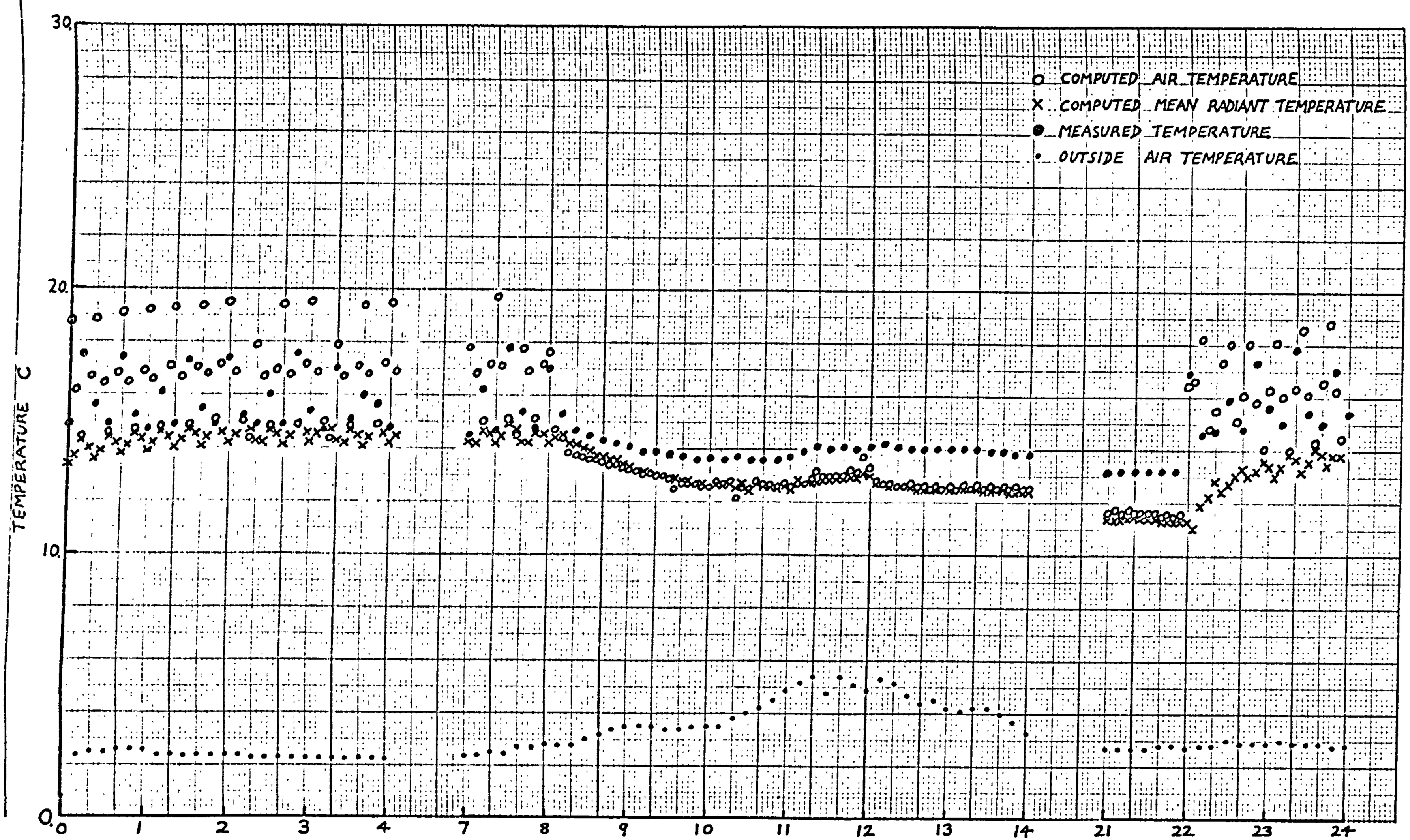

Figure 4.10 Measured and Computed Temperatures in Bedroom C - 15.3.76

The largest discrepancy between measured and computed energy consumptions is in the bedrooms, where the measured consumptions were much less than those computed by the model. On the other hand, the total energy consumptions agree to within 2%. The most likely explanation is that the heat transfer from the downstairs to the upstairs rooms was underestimated. This would also result in a lower computed energy consumption for the downstairs rooms, as is the case, with the two deviations cancelling one another out. This hypothesis is further supported by the fact that the bedroom temperatures were modelled consistently low during the daytime, when the heating upstairs was off, but downstairs was on. This too would result if a lower heat gain from the roomsbelow were predicted than actually occurred.

4.3.3 Ventilation Rates

The average daily ventilation rates are shown in Table 4.3 . Only the living room ventilation rate was measured on the test day used here, and this value is also given.

Living room	.77 (measured .76)
Kitchen	1.5
Hall/landing	2.7
Bedroom A	1.1
Bedroom B	1.9
Bedroom C	2.0

Table 4.3

Computed Mean Ventilation Rates

It was found that the ventilation rates did not vary much from these values, and most of the modelled ventilation is in fact induced by thermal density difference, i.e. stack effect, between the inside and outside of the house.

A study of Table 3.4 would suggest that some variation in ventilation rates would be expected, and it is probable that two factors contributed to this poor level of agreement. If the leakage areas of the external envelope were underestimated, this would tend to reduce the overall ventilation in the house. On the other hand, overestimation of the internal leakages would increase ventilation due to stack effects, and this is probably the case for the estimates produced by the model.

The second possibility is that the network of ventilating air flows, as depicted in Figure 4.2 is wrong. No account has been taken of flows in the wall cavities, and the ceiling-floor spaces. These flows could be quite considerable in this house and would completely alter the ventilation patterns obtained.

4.4 THERMAL PERFORMANCE MODELLING

To illustrate the aspects of a building's thermal behaviour that a computer modelling technique can simulate, some examples of heat transfers as computed by the model will be presented.

One important variable often omitted from manual design methods is the heat transfer through internal partitions in a building. This is particularly the case

in the test house, where the upstairs and downstairs rooms operate to different time clock schedules, and we will examine these heat flows in more detail.

Figure 4.11 shows the heat flows at the various levels of a vertical 'pole' through the living room and bedroom 'A' for each hour on 15.3.76. Large fluctuations occur at the external ground surface, due to day time solar radiation on the one hand and night time cooling due mainly to long wave radiation emission on the other. The thermal resistance and capacity of the ground attenuate these fluctuations, and the heat flow from the underfloor space into the ground is very small - less than $3W/m^2$ on average.

The solum heat gain fluctuations are probably more influenced by the radiation effect from the underside of the living room floor which varies with the living room temperature. On the living room floor top surface the increased flow due to heat storage in the floor is clearly seen, and a peak at around 11.00 is predicted.

Heat flow at the living room ceiling is greater than at floor level due to the thermal stratification, and the fact that the surface convection coefficient is higher for upward heat flow. Much of the upward flowing heat is re-radiated downwards at night and a less variable heat flow appears at the bedroom floor.

Heat flow into the bedroom ceiling is fairly small except at the 22.00 hours heater switch-on time, due to the high resistance of the loft floor insulation. The heat flow into the loft is uniform except at around mid-day when a

FIGURE 4.11 VERTICAL "POLE" HEAT FLOWS

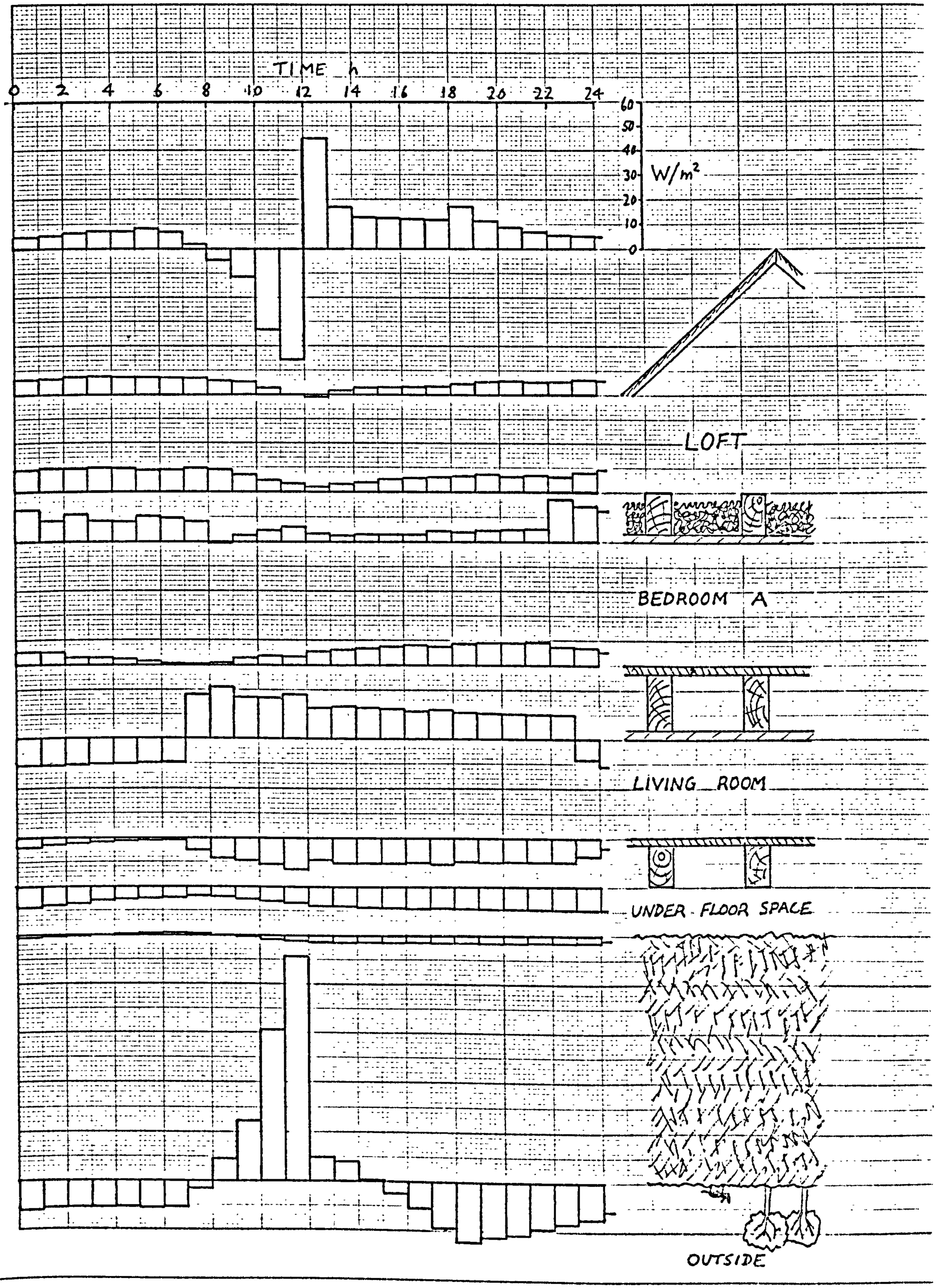

sharp drop occurs. This is probably due in part to the reduction in the roof heat loss due to the solar gain occurring at this time. Most of the solar gains are in fact re-radiated from the outer roof surface.

Clearly, there are many interacting factors affecting the heat flows depicted in Figure 4.11 which could only be reproduced by a simulation of the actual energy flows involved.

4.5 MANUAL CALCULATIONS

The test house which has been used for these comparisons is of lightweight construction and therefore there is the possibility of obtaining fairly good agreement between manual design calculations and the measured data, as thermal storage effects are fairly small. Additionally, the observed performance is such that near steady state conditions are obtained very quickly in the morning after the initial warm up period, at least on the test day of 15.3.76. The heating schedule is thus very intermittent, and such techniques as the IHVE admittance procedure based on 24-hour cyclic variations will not be likely to work well on this building in winter. The 1970 IHVE Guide data for steady state conditions is therefore used throughout. (2)

4.5.1 Sol-air Temperature

The first step must be to compute Sol-air temperatures for the external surfaces. To aid the comparison the computed values of solar radiation falling on the surfaces

will be used along with the measured outdoor air temperatures.

Using equation A6.4 of the Guide,

$$t_{eo} = t_{ao} + \left[R_{so} \left(\alpha I_t - \epsilon I_L \right) \right] \qquad 4.1$$

where t_{eo} = sol-air temperature

t_{ao} = outdoor air temperature

α = absorption coefficient applying to the outer wall surface

I_t = direct + diffuse solar radiation, W/m^2

ϵ = emissivity of outer surface to long wave radiation

I_L = long wave radiation from a black surface at air temperature

R_{so} = external surface resistance.

The values used in equation 4.1 are

α = 0.4

ϵ = 0.9

I_L = 0

R_{so} = 0.05 m^2C/W for walls

R_{so} = 0.04 m^2C/W for roof

so $t_{eo} = t_{ao} + 0.02\ I_t$ for walls)

and $t_{eo} = t_{ao} + 0.016\ I_t$ for the roof) 4.2

	$\bar{t}_{ao}$,C	$\bar{I}_t$, W/m²	$\bar{t}_{eo}$,C
front wall	3.4	30.4	4.0
back wall	3.4	18.9	3.7
roof	3.4	49.9	4.2

Table 4.4

Mean Sol-air Temperature Calculations for the Period 7.00 - 23.00 Hours on 15.3.76

Table 4.4 gives the results of the calculations for the front wall, back wall, and roof surface. These data apply to the 16 hours between 7.00 and 23.00 hours. The mean value of t_{ao} is that measured at the test house, and values of I_t are the means of those computed by the model simulation program.

4.5.2 Internal Temperature

To find the internal environmental temperature needed to compute fabric losses, we must use equation A5.7 of the IHVE Guide, so

$$t_{ei} = t_{ai} \frac{- \Sigma Qf}{4.8 \Sigma A} \qquad 4.3$$

where ΣQf = rate of heat transfer through building structure

ΣA = total area of surfaces bounding the enclosure

Also, since

$$t_{ei} = \frac{1}{3} t_{ai} + \frac{2}{3} t_{ri} \qquad 4.4$$

values of t_{ri} can be obtained.

Table 4.5 presents these results for each of the heated spaces in the test house. Again mean measured values of air temperatures are used.

	Measured Mean Air Temperature t_{ai} °C	Approximate ΣQ_f W	A m^2	Environmental Temperature t_{ei} °C	Mean Radiant Temperature t_{ri} °C	Ventilation Rate a/c/hr.	Volume m^3	Ventilation Heat Loss W/°C
Living Room	24.0	1000	77	21.0	19.5	.76	42	10.5
Kitchen	16.5	300	48	15.0	14.0	1.5	22	10.9
Hall	17.0	350	99	16.0	15.5	2.7	49	43.7 (22.4*)
Bedroom A	16.0	350	77	15.0	14.5	1.1	42	15.3
Bedroom B	15.5	350	48	14.0	13.0	1.9	22	13.8
Bedroom C	16.0	250	36	14.5	13.5	2.0	14	9.2

* Due to outside air only.

TABLE 4.5 : ENVIRONMENTAL DATA FOR THE HEATED SPACES IN THE TEST HOUSE .

4.5.3 Heat Losses

To calculate total fabric losses we must include those losses and gains to and from adjoining rooms where these are significant. Tables 4.6 to 4.11 give, for each heated space, the results of the calculations of fabric loss for each wall, window, door, partition, floor and ceiling. Only those components through which a significant heat transfer occurs are included. The U-values are calculated from the data presented in Table 3.1. All temperatures are mean internal environmental or external sol-air temperatures, except for the ventilation load, where air temperatures are used.

The ventilation heating loads are calculated from equation A5.16 (a) of the IHVE Guide, i.e.

$$Q_v = 0.33NV(t_{ai} - t_{ao}) \qquad 4.5$$

where Q_v is the ventilation load, W

N is the air change rate, hr^{-1}

V is the room volume, m^3

Values of ventilation rate and room volume are given in Table 4.5 for the heated spaces, and the ventilation loss per unit temperature difference is computed.

The ventilation losses are computed in Tables 4.6 to 4.11 by assuming that the ventilating air for the downstairs rooms comes from outside, and for the upstairs rooms comes from the hall. This is a better assumption than assuming that all ventilating air comes from outside. In the hall, special allowance can be made for the fact that air from the kitchen and living room passes into the hall. Therefore the

hall ventilation load is calculated as follows :-	l/s
Total hall ventilation rate (from computer model)	36.8
Living room air to hall	- 8.9
Kitchen air to hall	- 9.2
Therefore hall ventilation rate due to outside air	18.7

This results (from equation 4.5) in the reduced load shown in Table 4.5 of 22.4 W/^{o}C and this is the value used in Table 4. 8.

Since a significant temperature difference of 7C^{o} exists between the living room and the hall, the resultant ventilation heat gain is subtracted from the hall heat load at the rate of 10.5 W/^{o}C.

LIVING ROOM	Ouside Surface Resistance m^2 °C/W	Fabric Thermal Resistance m^2 °C/W	Inside Surface Resistance m^2 °C/W	Overall Thermal Transmittance =U-value, W/m^2C	Outside Temperature °C	Inside Temperature °C	Δt °C	Area m^2	Heat Loss W
Outside wall	.05	.73	.123	1.11	4.0	21.0	17	5.8	109
Window	-	-	-	5.6	4.0	21.0	17	2.6	248
Floor	-	-	-	0.65 (1)	4.0	21.0	17	18.3	202
Gable Wall	.05	.72	.123	1.11	4.0	21.0	17	4.2	79
Loss to Bedroom	.106	.69	.106	1.11	14.0	21.0	7	18.3	142
Loss to Hall	.123	.30	.123	1.84	16.0	21.0	5	11.8	109
Loss to Kitchen	.123	.30	.123	1.84	15.0	21.0	6	8.1	89
Loss to next House	.123	1.03	.123	.78	16.0	21.0	5	7.6	30
Ventilation	-	-	-	-	3.4	24.0	20.6	-	219
Solar Direct Gain	-	-	-	-	-	-	-	2.6	-60
TOTAL									1167

(1) IHVE Guide, Table A3.19, 7.5m x 7.5m

TABLE 4.6 : HEAT LOSS FROM LIVING ROOM 7.00 -23.00 HRS. 15.3.76

KITCHEN	Outside Surface Resistance m^2 °C/W	Fabric Thermal Resistance m^2 °C/W	Inside Surface Resistance m^2 °C/W	Overall Thermal Transmittance =U value W/m^2°C	Outside Temperature °C	Inside Temperature °C	Δt °C	Area m^2	Heat Loss W
Outside Wall	.05	.73	.123	1.11	3.7	15.0	11.3	6.9	87
Window	-	-	-	5.6	3.7	15.0	11.3	1.23	78
Floor	-	-	-	0.65 (1)	3.7	15.0	11.3	9.8	72
Gain from Living Room	.123	.3	.123	1.84	21.0	15.0	-6.0	8.1	-89
Ventilation	-	-	-	-	3.4	16.5	13.1	-	143
Direct Solar Gain								1.23	-18
TOTAL									273

(1) IHVE Guide, Table A3-19, 7.5m x 7.5m

TABLE 4.7 : HEAT LOSS FROM KITCHEN. 7:00 - 23:00 hrs. 15.3.76

HALL/LANDING	Outside Surface Resistance m^2 °C/W	Fabric Thermal Resistance m^2 °C/W	Inside Surface Resistance m^2 °C/W	Overall Thermal Transmittance U-Value W/m^2°C	Outside Temperature °C	Inside Temperature °C	Δt °C	Area m^2	Heat Loss W
Front Wall	.05	.73	.123	1.11	4.0	16.0	12.0	1.92	26
Front Door	.05	.24	.123	2.41	4.0	16.0	12.0	1.94	56
Front Window	-	-	-	5.6	4.0	16.0	12.0	.68	46
Back Wall	.05	.73	.123	1.11	3.7	16.0	12.3	3.6	49
Back Door	.05	.10	.123	3.7	3.7	16.0	12.3	.40	18
Back Window	-	-	-	5.6	3.7	16.0	12.3	.53	37
Gable Wall	.05	.72	.123	1.11	.7	16.0	12.3	4.2	57
Floor	-	-	-	0.65 (1)	4.0	16.0	12.0	15.8	123
Landing Ceiling/Roof	-	-	-	0.5 (2)	4.2	16.0	11.8	5.7	34
Gain from Living Room	.123	.30	.123	1.84	21.0	16.0	- 5.0	11.8	-109
Gain from next House	.123	1.03	.123	.78	16.0	21.0	- 5.0	7.6	- 30
Ventilation Loss					3.4	17.0	13.6	-	303
Ventilation Gain From living Room					24.0	17.0	7.0	-	-74
Front window solar gain								.68	-16
Back window solar gain								.53	- 8
TOTAL									512

(1) IHVE Guide Table A3.19, 7.5m x 7.5m
(2) IHVE Guide Table A3.14, No. 3

TABLE 4.8 : HEAT LOSS FROM HALL/LANDING 700-2300 HRS. 15.3.76

BEDROOM A	Outside Surface Resistance $m^2{}^oC/W$	Fabric Thermal Resistance $m^2{}^oC/W$	Inside Surface Resistance $m^2{}^oC/W$	Overall Thermal Transmittance =U-Value $W/m^2{}^oC$	Outside Temperature ^oC	Inside Temperature ^oC	Δt ^oC	Area m^2	Heat Loss W
Outside Wall	.05	1.03	.123	.83	2.5	15.0	12.5	6.9	72
Window	-	-	-	5.6	2.5	15.0	12.5	1.23	86
Gable Wall	.05	.72	.123	1.11	2.5	15.0	12.5	4.2	58
Ceiling/Roof	-	-	-	0.5 (1)	2.5	15.0	12.5	18.3	114
Ventilation	-	-	-	-	11.0	16.0	5.0	-	77
TOTAL									407

(1) IHVE Guide Table A3.14, No. 3

TABLE 4.9 : HEAT LOSS FROM BEDROOM A, 22.00 - 8.00 HRS. 15.3.76. THE CEILING U-VALUE INCLUDES THE ROOF SPACE. HEAT LOSS TO THE LANDING AND TO THE LIVING ROOM ARE NEGLECTED.

BEDROOM B	Outside Surface Resistance $m^2{}^oC/W$	Fabric Thermal Resistance $m^2\ {}^oC/W$	Inside Surface Resistance $m^2\ {}^oC/W$	Overall Thermal Transmittance U-Value $W/m^2{}^oC$	Outside Temperature ^oC	Inside Temperature ^oC	Δt ^oC	Area m^2	Heat Loss W
Outside Wall	.05	1.03	.123	.83	2.5	14.0	11.5	6.9	66
Window	-	-	-	5.6	2.5	14.0	11.5	1.23	79
Ceiling/Roof	-	-	-	0.5 (1)	2.5	14.0	11.5	9.8	56
Ventilation	-	-	-	-	11.0	15.5	4.5	-	62
TOTAL									263

(1) IHVE Guide Table A3.14, No. 3

TABLE 4.10: HEAT LOSS FROM BEDROOM B 22.00 - 8.00 HRS. 15.3.76

THE CEILING U-VALUE INCLUDES THE ROOF SPACE. HEAT LOSSES TO THE LANDING AND KITCHEN ARE NEGLECTED.

BEDROOM C	Outside Surface Resistance m^2 °C/W	Fabric Thermal Resistance m^2 °C/W	Inside Surface Resistance m^2 °C/W	Overall Thermal Transmittance =U-Value W/m^2°C	Outside Temperature °C	Inside Temperature °C	Δt °C	Area m^2	Heat Loss W
Front Wall	.05	1.03	.123	.83	2.5	14.5	12.0	3.7	37
Window	-	-	-	5.6	2.5	14.5	12.0	.81	54
Ceiling/Roof	-	-	-	0.5 (1)	2.5	14.5	12.0	6.2	37
Ventilation					11.0	16	5.0	-	46
TOTAL									174

(1) IHVE Guide Table A3.14, No. 3

TABLE 4.11 : HEAT LOSS FROM BEDROOM C 22.00 - 8.00 HRS. 15.3.76. THE CEILING U-VALUE INCLUDES THE ROOF SPACE. HEAT LOSSES TO THE LANDING AND HALL ARE NEGLECTED.

From Table A6.12 of the IHVE Guide a solar gain factor of 0.76 for the windows is obtained. Solar gains for all windows are thus computed from

$$Q_s = S.A.\bar{I}_t$$

where Q_s is the solar gain, W

S is the solar gain factor

A is the window area

$\bar{I}_t$ is the mean solar radiation at the window surface for the period 7.00 - 23.00

Values of Q_s are included in Tables 4.6 to 4.8 where they are appropriate.

4.5.4 Total Energy Consumption

The total energy consumptions can be calculated for the day 15.3.76 by multiplying the net heat losses by the hours of operation of the heating system. To these values must be added the pre-heating load to bring the room temperatures up to their "steady-state" values. These loads can be estimated from Table A9.3 of the IHVE Guide. Using the living room as an example, the installed heater capacity in the test house was 3.12 KW. Now, at our inside/outside temperature difference of 17 C^o, a load of 1.17 KW has been calculated. Therefore a design load based on a 20 C^o rise would be approximately $1.17 \times {}^{20}/17 = 1.38$ KW. Therefore the "plant size ratio" as defined in IHVE Guide Table A9.3 is 3.12/1.38 = 2.3.

	INSTALLED HEATER CAPACITY kW	CALCULATED LOAD kW	INSIDE/ OUTSIDE TEMPERATURE DIFFERENCE C	"DESIGN LOAD" (20C) kW	PLANT SIZE RATIO	PREHEAT TIME H	PREHEAT LOAD kW h	STEADY STATE LOAD kW h	TOTAL ENERGY CONSUMPTION kW h
Living Room	3,12	1.17	17	1.38	2.3	0.5	1.17	18.72	19.9
Kitchen	.888	.273	11.3	.48	1.8	0.8	.49	4.37	4.9
Hall/Landing	1.77	.512	12.0	.85	2.1	0.5	.63	8.19	8.8
Bedroom A	.98	.407	12.5	.65	1.5	1.7	.97	4.07	5.0
Bedroom B	.92	.263	11.5	.46	2.0	0.7	.46	2.63	3.1
Bedroom C	.85	.174	12.0	.29	2.9	0.4	.27	1.74	2.0
TOTAL ENERGY CONSUMPTION									43.7

FIGURE 4.12: "STEADY STATE" AND PRE-HEAT ENERGY CONSUMPTIONS.

For a short response plant in a lightweight building this gives, with some interpolation, a preheat time of approximately 0.5 h. Therefore the calculated pre-heating additional energy consumption is (3.12 - 1.17) x 0.6 kWh = 1.17 kWh.

The same procedure has been carried out for the other heated spaces and the results are shown in Table 4.12. The values of measured and computed energy consumptions in Table 4.2 are repeated here in Table 4.13 along with the values calculated above.

	Measured kWh	Computed kWh	Manual (IHVE) Calculation kWh
Living room	22.3	20.4	19.9
Kitchen	6.5	5.8	4.9
Hall	12.8	11.6	8.8
Bedroom A)		5.3	5.0
Bedroom B)	7.6	4.3	3.1
Bedroom C)		2.8	2.0
Total	49.2	50.2	43.7

Table 4.13

Measured, Computed and Hand Calculated Energy Consumptions

Clearly the manual calculation gives results that are consistent with those measured, although all the values are low. This could be partially due to the manual method's failure to make adequate allowance for outgoing longwave radiation from the external building surface even with cloud cover.

The computer model results and the measured data provided much of the input data that would normally have to be calculated or obtained from design data, such as is contained in the IHVE Guide. There is a clear indication, however, that less precise calculation techniques could be used in a model that retained the advantages of the ability to use hourly weather data with a finite time step. The extent to which simplification along these lines can be pursued will depend on the errors introduced when considering energy transfers into and out of thermal storage in the building fabric.

Summary of Chapter 4

The input data required for the computer model is described. Problems associated with interference between the five minute time step, and thermostat cycling are discussed. The comparisons between measured and computed temperatures, energy consumptions and ventilation rates indicate various levels of agreement and possible reasons for discrepancies are given. Comparisons with manual calculations are possible due to the low thermal capacity of the house. The manual results are consistent with the measured and computed data, and indicate some scope for simplification of the calculation procedures.

CHAPTER 5

THE ASSESSMENT OF DOUBLE GLAZING INSTALLED IN THE TEST HOUSE

5.1 INTRODUCTION

To further assess the performance of the computer model a comparison was carried out between the test house as previously described with single glazing, and the same house if double glazed windows were installed throughout. The test house was not modified in this way, and no actual measurements were carried out. The object of this exercise was to examine the model predictions and to determine its possible usefulness for this type of comparison.

5.2 HEAT TRANSFER THROUGH WINDOWS

Table 5.1 shows the proportions of total heat loss through the various fabric components of the house for the day 15.3.76.

	Fabric heat loss MJ	% of total heat loss
Roof	22	11
Upstairs walls	27	14
Downstairs walls	43	23
Upstairs windows	17	9
Downstairs windows	28	14
Ground	10	5
Ventilation	45	24
Total losses	192	100
Heat input	181	

Table 5.1

Heat Losses Through Fabric Components 15.3.76 - Single Glazing

Any solar gain transmitted through the windows into the house is included in these losses, as they represent the heat flows at the building's internal surfaces. The heating system energy consumption is therefore slightly less than the heat loss. This table indicates that 23% of the total losses are through the windows, and there would therefore appear to be a considerable saving obtainable if this figure could be reduced by installing double glazing. Table 5.2 gives details of the glass used in the comparison.

Figure 5.1 shows for the day 15.3.76, the heat flows through the single glazed living room window, both at the inner and outer surfaces. Also shown in this Figure are the window glass temperature, the outside and inside air temperatures and the room mean radiant temperature. All data are hourly means.

In order to obtain a heat balance, the solar absorption in the window glass has been added to the heat gain to the inner glass surface. Any difference between this total and the heat flux at the outer surface is therefore due to thermal storage in the glass, and does not exceed a few watts at any time. The heat flows are split into convective and long wave radiative components. It is interesting to note that the radiative component is a substantial proportion of the total heat transfer, but is not a constant proportion.During the day, for example, the room mean radiant temperature is less than the air temperature. At night however, the air temperature drops more rapidly than the mean radiant temperature and hence

the radiative heat transfer to the glass remains relatively high as the convective component drops.

The effect of the small quantity of solar absorbtion before mid-day is to increase the external losses and reduce the internal gains at the glass surfaces. The radiation component at the inner glass surface remains almost constant however, largely due to the room mean radiant temperature rising at approximately the same rate as the glass temperature.

Sheet thickness	3 mm
Thermal conductivity	1.05 W/mK
Density	2500 kg/m^3
Specific heat	.75 kJ/kgK
Absorption coefficient	50 m^{-1} (eqn. 2.30)
Reflectivity (normal incidence)	
single	.06
double	.10

Table 5.2

Glass Properties

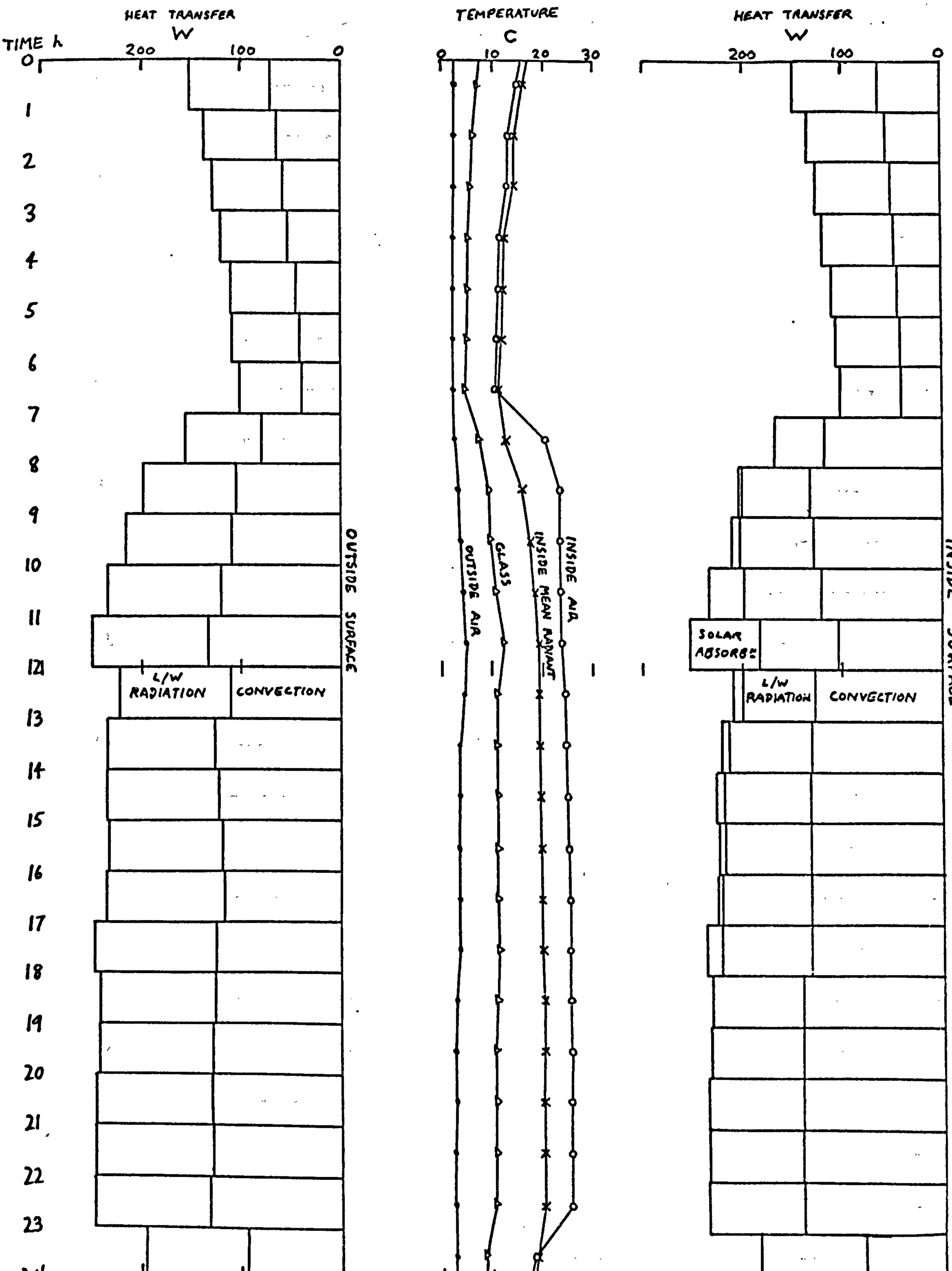

FIGURE 5.1 Window Heat Transfer - Single Glazing

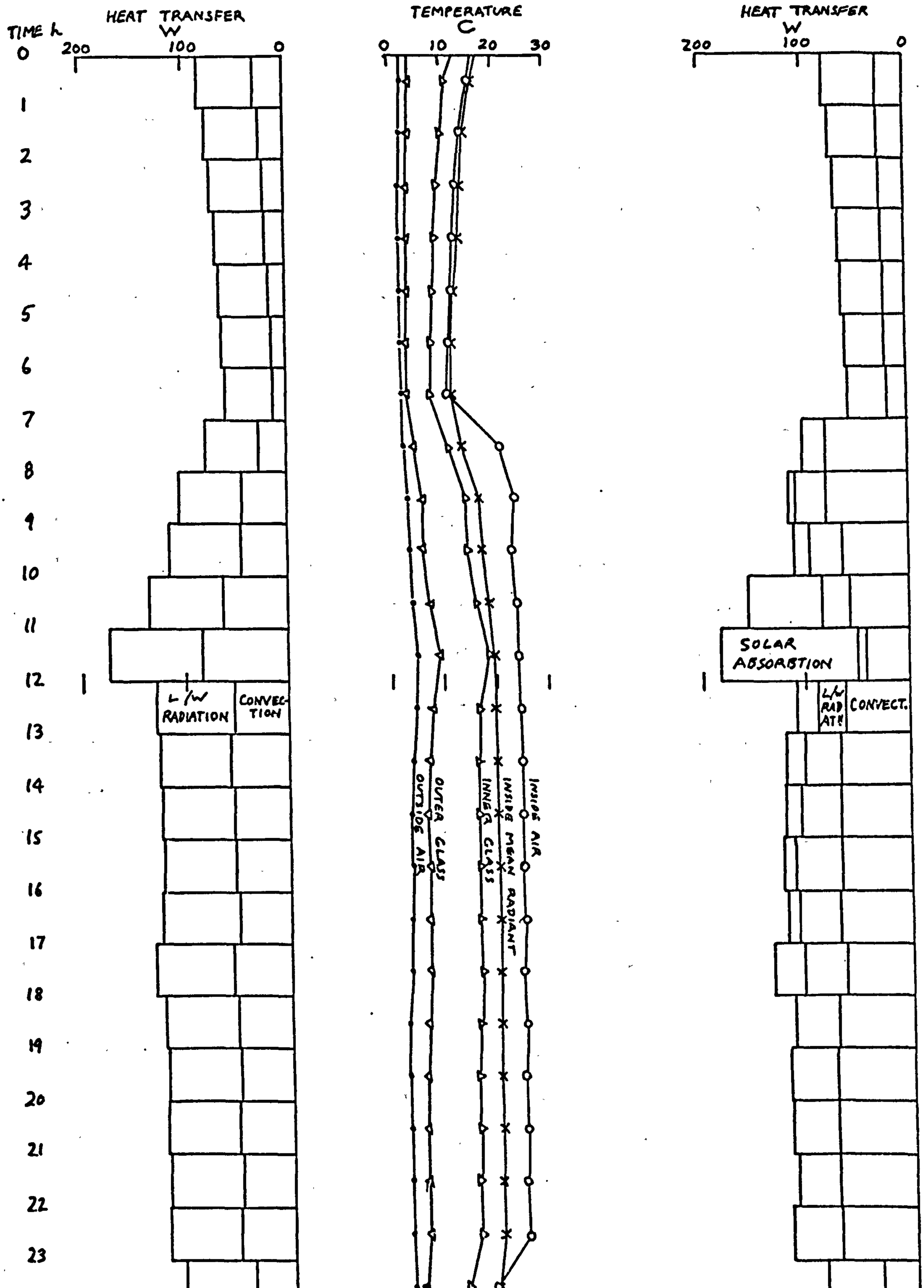

FIGURE 5.2 Window Heat Transfer - Double Glazing

Figure 5.2 shows, for the same day, the heat transfers with double glazing installed. Two sheets of glass described in Table 5.2 are used, with a 12mm air gap. Both radiative and convective components are approximately halved, and the behaviour is different, with two glass temperatures now involved. At the outside surface the radiative component is the larger component of total radiation. Even when the air and outside glass temperatures are almost equal, as they are around 6.00 hours, there still exists a high outgoing radiation to the sky. At the inner surface a higher glass temperature reduces both components of radiation. During the period of direct solar radiation, just before mid-day, heat is absorbed at both the outer and inner sheets of glass, and this has been added to the inner surface heat gain to obtain an energy balance, as before. In this case, even though only a small quantity of solar radiation is involved, the radiative heat loss to the inner glass is reduced almost to zero due to the rise in glass temperature, which approaches the room mean radiant temperature. Table 5.3 shows the new proportions of heat loss with double glazing installed.

Comparison with Table 5.1 shows that the heat loss through the glazing has been halved, and the reduction in total heat loss (at the internal surfaces) is 11%. The reduction in energy consumption is 9%, the 2% difference being due to the reduction in solar transmission through the glass due to the additional glass sheet.

	Fabric heat loss MJ	% of total heat loss
Roof	22	13
Upstairs walls	28	16
Downstairs walls	43	25
Upstairs windows	9	5
Downstairs windows	14	8
Ground	9	6
Ventilation	46	27
Total losses	171	100
Heat input	165	

Table 5.3

Heat Losses Through Fabric Components

- 15.3.76 - Double Glazing

5.3 ENERGY CONSUMPTION

All the comparisons discussed so far have been concerned with the test day of 15.3.76. To extend the comparisons further and to investigate more fully the seasonal variations in energy consumption, runs were carried out for summer and winter periods of two weeks each with continuous simulation throughout these periods. In each case a preliminary run up period of five days was added to eliminate the effects of the arbitrary initial starting conditions. The weather data used related to the

Abbotsinch meteorological station. This data happened to be convenient at the time and since no comparisons were being made with actual measurements, it was not felt to be essential to use weather data for the precise location of the test house. The periods chosen were January 1-14 1970 and June 4-17 1970.

Figures 5.3 and 5.4 show, for the test house with single and double glazed windows respectively, the mean daily heat losses and energy input for each day of the two 14-day periods. The data are plotted against daily mean outside air temperature. On each of these figures three sets of data are plotted.

(a) Fabric heat loss

This is computed as the total heat flow into the internal surfaces of external walls, windows, ground floors and bedroom ceilings, averaged over each day. There is clearly a strong correlation with outside temperature, and in each case a linear regression was carried out on the winter data. The resultant lines of best fit are plotted. The regression constants and coefficients of determination are given in Table 5.4. In neither case did this regression line pass through the summer data. In winter the heat flux is always towards the outside, but in summer heat flows in both directions at different times of day. The daily mean is an algebraic mean of the inward and outward heat flows

and this is a possible explanation of why the same regression line does not fit both sets of data. Another factor may be the non-linearity of heat flux as a function of outside temperature. Both the internal and external surface heat transfer coefficients are non-linear, the radiative component more so than the convective. By fitting a linear curve to the data we are ignoring this aspect which may be significant for the data presented here. As was noted earlier, the window heat losses do have a large radiative component, and the effective heat transfer coefficient will therefore decrease as the surface temperatures drop, due to the dependence on fourth powers of temperature, with the result that the expected shape of the curves of Figures 5.3 and 5.4 will be convex upward.

These fabric losses, for a given internal temperature pattern that does not vary significantly from day to day, should be almost independent of ventilation rates and direct solar gains, although they will be affected by solar absorption at the external fabric.

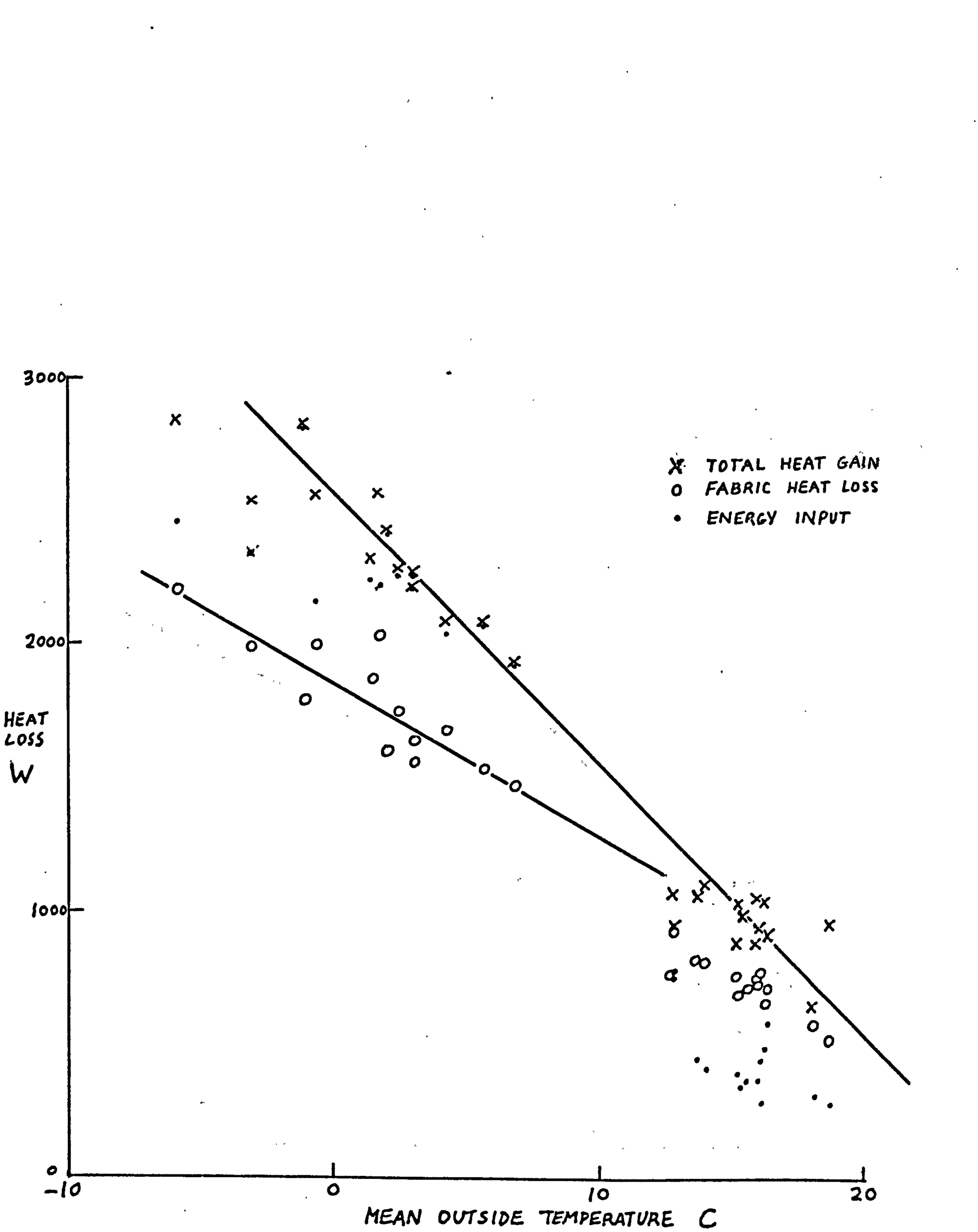

FIGURE 5.3

Energy Flows in Test House with Single Glazing

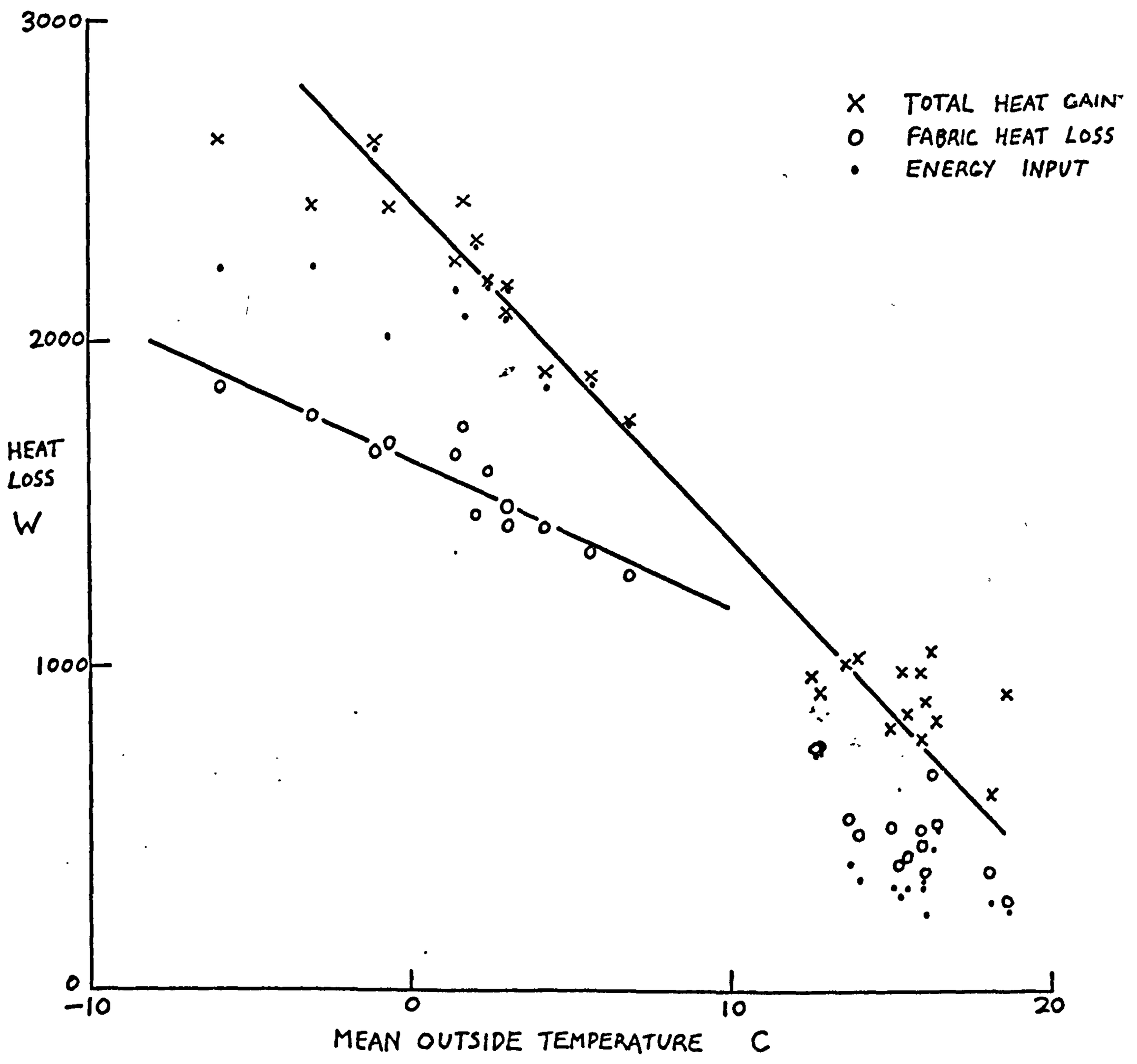

FIGURE 5.4

Energy Flows in Test House with Double Glazing

	a_o	a_1	coefficient of determination
Single glazing fabric loss	1856	-55.9	.75
Total heat gain	2582	-100.9	.87
Double glazing fabric loss	1642	-46.3	.85
Total heat gain	2454	-104.3	.91

Table 5.4

Regression Data for Figures 5.3 and 5.4

(b) Energy Input

This is the consumption of electrical energy in the spaces to maintain room conditions according to the operating schedules. These values differ from the fabric losses by amounts dependent on the ventilation losses and the direct solar heat gains. The scatter of these points is due mainly to the effects of direct solar heat gain in the spaces.

(c) Total heat gain

To account for the scatter a solar gain term was added and a best fit regression line obtained that corresponds to the total heat gain in the spaces. The solar gain term is a constant proportion of the solar radiation falling on the south facing vertical

wall of the house, since most of the solar gain to the spaces will be absorbed on this facade. The regression constants and coefficient of determination are given in Table 5.4. Again these lines were computed using only the winter data, but in this case the same regression lines pass through the summer data also, using the same solar gain term. In view of the previous comments regarding the non-linearity of the fabric loss data, this is probably a fortuitous result, but it gives us an opportunity to assess the magnitude of solar effects on this particular house construction.

The mean solar gain effect amounts to 3.2 times the solar radiation incident on the south facing external surface per unit area. Since the total area of this surface is 17.7 m^2, the effective solar gain to the internal spaces is 0.18 times the total solar gain incident on this external surface. For the winter period studied, the effective mean solar gain amounts to 83.8W. This compares with a mean total heat gain of 2312W in the case of single glazing, i.e. the effective solar gain is 3.6% of the total heat gain for the period of study. Another way of putting this is to say that the required heat input is offset by solar gains to the extent of a 3.6% reduction. The equivalent reduction for double glazing is 3.9% due to the reduced fabric loss. During the summer period, the mean effective solar gains are 17% and 18% of the total heat gain for single and double glazing respectively.

Ventilation accounts for most of the difference between the values corresponding to (a) and (c) above. Thus, in winter, the mean ventilation loss with single glazing amounts to 26% of the total heat gains as compared with 24% of the heat input as given in Table 4.2.

Summary of Chapter 5

The test house modelled with double glazing illustrates the complex heat transfer that occurs at windows. The comparisons are extended to a summer and winter period using Abbotsinch weather data. A study of the results shows the relative contributions of solar gains and ventilation to net energy requirements.

CHAPTER 6

THE PREDICTION OF VENTILATION IN BUILDINGS

6.1 INTRODUCTION

Prediction of infiltration, ventilation and air movement in buildings have always been the least certain aspects of thermal performance assessment with numerical values subject to arbitrary selection in most design techniques. The computer model described previously has successfully overcome the problems associated with the solution of a network with non-linear relationships for the flow through branches between nodes. The use of computerised techniques also enables the model to utilise climatological data containing hourly values of wind speed and direction.

There still remain problems of calculating the effects of building occupancy which have a larger effect on ventilation than on any other single aspect of building thermal behaviour. The difficulties of allowing for the wide variation in crack sizes around windows and doors have also to be considered. These variations in component tolerances again probably affect the validity of ventilation prediction more than the smaller variations in fabric thermal properties affect the other thermal calculations. This is because thermal properties are more readily measured and remain more consistent between samples.

One other aspect of ventilation which has up to now been neglected is the effect of turbulence in the wind on ventilation in buildings. Air does not flow around buildings in a steady streamline manner but as a turbulent

flow with large fluctuations in velocity and direction, and hence pressure, at any point. These fluctuations are present in the natural wind as it blows across the earth's surface as a boundary layer flow. Buildings also generate turbulence which adds to the complexity of assessing these effects on ventilation. We will now consider in turn the problems of predicting the effects of two of the factors described above.

6.2 OCCUPANCY

One approach to this problem is to consider it in two logical stages. Firstly the prediction of the presence of occupants and secondly their behaviour as affected by the room environment. It is not expected that this technique would accurately predict hour by hour occupancy and window openings, but that the seasonal variations in the effects of occupancy on ventilation and hence energy consumption in buildings will be simulated.

6.2.1 Estimation of Occupancy

One way of establishing occupancy in a building is simply to assign numbers to each space at different times of day. Whilst this is perhaps valid for large office buildings, or schools, a technique which embodies the inherent randomness of building occupancy is more realistic, particularly for smaller buildings. Let us

assign, for each type of space, time dependent probabilities that

(a) a person in a room will leave

(b) a person absent from a room will enter.

Movements to and from each room are determined at each time step by applying a uniform random number generator to each of these probabilities. The total number of people in a room is constrained to lie between zero and some maximum nominal number.

The room occupancy for an office, for example, would vary from empty overnight to full nominal occupancy during working hours, with occasional departures and arrivals during the day. Lunch breaks, etc. can be simulated easily using this approach, with separate probability functions for different week days. A separate total is kept of the number of movements at each time interval. This is later used to modify the air flow characteristic of doors in each room allowing for the time a door is opened.

More complex probability distributions could be assumed than the simple uniform distribution suggested here, but it is unlikely that anything more elaborate could be justified on the basis of improved predictive performance in relation to the amount of computation required.

6.2.2 Effects of Occupancy

Occupants in each space release heat and moisture to the space. These are added directly to the air as heat and moisture inputs.

As mentioned above, door opening varies according to occupancy. Window opening is also controlled by occupants, but in a more complex way. In a naturally-ventilated building window opening is dependent on the sensation of comfort perceived by occupants. Other factors, notably high moisture content and smell, are important, and the relative effect of different factors varies according to the type of building. However, only comfort will be considered here as an influencing factor.

In each building space, air temperature, mean radiant temperature, and moisture content, are known. Using this data, and assuming values of internal air velocity, the Predicted Mean Comfort Vote can be estimated using the equations for heat balance and thermal response developed by Fanger (49). The equation used is reproduced in Appendix 5 and is quite easy to solve iteratively for Predicted Mean Vote. Positive values of P.M.V. indicate "warmth" sensation and negative values indicate "cool" sensation. If a room window is closed at any time step, and the P.M.V. with zero room air velocity, is greater than 1.5 (between slightly warm and warm) the window is opened. If a window is already open, and the P.M.V. with a room air velocity of 0.3 m/s is less than -1.5 (between slightly cool and cool) the window is closed.

Clothing is assumed to vary to the extent that an occupant is likely to, say, remove a jacket, before opening a window, or replace a jacket before closing a window. By altering the "clo" value in the calculation in accordance with the window opening position, this effect can easily be incorporated.

6.3 WIND TURBULENCE

6.3.1 Previous Work

When air flows around a building with openings to its interior, air flow through the openings will be encouraged by a variety of factors which can be broadly classified into two groups: those which induce steady flow by virtue of their mean value, and those whose effect is due to their fluctuating nature. Factors which fall into the first group include the mean wind pressures on the building surfaces and the effect of temperature differences between inside and outside the building. The effect of the second group of factors becomes apparent if one considers the ventilation that takes place in a sealed room with only one window open to the outside. The mechanism whereby air exchange takes place across such an opening due to fluctuating external air velocity is obviously fairly complex and consists of a combination of effects. A low frequency variation in pressure at the opening will induce a fluctuating flow due to the compressibility of the air in the internal space. Higher frequency fluctuations will enable air exchange at the opening due to smaller scale turbulence with eddy sizes comparable with, or smaller than, the opening size, providing an additional contribution to ventilation in the internal space. If more than one opening exists then a fluctuating flow will be set up dependent on the correlation between the pressures generated at each opening.

Each of these factors will depend on a variety of parameters, e.g. the sizes and shapes of openings, the nature of the external air flow at the openings, the size of the internal space, and the magnitude of any net mean air flow through the openings.

Malinowski's experiments (50) using a model with air flow passing across the openings in a direction parallel to the wall containing the openings demonstrated some of these effects. He showed that ventilation rate increases as the spacing between two coplanar holes is increased, as mean air velocity is increased and, for a given mean air velocity, as turbulent intensity is increased. He also showed the effect of different wall thicknesses, and various permeable materials in place of the simple hole. There was no attempt, however, to quantitatively correlate the air flows with turbulence in the external air stream. Harris-Bass et al (51) used a model consisting of a cuboid with an opening in each of two opposite faces parallel to the air stream. Experiments were carried out both in the wind tunnel and full-scale and good correlations were obtained between the two sets of results. Again no measure of turbulence or correlation with ventilation rates was made other than on an empirical basis. It would be generally useful to be able to predict, for any given configuration, the air flows that will result under sets of external conditions. A small study was carried out to examine the feasibility of generating such a predictive facility.

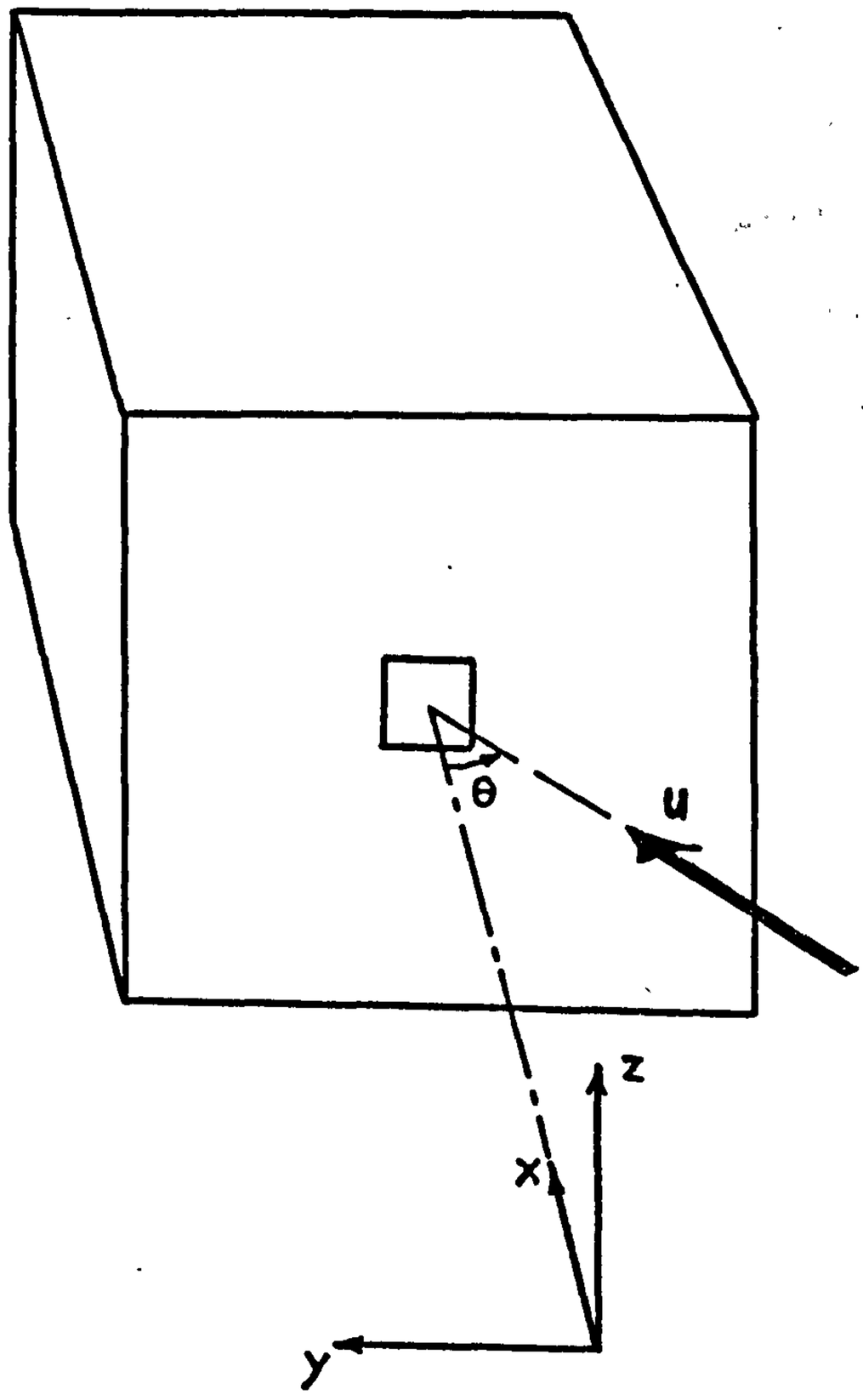

FIGURE 6.1 Schematic Diagram Showing Co-ordinate Representation

6.3.2 Derivation of a Simple Theoretical Model

Consider the case of an enclosure with only one opening in a plane wall, and an air stream moving with velocity u directed towards and impinging on the wall containing the opening (Figure 6.1) with components of velocity u_x, u_y and u_z in the x, y and z directions respectively. We define $u = \bar{u} + u'$ where $\bar{u}$ is the mean velocity and u' the fluctuating component with zero mean. Assume initially that $\bar{u}_y = \bar{u}_z = 0$, i.e. the airstream is directed along the normal to the plane surface containing the opening. As the airstream approaches the surface containing the opening, the x-component of velocity will decrease and the static pressure will increase. At the opening itself the mean velocities, denoted by $\bar{u}_x$, $\bar{u}_y$, $\bar{u}_z$ will all be zero, but the fluctuating components u_x', u_y', u_z', will not. This assumes that the opening coincides with the stagnation point of the airstream. There will be a fluctuating transfer of air through the opening in either direction. The low frequency content of the fluctuating velocity will produce a pulsating flow through the opening which will depend on the compressibility of the air in the enclosure, in other words, the size of the enclosure. Also at low frequencies, there will be a high correlation between velocities at different points within the opening. On the other hand, at high frequencies there will be a lower correlation between velocities at different points within

the opening. These high frequency fluctuations will produce a turbulent diffusion of air through the opening which will be less dependent on compressibility effects. The relative contribution to air flow through the opening due to fluctuations in different bands of the frequency spectrum will not be independent. For example a large, low frequency pulsating flow will tend to minimise the contributions due to smaller scale turbulence. For ventilation to take place within the enclosure, i.e. for a net exchange of air between the enclosure and outside to occur, some fraction of the fluctuating air flow passing through the opening must be mixed with the bulk of air within the enclosure, the remainder passing back out without mixing. This fraction will depend on the magnitude of the fluctuations, and on the spectrum of the turbulence at the opening, as well as the intensity of turbulence within the enclosure. It was decided to neglect for the present some of these factors and formulate a simple model to correlate external air flow with ventilation. Since it was expected that most of the turbulent energy would be contained in the low frequency part of the spectrum, and since the detailed analysis of the turbulent air motion at the opening would require quite an involved investigation and fairly extensive experimental work, it was decided to concentrate on the study of the low frequency pulsating air flow through the opening.

With the configuration of Figure 6.1 and the mean air flow directed along the normal to the plane of the opening, we will assume that the flow is quasi-steady, and that the stagnation pressure of the airstream is generated immediately outside the opening. Using the suffix a to represent conditions in the free airstream and o for conditions immediately outside the opening, the stagnation pressure of the air outside the opening p_o is given by

$$p_o = \tfrac{1}{2}\rho u^2 + p_a \qquad 6.1$$

where ρ is the density of the air, and

$u = u_{x,a}$, the x-component of velocity in the free airstream.

If we assume that the opening behaves as a sharp orifice and that the Reynold's number is high enough for Bernoulli's theorem to apply, then using the suffix i to represent conditions inside the enclosure and applying a coefficient of discharge C_D, the flow rate of air through the opening q is given by

$$q = \pm A C_D \left(2|p_o - p_i|/\rho\right)^{\frac{1}{2}} \qquad 6.2$$

where p_i is the static pressure inside the enclosure and A is the area of the opening. If we further assume that p_i is constant and equal to $\overline{p_o}$, we obtain from equation 6.1,

$$p_o - p_i = p_o - \overline{p_o} = \tfrac{1}{2}\rho\left(u^2 - \overline{u^2}\right)$$

Now, since $u = \bar{u} + u'$ and $\overline{u'} = 0$ we can obtain

$$u^2 - \overline{u^2} = 2\bar{u}u' + u'^2 - \overline{u^2}$$

and so

$$2|p_o - p_i|/\rho = |2\bar{u}u' + u'^2 - \overline{u^2}|$$

Hence substituting into equation 6.2

$$q = \pm A C_D (|2\bar{u}u' + u'^2 - \overline{u'^2}|)$$

and

$$\hat{q} = (\overline{q^2})^{\frac{1}{2}} = A C_D (2\bar{u}\,\overline{|u'|})^{\frac{1}{2}} \qquad 6.3$$

where $\hat{q}$ is the root mean square value of q.

As will be seen later, measurements of the mean airflow rate $\overline{|q|}$ into the enclosure are most readily obtained and we therefore require to relate the r.m.s. of q, as expressed above, to $\overline{|q|}$. Now if q is assumed to vary randomly and to be describable in terms of a Gaussian probability distribution, it can be shown that $\overline{|q|}$ is estimated by $(2/\pi)^{\frac{1}{2}}\,\hat{q}$; therefore

$$\overline{|q|} = A C_D (2/\pi)^{\frac{1}{2}} (2\bar{u}\,\overline{|u'|})^{\frac{1}{2}}$$

On the other hand measurements of $\hat{u}$, the root mean square of u' are more readily obtained than the mean $\overline{|u'|}$ contained in the above equation. Therefore by assuming that u' also varies randomly in a Gaussian manner, we can estimate $\overline{|u'|}$ by $(2/\pi)^{\frac{1}{2}}\,\hat{u}$ and thus,

$$\overline{|q|} = AC_b(2/\pi)^{\frac{3}{4}}(2\bar{u}\hat{u})^{\frac{1}{2}} \qquad 6.4$$

Clearly the assumption that both $u_{x,a}$ and q can be described in terms of Gaussian probability distributions cannot be strictly justified - they are related non-linearly as is shown in the derivation of equation 6.3 . However for the sake of simplicity we will use this assumption in order to obtain a simple function correlating these variables. Since $\bar{q} = 0$, the mean flow into and out of the enclosure being the same, the mean flow rate into the enclosure q_i is equal to $\frac{1}{2}\overline{|q|}$. Clearly all the air flowing into the enclosure, as represented by q_i does not necessarily contribute to the effective ventilation of the enclosure. Some of the inflowing "pulsations" of air will be exhausted before mixing has a chance to occur. This proportion will not be fixed by any means. As the frequency of the pulsating flow increases, with $\bar{u}$ and u' fixed, the amount of air mixed with the bulk of air in the enclosure will decrease, as the volume of the injected "slugs" of air reduces. In fact the frequency spectrum of the turbulent airstream will determine, in a complex way, the actual proportion of air involved in ventilating the internal space. We will call this proportion f. Therefore the net mean effective flow rate of ventilating air q_{eff} into the enclosure is given by

$$\overline{q_{eff}} = f\,\overline{q_i} = \tfrac{1}{2} f\,\overline{|q|} \qquad 6.5$$

The value of f would be expected to lie in the range $0 < f < 1$.

Measurements of $\bar{u}$ and $\hat{u}$ can be readily obtained using conventional instrumentation, and some measure of correlation with q_{eff} should be possible. However, since modern instrumentation allows us to record and electronically process varying signals, a slightly more sophisticated version of this simple model can be constructed which will still be capable of direct comparison with experimental results. This will overcome some of the inherent shortcomings of the foregoing analysis, avoiding the more gross approximating assumptions. It was stated previously that since low frequency turbulence was expected to be dominant, pulsating flow would occur through the opening and that this would depend on the compressibility of the air within the enclosure. The effect of compressibility has so far been neglected, and led to the simplicity of the above result. We will now develop the analysis further to include this effect. If we assume the enclosure to be an adiabatic system,

$$p_i (V_i - v)^{\gamma} = p_a V_i^{\gamma} \qquad 6.6$$

where V_i is the total volume of the enclosure, and $v = \int_0^t q\, dt$ represents the decrease in volume of the mass of air inside the enclosure at time $t = 0$, when $P_i = P_a$. Since $|v| \ll V_i$

and $|(p_i - p_a)| \ll p_a$, equation 6.6 can be simplified to

$$(p_i - p_a)/p_a - \gamma v/V_i = 0$$

so from equation 6.1,

$$p_o - p_i = \tfrac{1}{2}\rho[u^2 - (2\gamma p_a/\rho)\, v/V_i]$$

and substituting into equation 6.2 gives

$$q = \frac{dv}{dt} = \pm A C_D \left| u^2 - (2\gamma p_a/\rho)\, v/V_i \right|^{\frac{1}{2}} \qquad 6.7$$

Equation 6.7 is a non linear differential equation which can be solved for q given the velocity u. Hence q_{eff} can be obtained from equation 6.5 .

There is one more adaption which can be made where, in the context of building ventilation, the effect of variations in the direction of mean flow of the free airstream is of interest. Suppose the mean velocity is directed in the x-y plane towards the centre of the opening at an angle θ to the normal to the plane of the opening (Figure 6.1). Then

$$\bar{u} = \overline{|u_a|} \cos\theta \qquad 6.8$$

and this value can be substituted into equation 6.4.

At greater angles of incidence than, say, 60^{o}, the complexity of the flow is outwith the scope of this study.

In the foregoing analysis we have neglected to allow for the fact that there is considerable distortion of the flow in the vicinity of the opening, and this will undoubtedly affect the relative values of the components of turbulent velocity in the direction of the three co-ordinate axes. The above equation can only be described as an approximation and, at the level of this analysis, it is unlikely that we can proceed much further.

6.3.3 Experimental Study

In an attempt to assess these models for flow through an opening in a sealed enclosure it was decided to carry out an experimental investigation to correlate ventilation in the enclosure with turbulence in the impinging airstream with the intention of proceeding to full scale at a later stage. A large wooden box was constructed with dimensions approximately 1.2 x 1.2 x 2.4m. This was completely sealed except for a 15.2cm square opening in the centre of one of the small faces. The box was laid with this face lying in a vertical plane. A variable speed fan with an outlet 40.7 cm wide and 25 cm high was placed with the plane of the outlet situated 2.18m away from the opening and the centreline of the outlet lined up to the centre of the opening. When it was desired to reduce the intensity of turbulence in the airstream a 1.68m length of 40 cm dia. duct was inserted at the fan outlet. A D.I.S.A. Hot-wire anemometer operating in constant temperature mode was placed on the centre line of the fan, 30cm from the enclosure. This had a uniform

frequency response up to 250kHz, which was adequate for the purposes of this study. The instrument gave direct readings of mean and r.m.s. velocity to an accuracy within $\pm$ 3%. The ventilation rate was measured by releasing a small quantity of nitrous oxide gas into the box, allowing this to mix with the air in the box, and then measuring the decay in concentration of gas using an infra-red gas analyser and recording the output on a chart recorder. The effective mean ventilation flow rate q_{eff} was then obtained to an accuracy within $\pm$5% by the method described in Chapter 3.

A small circulating fan was placed on the floor near the centre of the box in order to maintain a uniform gas concentration within the box. The airstream from this fan was directed away from the opening. The air sample point was located at the inlet to this fan. The magnitude of ventilating airflow which occurred at the opening resulting from the action of this fan and the ambient turbulence in the laboratory was measured as 0.3 l/s, the highest velocities being about 50 mm/s in the region of the opening. This was considered to be an acceptably small background level. A Solartron HS7-3A analogue computer was programmed to solve equation 6.7. The anemometer signal was transmitted to the computer which evaluated q_i to an accuracy within $\pm$6%.

In order to assess the assumptions made regarding the spectra of the velocity fluctuations, recordings were made of the anemometer output signal during a number of test runs. These were later analysed using a B&K sound spectrum analyser.

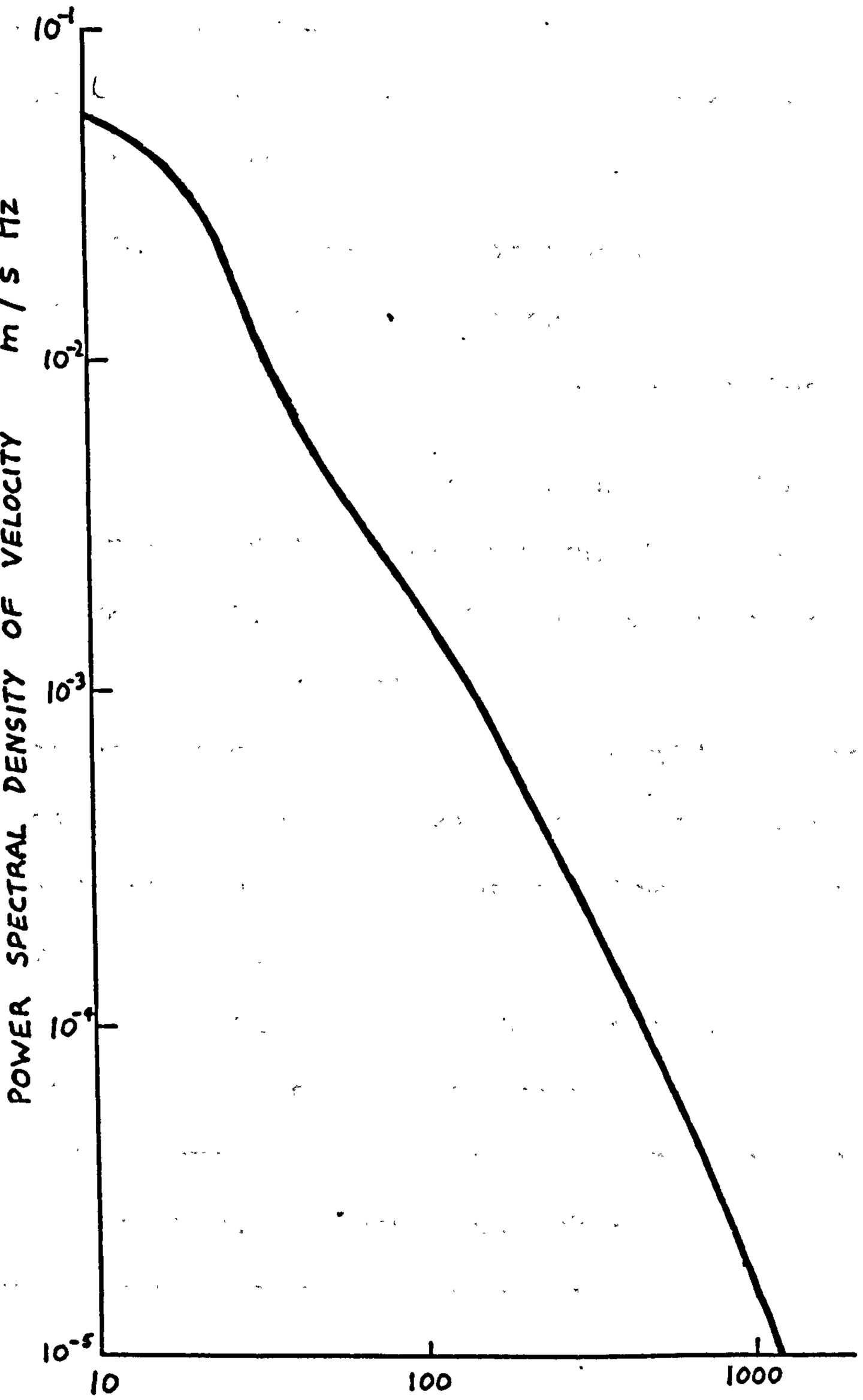

FIGURE 6.2 Power Spectral Density of Impinging Air Velocity

In addition, a sample of data was digitised and the power spectral density function evaluated by a digital computer program using the Blackman-Tukey method (52) and smoothing using the Hamming window function.

Experiments were conducted to assess, over a range of mean air velocities, the effects of:

a) two different intensities of turbulence;

b) two different sizes of opening;

c) airflow impinging normal, and at two angles, to the plane of the opening.

The spectral density function of a sample of digitised data is shown in Figure 6.2. There are no sharp peaks evident in the record. Certainly most of the energy is contained in large scale eddies, although smaller scale turbulence is present at frequencies up to 1000Hz. This could be interpreted as being indicative of the relative quantities of air transferred by a low frequency pulsating flow, and high frequency eddy diffusion.

The velocity magnitude spectra expressed as dB re the r.m.s. velocity were plotted against wavenumber k, which was obtained using the approximate relationship $k,=\omega/u$ where ω is the radian frequency. It was found that, for each of the two experimental configurations - one for high and one for low turbulent intensity - the spectra obtained for each record over the range of mean velocities fitted the same curve. The two curves, corresponding to mean values of $\hat{u}/\bar{u}$ of 0.252 and 0.104 for high and low turbulent intensities respectively are shown in Figure 6.3.

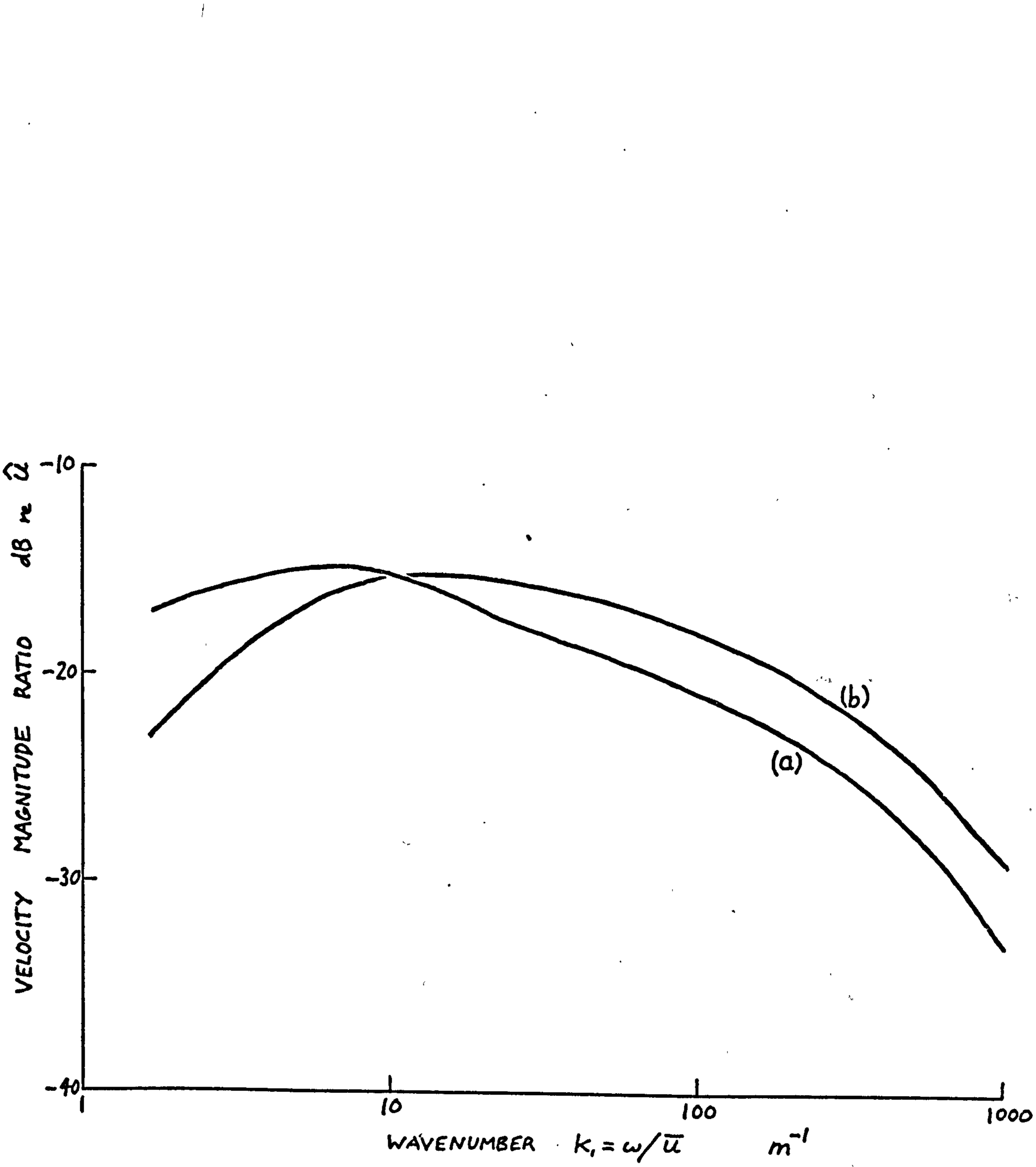

FIGURE 6.3 Velocity Magnitude Spectra

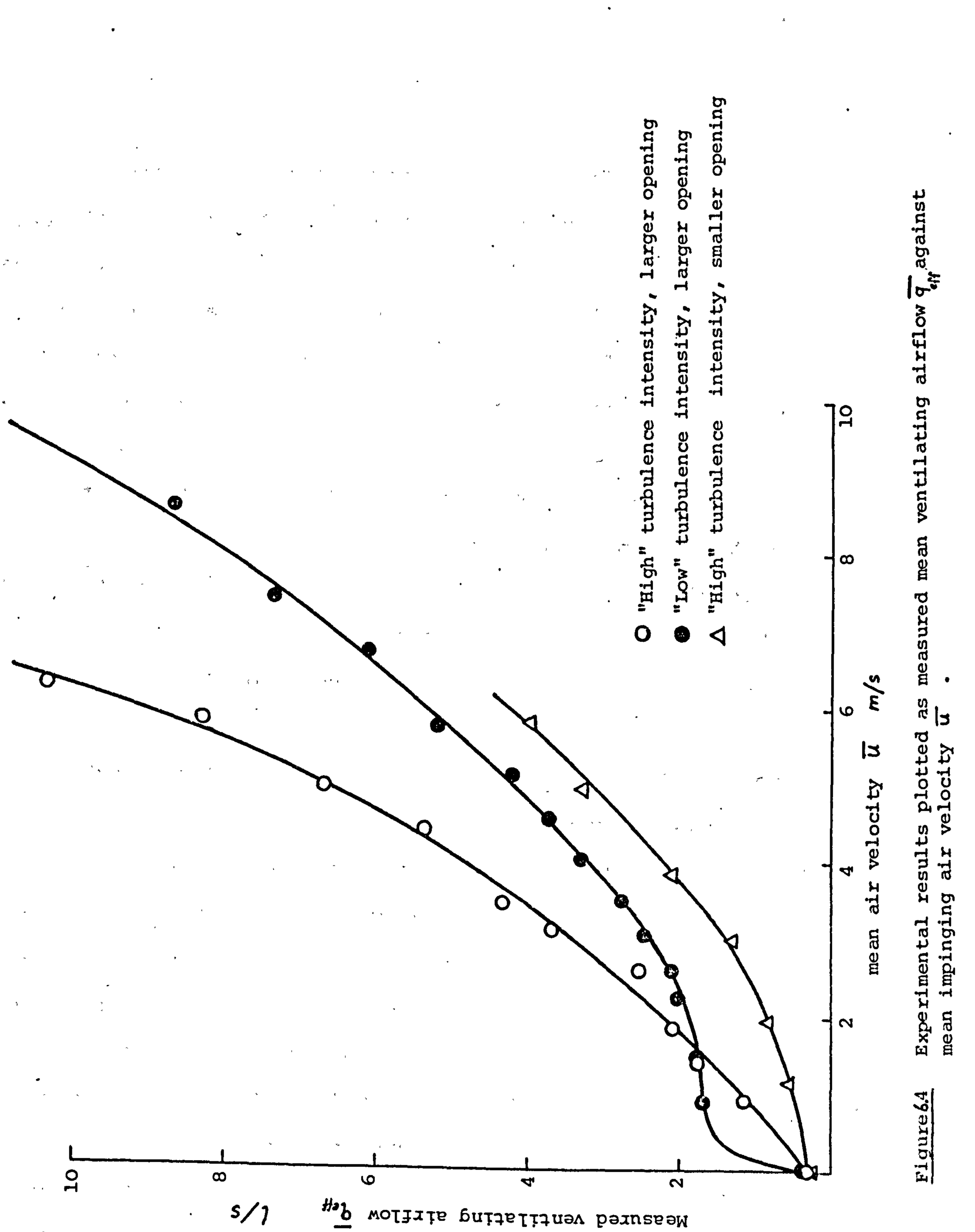

Figure 6.4 Experimental results plotted as measured mean ventilating airflow $\overline{q}_{eff}$ against mean impinging air velocity $\overline{u}$.

Figure 6.4 shows the measured ventilating flow rates q_{eff} plotted against $\bar{u}$. $\hat{u}$ was approximately proportional to $\bar{u}$ for each experimental configuration. The ventilating airflow was less at corresponding values of $\bar{u}$ when the turbulent intensity was reduced and less still with the smaller opening area. Clearly the mean velocity cannot be used to predict ventilation rates.

If the length of the opening side is taken as a characteristic dimension, then at a velocity of 0.5 m/s a Reynold's number of about 5000 is obtained. Therefore, within the limits of our assumptions, the models derived previously ought to be valid over the range of variables tested.

The results for airflow normal to the opening using the simple model and the analogue computer model are shown in Figure 6.5. A value of $C_p = 0.65$ was assumed. q_{eff}, as measured by gas concentration decay is plotted against the computed flow inwards through the opening, q_i. There is a substantial difference between the correlation obtained for the computer model and the simple model which ignored compressibility and the frequency distribution of the velocity. The fact that both curves have a mean gradient less than unity demonstrates a mean value of f in equation 6.5 of between zero and one. The gradient of the linear section of the graphs in Figure 6.5 gives a value of $f = 0.37$ in other words, only about one third of the airflow passing into the enclosure is ultimately mixed with the bulk of the air within the enclosure.

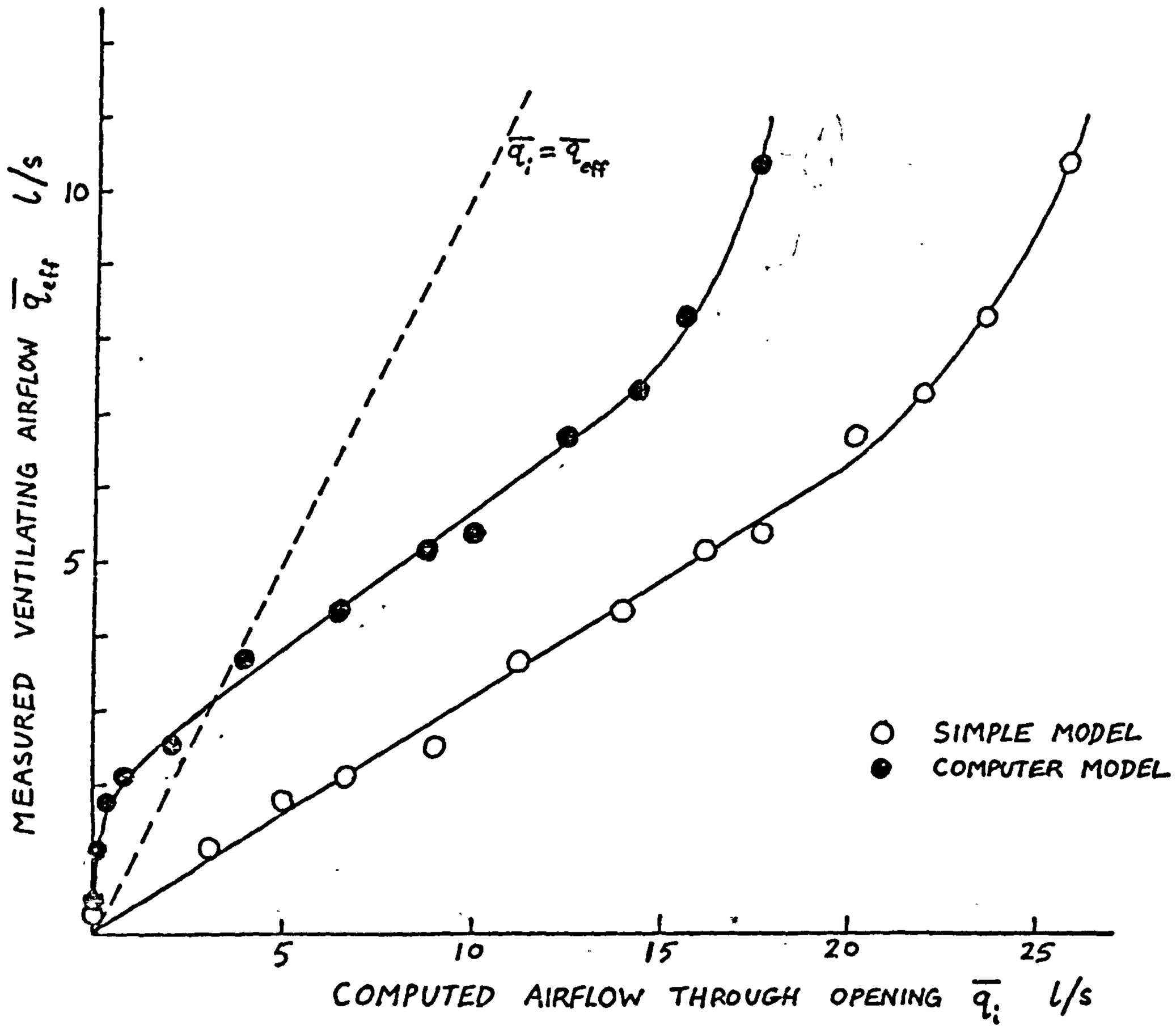

FIGURE 6.5 | Measured Mean Ventilating Airflow $\overline{q}_{eff}$ Plotted Against Computed Mean Airflow Through Opening $\overline{q}_i$

The interpretation of the shape of the curve for the computer model may shed some light on the physical processes involved in the air transfer through the opening. As the air velocity increases from zero, the measured ventilation rate increases quite rapidly. At these very low speeds the pulsating flow will be minimal and small scale eddies will have maximum effect, encouraging turbulent diffusion at the opening. This is not accounted for in the model and hence the initial gradient of the curve (1/f) is high. As the velocity increases this smaller scale turbulent diffusion is masked by the increasing pulsating flow due to low frequency velocity fluctuations. Therefore, although the relative quantities of energy in the wavenumber spectrum remain unaltered, the higher frequencies have less effect on q_{eff} and hence the errors inherent in the model are reduced. Also the gradient of the curve is less than unity indicating the proportion f of the airflow entering the enclosure which mixes with the air inside the enclosure. A possible cause for the levelling off effect at very high velocities could be the fact that, as the turbulence within the enclosure increases due to the increased activity at the opening, so the value of f is increased.

Figure 6.6 shows the effect of reducing turbulence intensity by inserting a length of duct at the fan outlet. These results correlate reasonably well with those for the high turbulence case. The results obtained when the size of the opening was reduced to 10.15 cm square are also shown in Figure 6.6. This corresponds to an area of 44.5% of the

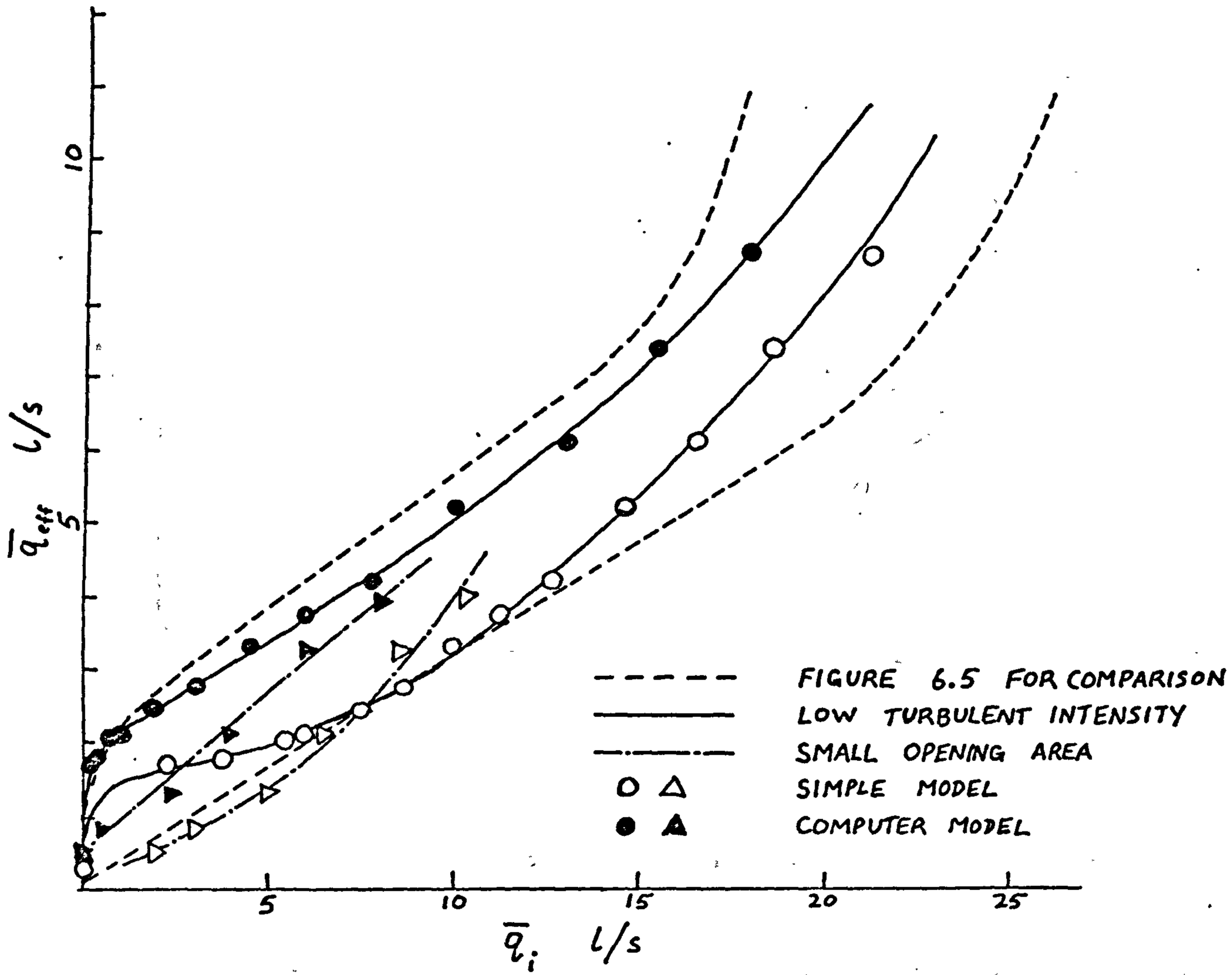

FIGURE 6.6 Measured Mean Ventilating Airflow $\overline{q}_{eff}$ Plotted Against Computed Mean Airflow Through Opening $\overline{q}_i$ for Low Turbulent Intensity and Smaller Opening Area

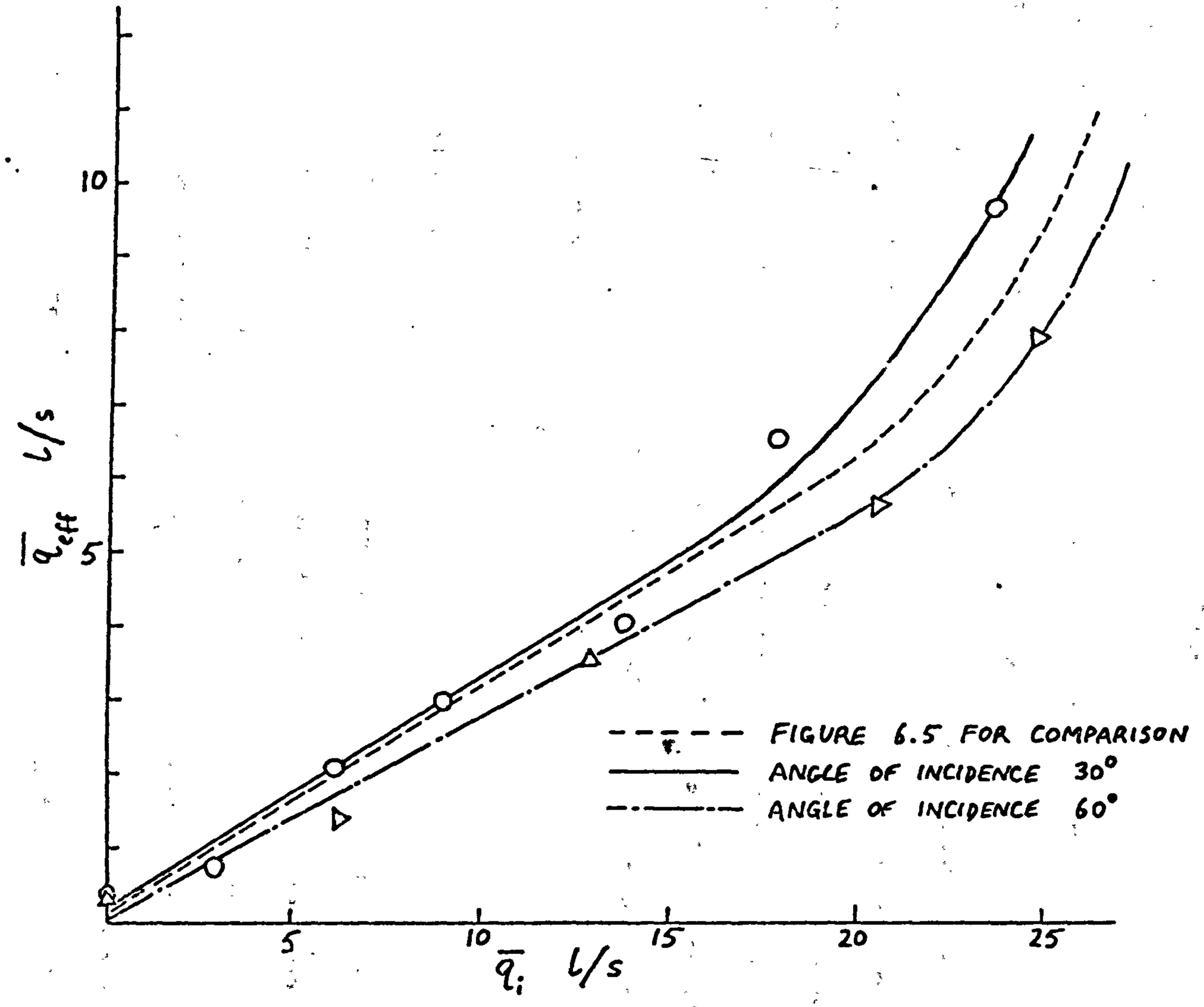

FIGURE 6.7 | Measured Mean Ventilating Airflow $\overline{q}_{eff}$ Plotted Against Computed Mean Airflow Through Opening $\overline{q}_i$ for Angles of incidence of 30° and 60°

original opening. Although the shapes of the curves differ from the results using the larger opening the mean gradients remain unaltered. One effect of reducing the opening area is to reduce the effect of small-scale turbulent diffusion throughout the velocity range. The absence of a high gradient portion at low $\overline{q_{eff}}$ in the curve of Figure 6.6 for the adapted model supports this argument.

For experiments using airflow from two different directions - one at 30^{o} and one at 60^{o} to the normal to the plane of the opening - the modification discussed previously was made to the simple model to account for the change in direction of the impinging airstream. The results are shown in Figure 6.7. Again a reasonably good agreement with the original curve was obtained.

6.3.4 Conclusions

Clearly the physical processes involved in this type of airflow are much more complex than has been given credit for in this discussion and more theoretical and experimental work would be necessary to investigate the relative magnitude of the various effects discussed here. Nevertheless the experimental work provides consistent results which suggest that further work would be rewarded with better correlation between theory and experiments. It is interesting to note that in this investigation the more complex computer model did not provide significantly better overall correlations than the simple model, despite the

apparent shortcomings and assumptions inherent in the latter. The work described does show that about one third of the fluctuating airflow into the enclosure was finally mixed with the bulk of air in the enclosure.

Summary of Chapter 6

Some of the difficulties of estimating ventilation in buildings are discussed. An approach to the estimation of the effects of occupancy is described. The effects of wind turbulence on ventilation has been investigated using a model, and a theory for predicting this component of ventilation in an idealised case is tested.

CHAPTER 7

CONCLUDING DISCUSSION

7.1 REVIEW OF THERMAL SIMULATION TECHNIQUES

Before examining the way in which future developments might enable complex thermal simulations to become firmly established in practice, the scope of the computer program described and used for this thesis will be reviewed. This will indicate those areas where more work is required and will enable an assessment of the validity of the overall approach to be made.

7.1.1 Solar Radiation

The solar radiation calculations described in Chapter 2 enable predictions of solar radiation on any plane for any atmospheric conditions and at any site. They are almost absolute predictions, relying to a minimum extent on empirical constants, and can be applied universally at any site. The calculation procedure is lengthy however, although in terms of computation time, not excessive compared with the total time required to run the complete thermal simulation model. Some simplification in the calculation procedure could be usefully accomplished, probably the most obvious simplification being to reduce the number of wavebands to below the present 22. This would affect the accuracy of the computation to some extent and the amount of simplification possible would be largely dependent on this. Corrections for ozone and carbon dioxide are secondary and could probably be removed altogether, provided sufficient allowance was made in the other transmission coefficients.

7.1.2 Conduction

The calculation methods for conduction through building fabric are extremely efficient and are as accurate as the input data allows. This is particularly so in the air cavities where the coefficients (strictly convection and radiation) can be made dependent on the direction of heat flow. The main problem here is the acquisition of reliable thermal property data for the fabric. At present there is no allowance made for variations in conductivity dependent on moisture content, for example. This could easily be incorporated into the existing model if adequate data were available, and if a method were found for computing moisture content given the weather data (humidity, rainfall, etc.) already present in the weather data input to the program.

7.1.3 Convection

The present method is far superior to any previous technique, but still does not depend on internal air movements. The difference in convection coefficient for a wall in a naturally-ventilated and an air-conditioned room is probably significant, and a means of allowing for this would be desirable. On the other hand, the calculation of a non-integer power at every time step is probably unnecessary, and a simpler, temperature dependent, correction factor could be used.

The external convection which is clearly wind dependent, needs more investigation. This is an important factor in building heat loss calculations, particularly at windows.

7.1.4 Radiation

By far the most time-consuming part of the overall calculation procedure is the estimation of internal radiation transfers. Even with only six surfaces in a room, fifteen radiative interchanges are involved, and there is clear scope for a reduction here. As was shown in Chapter 4, a manual calculation using the environmental temperature concept is consistent, and a compromise could probably be attained using a mean radiant temperature for all room radiation exchanges. This would reduce the number of interchanges from fifteen to six, and would reduce computation time by an even greater ratio. The very sophisticated angle factor calculation procedures would no longer be required. This is unfortunate, considering the effort expended in developing the routines, although other applications may exist, for example in the computation of daylighting.

The study of heat transfer at windows in Chapter 5 showed the importance of including the effects of outgoing radiation at the external surfaces of a building. This is clearly an atmosphere dependent phenomena, and its inclusion is a positive step towards better energy prediction techniques in buildings.

7.1.5 Air Temperature Calculations

The calculation of air temperatures in rooms relies on the assumption that the heat input and surface heat transfers

to the room air apply homogeneously throughout the room volume. This is clearly not the case, as is evident in Chapter 4, where the rate of heat input in the model caused much more rapid temperature rises than was measured in the test house rooms. Heat is transferred to room air which is heated locally and causes convection currents to be set up. This air movement, along with ventilation induced air movement, distributes the heat by diffusion and turbulent mixing to other parts of the room. This mixing is never perfect, and some stratification will always be present. A model which takes account of these air movements is required. Although the present model includes a stratification effect, this is a relatively crude, fixed, correction. A more realistic, dynamic technique is necessary.

7.1.6 Ventilation

The present model is unique in the concept of providing simultaneous air and heat transfer calculations. However, there remains much work to be undertaken before ventilation can be fully modelled. Chapter 6 indicates some of these aspects but a broader review will follow in Section 7.2.

7.1.7 Occupancy

The estimation of occupancy and its effects on building usage will never be attained with the same reliability as calculations of the physical behaviour of buildings. It is

not necessary in the majority of applications to have a precise simulation of building occupancy. To be able to model the essential characteristics of occupancy will suffice in most practical instances. As was discussed in Chapter 6, occupancy has its least predictable effect on ventilation in naturally ventilated buildings, and a major step forward is offered by the procedures suggested there. More work is required to refine these techniques to model different occupancy types, and to include other motivation effects besides comfort.

7.1.8 Mechanical Systems

The program described in Chapter 2 is currently able to model energy inputs and air flows in buildings, but actual plant items such as boilers, water circulation systems, chillers, and so on, which are required to enable estimates of actual energy consumption in buildings, are not yet included. The electrically heated test house was easy to model in this respect, but more complex non-electric services will require more sophisticated plant modelling routines. To be universally applicable a modular approach is required, so that a single system, e.g. domestic boiler, water circulation system, radiators and thermostat/timer control, can be modelled, whilst on the other hand, complex systems incorporating heating and cooling, energy recovery, modulating controls, external temperature compensation and so on, can be assembled into the model. The existing program, with its network concept, can be extended so that

the branches represent plant items and the nodes represent the points of energy and air transfer between plant items. This can already be done to a limited extent by making the branches represent air ducts and fittings, and the nodes the points at which ducts branch.

The expansion of the program to include mechanical systems in this way will open up a new range of applications beyond building design, as will be discussed in Section 7.3.

7.1.9 Conclusion

The results presented in Chapters 4 and 5 are indicative of the value of having the ability to model the thermal performance of a building in more detail than a manual method permits. There are practical drawbacks, to be discussed in Chapter 7.3, and there are several areas where more work is required to improve the quality of individual aspects of thermal modelling.

However, every improvement in a particular aspect has a far greater effect insofar as the whole modelling technique gains from such improvements. The following list summarises those aspects of thermal modelling which gain most from computerised techniques.

Non-linear heat transfer at building surfaces.

Thermal storage in building fabric.

Solar radiation effects.

Use of actual weather data.

Ventilation.

7.2 VENTILATION

Ventilation is probably the one topic that presents the most problems and needs the most further work done to improve predictive techniques. There are several aspects which require attention and these will be dealt with in the following discussion.

7.2.1 Wind and Building Surface Pressures

The characteristics of the natural wind are well understood, but the local effects of surrounding buildings and structures are difficult to predict, and some work is needed in this field. It should be remembered, however, that the desire for accurate prediction techniques must be tempered to some extent by the knowledge that other aspects, for example building occupancy, can have large effects on ventilation and that if these other effects can be estimated to within, say ±20%, there is little to be gained from predicting wind velocities and turbulence to within ±2%. Wind tunnel studies have always been a valuable tool in the past, and it is possible that large scale three-dimensional matrix techniques could supplement these studies in an effort to improve our understanding of local wind around buildings.

Building surface pressures cause the actual air flows in buildings and again wind tunnel studies are invaluable. A technique which does not require a series of wind tunnel tests for every new building is needed. This could also be the product of three-dimensional modelling techniques.

7.2.2 Open Windows

The study of wind turbulence and its effects on a single opening discussed in Chapter 6 are directly relevant to natural ventilation in buildings. It is unlikely that wind tunnel studies will ever be of value in predicting air flows through open windows because of scaling difficulties, and full-scale work is therefore required. There are several different types of flow which can occur, as described in Chapter 6. When more than one opening exists the flow depends on the correlation between turbulence effects at each opening, and this could lead to quite complex requirements for the description of the wind pressures and air flows around buildings.

7.2.3 Air Flows Within Buildings

The model described in Chapter 2 calculates air flows within buildings using an efficient technique that is ideally suited to incorporation into the thermal simulation, and utilising the same network to describe air and heat flows. The calculation of room air movement and its effects on surface convection coefficients and room air mixing are required for a complete understanding of air flows within buildings. This was discussed in Section 7.1. Clearly the effects of air flows at open windows and the turbulence effects already discussed will have its implications here. The problems that remain are those of determining exactly where the air flows and leakages take place, and what values

to use to describe the cracks and other restrictions that form the network. This was a major difficulty in the comparisons with measurements at the test house.

7.3 THE ROLE OF THERMAL SIMULATION TECHNIQUES

7.3.1 Design of Buildings and Mechanical Systems

Simulation of the energy flows in a building using the computerised methods described in this thesis have clearly a role in the design of buildings and mechanical systems in buildings. The use of computers has a number of clear advantages which have already been discussed. There are practical drawbacks however, which will now be considered.

Although the techniques used in developing the program enabled large quantities of file data to be referenced, avoiding the need for direct input of frequently recurring construction properties, weather data, and so on, there was still a large quantity of input required to the program, and this can be time-consuming to enter, as well as being a potential source of errors. The simplifications in calculating internal radiation exchanges suggested in Section 7.1 would remove the requirement for a large portion of the geometric data required at present. It is very important nevertheless, that data input routines should check input for range and compatibility. Graphical input techniques would be the most valuable in minimising the error rate, as well as speeding up the data input process.

Provided programs based on these general guidelines can be developed, it is probable that practising designers will accept some additional time overhead in return for the advantages of more accurate, reliable and versatile design, than current manual methods can offer.

7.3.2 Energy Targets

A possible application of computerised methods of building energy consumption estimation are in developing energy targets. These targets are used by building owners and energy managers to assess the standard of building energy use in individual cases. The target figure is not an estimate of the energy consumption of an actual building, but is an estimate of the energy consumption in a building with the same internal occupancy and general dimensions, insulated to a good standard in relation to current practice, and with properly designed, installed and maintained heating and cooling services. It is therefore a figure that one might not expect to achieve in practice, but which one may use to indicate those areas needing attention in respect of insulation or services.

There is therefore a belief that the techniques used for deriving such a target figure need not be rigorous, and that an approximate estimate of energy consumption in an idealised case is adequate. This is not the case. Although a target does not represent an estimate of actual energy consumptions, it does represent a figure to which actual

consumptions are being compared, and, if inconsistent errors occur, credibility will be lost. A computerised technique for energy consumption calculation can enable targets to be computed with the necessary accuracy, and using weather data applicable to the sites under consideration.

7.3.3 Design of Plant

Insulation of buildings is now a very popular method of energy conservation and new products are continually appearing on the market. Novel items of mechanical plant are also under development as more sophisticated energy conservation techniques are exploited.

It is now possible, using the computer model as a theoretical "test-bed", to carry this development work to a more advanced stage than was previously possible, before prototype trials are required. This applies particularly, for example, to heat recovery devices, where the optimum device will take maximum advantage of the availability and requirements of energy in a range of applications under different climatic conditions.

Such a tool could be developed even further, to include such complexities as simultaneous heat and power generation, and could be used directly for large projects to enable accurate load matching and feasibility studies to be carried out in individual cases.

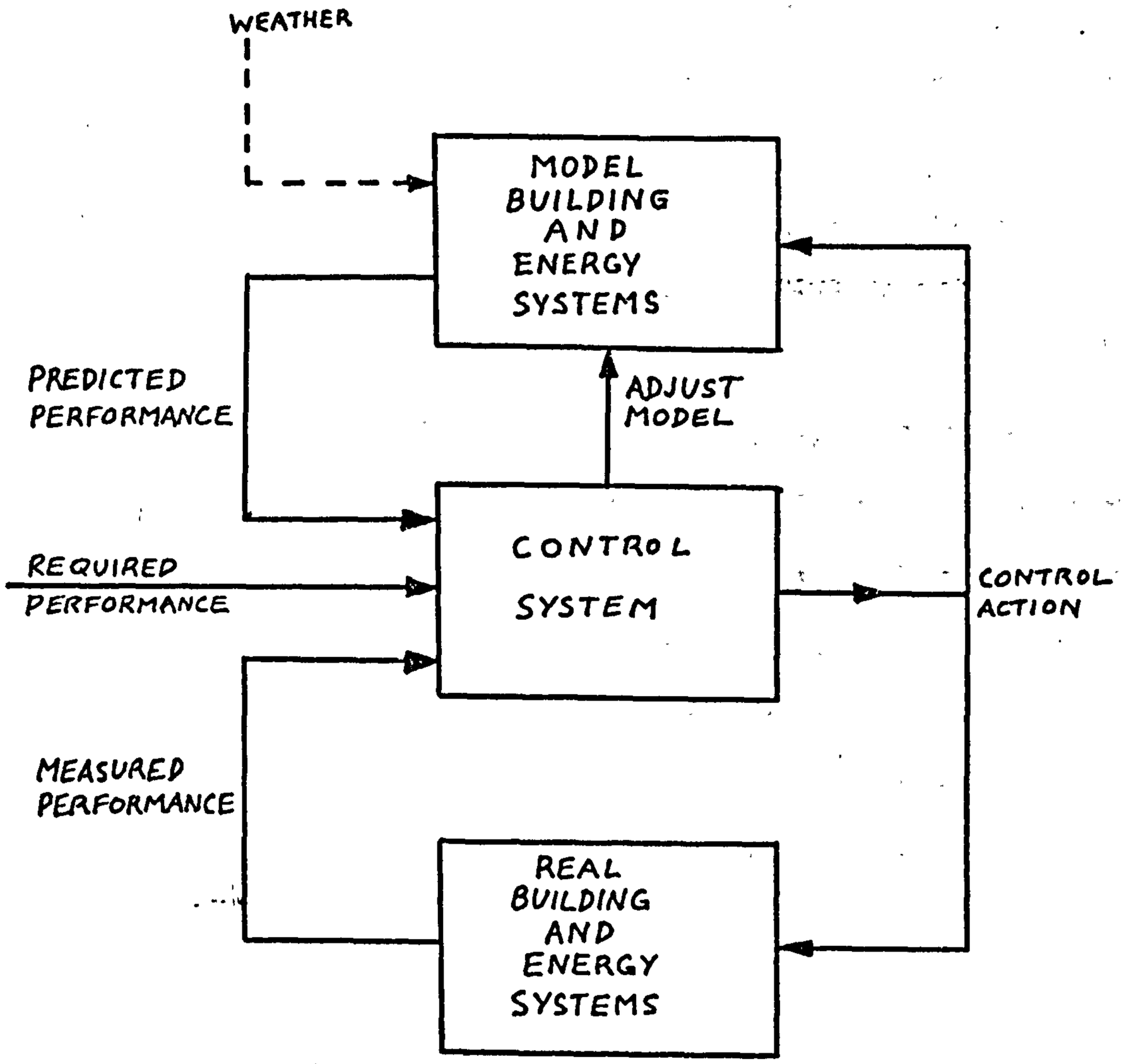

FIGURE 7.1 Use of a Thermal Model in Building Services Control

7.3.4 Control Systems

In large and complex building projects, the installation of control systems can represent a large portion of the total services contract, and a need exists for designers to be able to compare different approaches and to enable comparative predictions of energy savings. This may permit the approval of more expensive techniques which can be shown to have advantages over simple control systems.

The model described in this thesis, extended to include plant and associated control systems, would enable the very complex interactions to be modelled in a way which, hitherto, has not been possible. The full effects of, for example, external temperature compensation, and computed optimum pre-heat time, could be modelled and as a result the cost of these additional energy saving items may more readily be justified.

It is even possible that, in future buildings incorporating computerised systems control, the control program might include a model of the actual building, with actual internal and external conditions used as input to predict optimum control policy on a real-time basis. Building services systems would thus respond accurately to varying conditions the instant these variations occur.

Figure 7.1 illustrates a possible arrangement for such a scheme.

7.4 CONCLUDING STATEMENT

It is believed that the development of computerised energy prediction techniques, based on the program described in this thesis, will improve the way in which buildings are designed at present, and will enable more emphasis to be placed on the conservation of energy, in relation to both building design and plant systems design.

Furthermore, a wide range of additional applications will become available which will extend the potential for energy savings in buildings even further, allowing the manufacturers of plant items access to design methods which are at present unavailable.

The effect of these advances in building services technology will be beneficial to the building services profession as a whole, and to its interaction with the other professions involved in the design process.

APPENDIX 1

AIRNET - COMPUTER AIDED THERMAL AND VENTILATION ASSESSMENT BY SIMULATION.

Introduction

This suite of programs enables the air and heat transfer within a building to be simulated in a stepwise fashion, using actual meteorological data as supplied by the Meteorological Office on magnetic tape as input.

Account is taken of the convective and radiative heat transfers at all the external and internal building surfaces, and the conduction of heat through composite materials including air-spaces contained in either horizontal or vertical partitions. Air flows are calculated on the basis of the flow equations at each crack or opening in the building fabric, and internal flows can be bi-directional at large vertical openings where a temperature difference exists across the opening. The effects of solar radiation on all the external surfaces is accounted for, as well as the transmission through window glass and subsequent dissipation internally.

The geometric data structure can be conceived of as a network of communicating branches between nodes (see figure). Each branch represents an interface such as a wall, floor, or ceiling, between two spaces, such as rooms, stairwells, corridors.

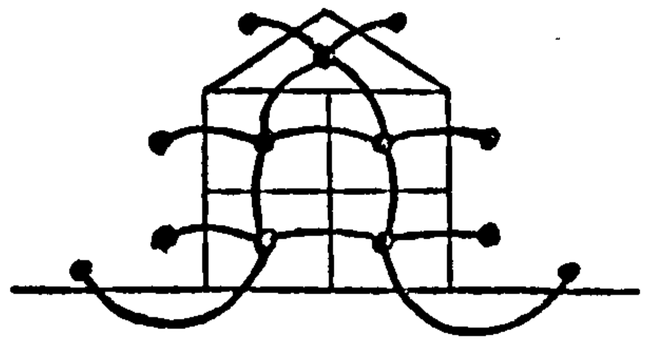

If the branch is an interface between a room and outside, then the outside "space" is conveniently described as the external surface.

Internal spaces are considered to be cuboid shaped. More complex shapes can either be approximated to be cuboid, or represented by two or more adjacent cuboids. Each of the six cuboid surfaces is defined as a main surface for the bounding interfaces, and the surfaces of co-planar interfaces such as windows and doors are specified as sub-surfaces. Internal inclined surfaces cannot be modelled. However, solar radiation on, for example, a sloping roof, is accurately determined by specifying the attitude of the external surface when inputting "space" data. The internal surface of such a partition can be approximated by either a vertical partition, a horizontal partition, or one of each.

The bulk of material properties are stored in data files, and are retrieved by specifying a particular composite structure for each partition, along with co-ordinate data which locates each particular component in the simulation network. This approach has reduced the amount of data input to a minimum.

The suite is divided into a number of main program segments which communicate via common data files and access a subroutine library for performing specific functions, such as calculation of solar radiation, or solution of heat transfer equations. These programs can be executed interactively, and rapid editing facilities enable assessments of modified structure, services, orientation, or indeed any input variable. The effect of re-siting a building can be evaluated simply by changing the Meteorological Office tape used for climatological data input.

1. RDSPDA - read, check and edit space data.
   For each building space (represented by a network node and hence including the external building surfaces which enable boundary conditions to be fixed) the following data is required.

(a) Type of space; e.g. internal room, section of corridor or stairwell, external surface. If a space type is specified as "external surface", then only item (c) of data is required.
(b) Maximum occupancy.
(c) Space dimensions or external surface orientation.
(d) Zoning of space (for heating control).

In addition, the thermostat upper and lower switching points in each zone may be specified.

2. RDINDA - read, check and edit interface data.

For each interface between building spaces through which air, heat or both are transferred, the following data is required.

(a) Interface type: e.g. external wall, internal partition, floor on ground, intermediate floor/ceiling, roof, window, door, stairwell or corridor interface, air supply or extract, heat supply (controlled by a zone thermostat).
(b) Interface class: this enables data on composite constructions such as thermal properties, air flow/pressure relationship, and surface heat transfer properties to be retrieved and incorporated into a secondary input data file by INITAL.
(c) Positive and negative space identifiers. The positive and negative surfaces of each interface type are defined by convention and the specification of the spaces on either side locates the interface as an interconnecting branch between two nodes.
(d) Airflow areas. Normally a closed and open flow area is specified which in the case of a window indicates the range of openings available, and simulation of the effects of variable window openings is thus possible.

(e) Interface orientation. If an interface is co-planar with another interface, then this is specified here, otherwise the position of the interface as one of the six internal main surfaces of a cuboid shaped space is specified for each interface surface. This enables heat transfer at each surface to be correctly determined in relation to the other surfaces bounding a space.

(f) Interface dimensions.

(g) Interface co-ordinates. Where an interface is specified as being coplanar with another interface, the co-ordinates of a reference origin are specified to determine its position relative to the main interface.

(h) Heating effect. This may be the heat input to a heating device, to an air supply system, or to a layer within an interface, e.g. a radiant panel ceiling. The quantity specified here will be modulated by control systems associated with a particular zone.

(i) Air supply, for supply systems. Negative supply indicates an exhaust.

(j) Window recess.

In the interactive version of the program, not all the above information is required to be input for every interface. For example, air supply is not specified unless the interface type indicates this to be required.

3. INITAL - initialisation program

This program accepts the user's input data and generates an additional input file defining the structure and material properties of each interface, and surface properties which enable radiative, absorptive and transmissive behaviour to be modelled. Angle factors are calculated from the geometric data input by RDINDA.

4. SIMULT - Air and Heat transfer Simulation

This is the main program which carries out the simulation process. The date and starting time are input which causes a search for the appropriate meteorological data. This is read in as twenty-four hourly values of:-

Cloud amount
Dry bulb temperature
Vapour pressure
Sea level pressure
Wind direction
Wind speed
Duration of bright sunshine.

Solar radiation calculations are performed based on the above data and the information given on the building site and orientation of external surfaces. Calculations of the scattering the depleting effects of atmospheric water vapour, ozone and dust are included. The components of direct, diffuse and ground reflected radiation in four wavebands are obtained.

An alternative subroutine may be specified here which, instead of using the standard Met. Office tape, will input the users own data.

Other data files provide details of the type of room occupancy, pressure distributions on the building external surfaces at different wind directions, and the heating control system. These files will not normally require alteration for a given building, but can easily be amended as required.

The calculations proceed with a five minute time interval between steps, and a number of separate calculations take place at each step:-

a) Using a probability model, an estimate is obtained of the numbers of persons entering or leaving a space in that interval. The air and mean radiant temperatures are used to determine a thermostat response temperature, which indicates whether the thermostat is on or off. Heat inputs are set accordingly.

b) Calculates shading of windows and the transmission and absorption of radiation at windows and on external surfaces of the building.

c) Calculates radiation between the internal surfaces of the building using the angle factors constructed by INITAL.

d) Calculates convection at all building surfaces, based on surface dimensions, orientation and direction of heat flow.

e) Using the calculated heat flows, obtains a new temperature distribution in each heat transferring interface by solution of the multilayer simultaneous equation set.

f) Calculates all external building surface pressures based on wind speed and direction and data in the pressure distribution file. From current data assesses comfort conditions in each space and sets window and door openings according to occupancy patterns. Proceeds to iteratively calculate internal air flows through open and closed doors, windows, cracks due to floor boarding, roof construction, etc. Bi-directional flows across open doorways due to temperature differences may occur.

g) Using the flow and temperature data for interfaces, calculates space heat flows and new space air temperatures.

h) Outputs to assessment file all variable data and moves to next time interval.

5. ASSESS

This program reads the output file from SIMULT and is used to obtain the information required by the program user. This may be complete listings of temperatures, pressures, airflows and heat flows, or a statistical summary enabling rapid convergence on particular performance characteristics which can then be examined in more detail. A user may prefer to develop his own post-processors to carry out analyses relevant to his own problems.

TITLE AND FUNCTION OF PRINCIPAL SUBROUTINES

FYPAR	Calculates angle factor between any two parallel plane rectangular surfaces.
FYPER	Calculates angle factor between any two perpendicular plane rectangular surfaces.
AFELT	Calculates angle factor between a plane rectangular surface and an elemental surface.
AFPONT	Calculates angle factor between a plane rectangular surface and a point source.
FYROOM	Calculates angle factor between any two room surfaces, selecting subroutines FYPAR, FYPER as appropriate.
TIMSET	Reads meteorological data tape, sets input variables for each time interval.
RADIAT	Calculates radiative heat transfer between room surfaces.
CONVEC	Calculates convective heat transfer at room surfaces.
TSOLVE	Calculates temperature distribution in multi-layer partition.
PMVC	Calculates predicted mean vote.
FLOWS	Calculates air flows in building flow network.
SOLRAD	Calculates direct, diffuse, reflected and global solar radiation on a plane inclined surface in four wave-bands.
SUNPOS	Computes sun position.

APPENDIX 2

CALCULATION OF ANGLE FACTORS

The preprocessing program INITAL calculates angle factors between all pairs of parallel or perpendicular rectangular surfaces in common view. A surface is defined in the input data by specifying

1. The space enclosed
2. The surface dimensions
3. An integer between 1 and 6 specifying location relative to a reference surface, normally, though not necessarily, the inside surface of a vertical window wall.

or

4. For a sub-surface, the main surface which incorporates the sub-surface, together with the co-ordinates of the origin of the sub-surface relative to the main surface.

A complete set of angle factors is stored using four arrays. Arrays FYMP and FYMN contain the angle factors between each main surface and the five other main surfaces enclosing each space. The surfaces on the side of a partition which is defined as positive are contained in FYMP, and the negative surfaces are in FYMN. For each partition an array IDSS specifies any sub-surfaces in view of the surfaces on either side of the partition, and FYSS specifies the corresponding angle factor. To reduce the computation time for calculating radiative exchanges, angle factors less than .05 are excluded.

These arrays are set up automatically by INITAL and the main program proceeds to calculate radiative interchanges using the stored data directly.

The following equations are used to calculate the angle factors.

1. Parallel planes

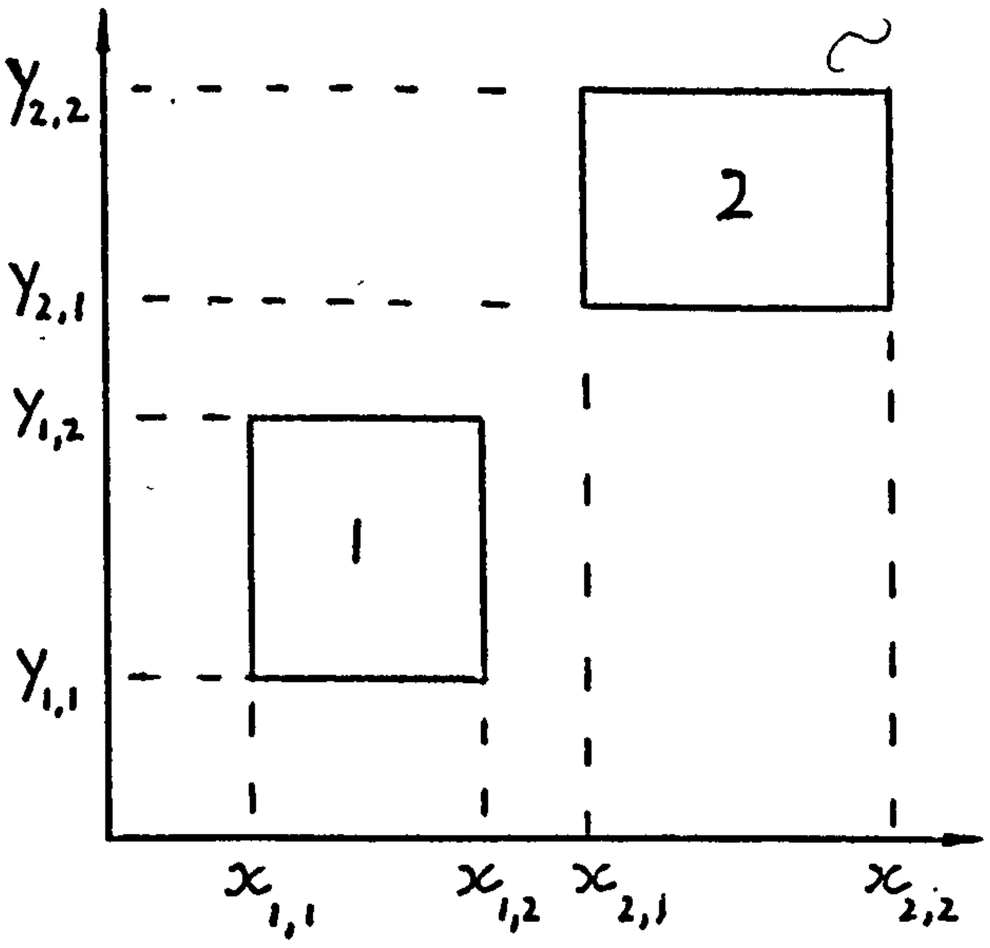

$z_2 - z_1 = c$

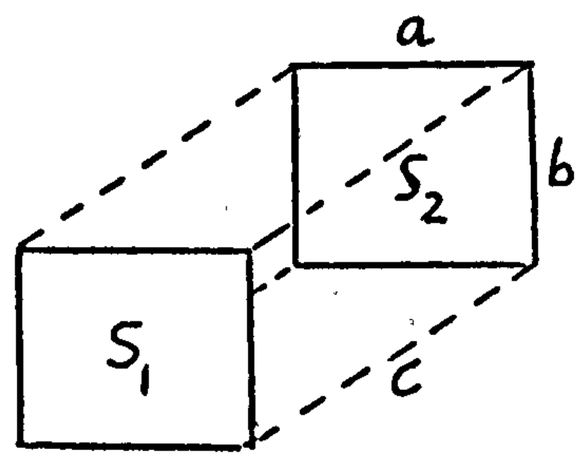

$\phi_1(a,b,c)$ is angle factor for radiation from S_1 to S_2, multiplied by area $(a \times b)$.

Angle factor for radiation from surface 1 to surface 2 is

$$F_{1\to 2}(x_{1,1}, x_{1,2}, x_{2,1}, x_{2,2}, Y_{1,1}, Y_{1,2}, Y_{2,1}, Y_{2,2}, z_1, z_2)$$

$$= \frac{1}{4(x_{1,2}-x_{1,1})(Y_{1,2}-Y_{1,1})}$$

$$\times \Big\{ \phi_1[(x_{1,2}-x_{2,1}),(Y_{1,2}-Y_{2,1}), c] + \phi_1[(x_{2,2}-x_{1,1}),(Y_{1,2}-Y_{2,1}), c]$$
$$+ \phi_1[(x_{1,2}-x_{2,1}),(Y_{2,2}-Y_{1,1}), c] + \phi_1[(x_{2,2}-x_{1,1}),(Y_{2,2}-Y_{1,1}), c]$$
$$- \phi_1[(x_{1,2}-x_{2,1}),(Y_{1,1}-Y_{2,1}), c] - \phi_1[(x_{1,1}-x_{2,1}),(Y_{1,2}-Y_{2,1}), c]$$
$$- \phi_1[(x_{2,2}-x_{1,1}),(Y_{1,1}-Y_{2,1}), c] - \phi_1[(x_{2,2}-x_{1,2}),(Y_{1,2}-Y_{2,1}), c]$$
$$- \phi_1[(x_{1,1}-x_{2,1}),(Y_{2,2}-Y_{1,1}), c] - \phi_1[(x_{1,2}-x_{2,1}),(Y_{2,2}-Y_{1,2}), c]$$
$$- \phi_1[(x_{2,2}-x_{1,2}),(Y_{2,2}-Y_{1,1}), c] - \phi_1[(x_{2,2}-x_{1,1}),(Y_{2,2}-Y_{1,2}), c]$$
$$+ \phi_1[(x_{1,1}-x_{2,1}),(Y_{1,1}-Y_{2,1}), c] + \phi_1[(x_{2,2}-x_{1,2}),(Y_{1,1}-Y_{2,1}), c]$$
$$+ \phi_1[(x_{1,1}-x_{2,1}),(Y_{2,2}-Y_{1,2}), c] + \phi_1[(x_{2,2}-x_{1,2}),(Y_{2,2}-Y_{1,2}), c] \Big\}$$

2. Perpendicular planes.

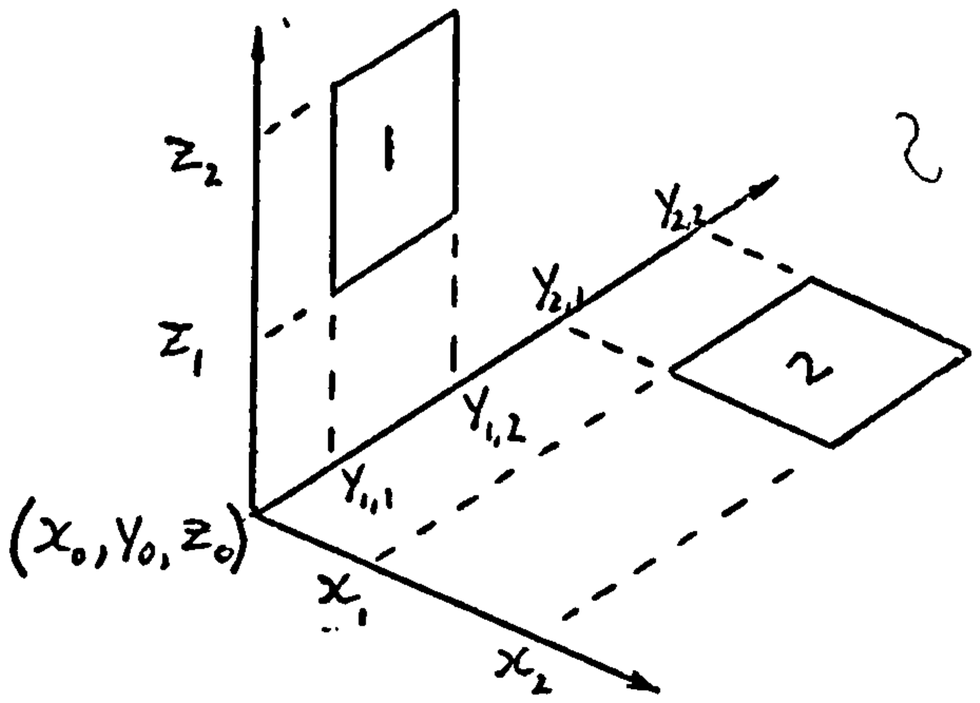

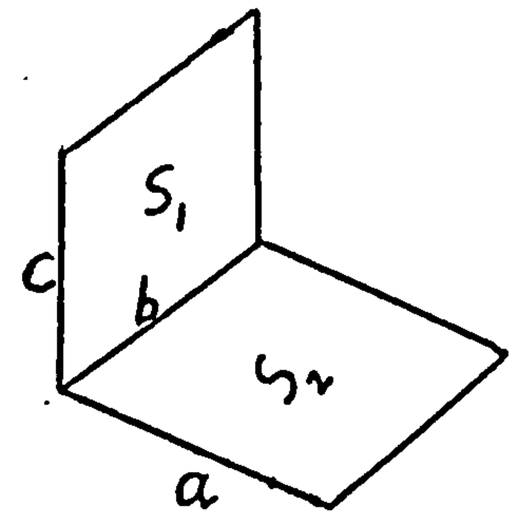

$\phi_2(a,b,c)$ is angle factor for radiation from S_1 to S_2 multiplied by area $(b \times c)$

Angle factor for radiation from surface 1 to surface 2 is

$$F_{1\to 2}(x_0, x_1, x_2, Y_{1,1}, Y_{1,2}, Y_{2,1}, Y_{2,2}, z_0, z_1, z_2)$$

$$= \frac{1}{2(Y_{1,2}-Y_{1,1})(z_2-z_1)}$$

$$\times \Big\{ \phi_2[(x_2-x_0),(Y_{2,1}-Y_{1,2}),(z_2-z_0)] - \phi_2[(x_1-x_0),(Y_{2,1}-Y_{1,2}),(z_2-z_0)]$$
$$+ \phi_2[(x_2-x_0),(Y_{2,2}-Y_{1,1}),(z_2-z_0)] - \phi_2[(x_1-x_0),(Y_{2,2}-Y_{1,1}),(z_2-z_0)]$$
$$- \phi_2[(x_2-x_0),(Y_{2,1}-Y_{1,2}),(z_1-z_0)] + \phi_2[(x_1-x_0),(Y_{2,1}-Y_{1,2}),(z_1-z_0)]$$
$$- \phi_2[(x_2-x_0),(Y_{2,2}-Y_{1,1}),(z_1-z_0)] + \phi_2[(x_1-x_0),(Y_{2,2}-Y_{1,1}),(z_1-z_0)]$$
$$- \phi_2[(x_2-x_0),(Y_{2,1}-Y_{1,1}),(z_2-z_0)] + \phi_2[(x_1-x_0),(Y_{2,1}-Y_{1,1}),(z_2-z_0)]$$
$$- \phi_2[(x_2-x_0),(Y_{2,2}-Y_{1,2}),(z_2-z_0)] + \phi_2[(x_1-x_0),(Y_{2,2}-Y_{1,2}),(z_2-z_0)]$$
$$+ \phi_2[(x_2-x_0),(Y_{2,1}-Y_{1,1}),(z_1-z_0)] - \phi_2[(x_1-x_0),(Y_{2,1}-Y_{1,1}),(z_1-z_0)]$$
$$+ \phi_2[(x_2-x_0),(Y_{2,2}-Y_{1,2}),(z_1-z_0)] - \phi_2[(x_1-x_0),(Y_{2,2}-Y_{1,2}),(z_1-z_0)] \Big\}$$

APPENDIX 3

TEMPERATURES (C) IN TEST HOUSE ON 15.3.76

Channel	Location
4	Living Room
5	Living Room
6	Living Room
10	Front of Hall
11	Back of Hall
12	Kitchen
14	Bedroom 'A'
15	Bedroom 'B'
16	Bedroom 'C'
17	Landing
18	Bathroom
13	Outside air

15.3.76 Time	4	5	6	10	11	12	14	15	16	17	18	13
00.10	17.0	16.2	15.3	12.8	12.6	13.1	15.8	16.9	17.5	15.0	11.1	2.4
00.20	16.6	15.8	15.0	12.6	12.4	12.9	14.9	15.3	15.6	14.8	11.1	2.5
00.30	16.3	15.5	14.7	12.5	12.3	12.7	17.7	14.9	14.9	14.7	11.1	2.5
00.40	16.0	15.2	14.4	12.3	12.1	12.5	15.7	16.0	17.4	14.6	11.0	2.6
00.50	15.7	14.9	14.1	12.1	12.0	12.4	14.9	15.0	15.2	14.4	11.1	2.6
01.00	15.4	14.7	14.0	12.0	11.8	12.2	17.8	16.0	14.7	14.3	11.0	2.6
01.10	15.2	14.5	13.7	11.9	11.6	12.0	15.8	15.5	16.1	14.2	10.8	2.4
01.20	15.0	14.3	13.6	11.7	11.5	11.8	15.0	14.9	14.9	14.0	10.8	2.4
01.30	14.8	14.1	13.3	11.6	11.5	11.7	17.7	17.0	17.3	14.0	10.8	2.4
01.40	14.6	13.9	13.2	11.5	11.3	11.5	15.5	15.3	15.5	13.9	10.8	2.4
01.50	14.4	13.7	13.1	11.4	11.2	11.4	15.0	14.9	14.9	13.7	10.8	2.4
02.00	14.2	13.6	12.9	11.3	11.1	11.3	17.1	16.1	17.4	13.7	10.7	2.4
02.10	14.0	13.4	12.7	11.2	11.0	11.2	15.2	15.0	15.2	13.6	10.6	2.4
02.20	13.9	13.3	12.6	11.1	10.9	11.1	16.5	16.2	14.9	13.6	10.6	2.3
02.30	13.7	13.1	12.4	11.0	10.8	11.0	16.1	15.5	16.0	13.5	10.5	2.3
02.40	13.6	13.0	12.3	10.9	10.7	10.8	15.0	14.9	14.9	13.3	10.5	2.3
02.50	13.5	12.9	12.3	10.8	10.7	10.7	17.4	16.6	17.6	13.3	10.4	2.3
03.00	13.3	12.7	12.1	10.7	10.5	10.7	15.5	15.2	15.4	13.3	10.4	2.3
03.10	13.2	12.6	12.0	10.6	10.4	10.6	14.9	15.3	14.7	13.2	10.3	2.3
03.20	13.1	12.5	11.9	10.6	10.4	10.5	17.5	15.7	17.0	13.2	10.2	2.3
03.30	13.0	12.4	11.8	10.5	10.2	10.3	15.2	14.9	15.1	13.1	10.2	2.3
03.40	12.9	12.3	11.7	10.4	10.2	10.3	16.0	16.7	16.0	13.0	10.2	2.3
03.50	12.7	12.1	11.6	10.3	10.2	10.2	16.2	15.2	15.7	13.0	10.2	2.3
04.00	12.7	12.0	11.5	10.3	10.1	10.2	14.9	15.3	14.8	12.9	10.1	2.3
04.10	12.5	12.0	11.5	10.2	10.0	10.0	17.2	15.5	18.3	12.9	10.0	2.3
04.20	12.4	11.9	11.3	10.2	9.9	10.0	15.6	14.8	15.4	12.8	10.0	2.4
04.30	12.4	11.9	11.3	10.1	9.9	9.9	14.7	16.3	14.7	12.8	9.9	2.4
04.40	12.3	11.8	11.2	10.0	9.8	9.8	17.7	14.9	16.4	12.7	9.9	2.4
04.50	12.2	11.6	11.1	9.9	9.8	9.8	15.4	16.2	14.9	12.6	9.9	2.4

Time	4	5	6	10	11	12	14	15	16	17	18	13
05.00	12.1	11.5	11.0	9.9	9.7	9.7	14.9	15.3	17.3	12.6	9.8	2.4
05.10	12.0	11.5	11.0	9.8	9.6	9.5	17.7	14.6	15.5	12.6	9.6	2.2
05.20	12.0	11.4	10.9	9.8	9.6	9.5	15.2	15.7	14.7	12.6	9.7	2.2
05.30	11.9	11.4	10.9	9.8	9.5	9.5	16.0	14.8	17.1	12.5	9.7	2.2
05.40	11.9	11.3	10.7	9.7	9.5	9.4	17.0	16.7	15.0	12.5	9.7	2.1
05.50	11.8	11.2	10.7	9.6	9.4	9.3	15.0	15.0	16.4	12.4	9.5	2.1
06.00	11.8	11.2	10.7	9.6	9.4	9.3	16.5	15.6	15.6	12.4	9.4	2.1
06.10	11.6	11.1	10.6	9.5	9.3	9.1	16.4	15.3	14.6	12.3	9.3	2.1
06.20	11.6	11.1	10.5	9.5	9.3	9.1	14.9	14.5	17.0	12.4	9.4	2.2
06.30	11.5	10.9	10.5	9.4	9.2	9.1	17.1	15.8	14.9	12.3	9.4	2.2
06.40	11.5	10.9	10.4	9.4	9.2	9.0	16.1	14.7	16.9	12.3	9.4	2.2
06.50	11.4	10.8	10.4	9.4	9.1	9.0	14.9	16.6	15.3	12.3	9.5	2.3
07.00	11.4	10.8	10.3	9.3	9.1	9.0	17.4	14.9	14.5	12.3	9.5	2.4
07.10	17.1	15.0	10.8	11.2	11.2	11.0	15.7	15.8	16.2	13.1	9.5	2.4
07.20	22.5	19.9	13.1	13.4	13.2	13.6	14.8	15.2	14.7	14.7	9.4	2.5
07.30	24.7	22.1	14.7	14.3	14.0	14.7	17.7	14.6	17.8	15.4	9.5	2.5
07.40	26.1	23.7	16.0	15.0	14.7	15.6	15.7	15.8	15.4	16.2	9.4	2.7
07.50	27.2	24.5	17.0	15.6	15.3	16.1	15.0	14.8	14.8	16.6	9.5	2.7
08.00	26.1	23.5	17.0	15.4	15.2	15.8	17.9	16.9	17.0	16.4	9.5	2.8
08.10	24.0	21.7	17.0	14.4	14.3	14.9	15.9	15.2	15.3	15.9	9.7	2.8
08.20	23.0	22.1	17.3	14.2	14.1	14.9	15.2	14.6	14.7	15.8	9.5	2.8
08.30	24.6	23.5	17.7	15.1	14.9	15.6	14.8	14.4	14.5	16.3	9.7	3.0
08.40	27.0	24.5	18.0	16.1	15.7	16.4	14.5	14.3	14.3	17.0	9.8	3.2
08.50	26.6	24.0	18.0	16.1	15.8	16.3	14.4	14.2	14.2	16.7	9.7	3.4
09.00	26.0	23.3	17.9	15.7	15.6	15.8	14.3	14.1	14.1	16.6	9.7	3.5
09.10	24.4	22.1	18.4	15.6	15.2	15.4	14.2	14.2	13.9	16.3	9.7	3.5
09.20	21.9	21.5	20.4	14.8	14.6	15.3	14.1	14.1	13.9	16.2	9.8	3.5
09.30	26.6	24.9	23.9	16.9	16.5	17.4	14.0	14.0	13.8	17.6	9.7	3.4
09.40	24.9	23.6	22.7	16.1	15.9	16.4	13.9	13.9	13.7	16.9	10.0	3.4
09.50	23.0	22.8	22.1	15.4	15.2	16.1	13.8	13.9	13.6	16.6	9.9	3.5

Time	4	5	6	10	11	12	14	15	16	17	18	13
10.00	27.1	25.4	23.7	17.0	16.7	17.5	13.8	14.0	13.7	17.7	10.0	3.5
10.10	23.3	20.7	16.7	17.6	17.3	15.8	13.7	14.0	13.6	17.3	10.2	3.5
10.20	22.8	21.9	18.8	16.3	15.7	15.7	13.7	14.4	13.7	16.7	10.4	3.8
10.30	24.0	23.0	19.1	16.2	15.9	16.3	13.7	14.2	13.6	16.9	10.5	4.0
10.40	26.7	24.9	19.1	16.9	16.9	17.3	13.7	14.1	13.6	17.8	10.5	4.1
10.50	26.5	23.8	18.8	16.9	16.7	16.9	13.7	14.2	13.6	17.4	10.6	4.5
11.00	23.6	21.5	18.7	15.8	15.6	15.9	13.8	14.3	13.7	16.6	10.8	4.9
11.10	23.1	22.2	19.1	16.0	15.7	16.0	14.0	14.4	13.9	16.6	10.7	5.2
11.20	25.3	24.0	19.4	16.7	16.5	17.0	14.1	14.5	14.1	17.1	11.1	5.4
11.30	27.5	24.7	19.3	17.2	17.1	17.3	14.1	14.4	14.0	17.9	10.8	4.8
11.40	25.0	22.4	19.1	16.9	16.7	16.4	14.2	14.5	14.1	17.3	11.0	5.4
11.50	22.3	21.6	18.8	16.4	16.1	15.9	14.1	14.4	14.0	16.7	11.0	5.1
12.00	23.8	22.9	19.1	16.5	16.2	16.6	14.1	14.5	14.1	17.0	11.1	4.9
12.10	26.6	24.8	19.4	17.1	17.1	17.5	14.2	14.6	14.2	17.9	11.3	5.3
12.20	26.5	23.7	19.0	17.3	17.0	17.1	14.1	14.5	14.1	17.8	11.1	5.2
12.30	24.0	21.6	18.7	16.3	16.0	16.2	14.0	14.4	14.0	16.9	11.0	4.7
12.40	22.6	21.8	18.8	16.1	15.8	16.2	14.0	14.5	14.0	16.8	11.2	4.4
12.50	24.0	23.0	19.0	16.5	16.3	16.7	14.0	14.4	14.0	17.3	11.0	4.5
13.00	26.5	24.7	19.1	17.2	17.1	17.5	14.0	14.4	14.0	18.0	10.9	4.2
13.10	26.6	24.0	18.8	17.4	17.0	17.3	14.0	14.4	14.0	17.9	10.9	4.1
13.20	24.8	22.2	18.7	16.6	16.2	16.5	14.0	14.4	14.0	17.3	10.8	4.2
13.30	22.4	21.7	18.7	15.8	15.7	16.0	13.9	14.4	13.9	16.9	11.0	4.1
13.40	23.5	22.6	18.8	16.2	16.0	16.4	13.9	14.4	13.9	17.0	10.9	4.0
13.50	25.0	23.8	19.0	16.7	16.5	17.0	13.8	14.2	13.8	17.5	10.9	3.7
14.00	27.3	24.7	19.0	17.6	17.2	17.8	13.8	14.3	13.8	18.1	11.2	3.2
14.10	25.5	22.9	18.7	16.8	16.5	17.0	13.7	14.3	13.7	17.5	11.2	3.1
14.20	22.2	21.5	18.6	15.7	15.6	16.1	13.7	14.3	13.7	16.9	11.0	3.1
14.30	23.2	22.4	18.8	16.0	15.8	16.5	13.7	14.3	13.7	17.1	11.1	3.1
14.40	24.7	23.7	19.0	16.6	16.4	17.1	13.7	14.3	13.7	17.5	11.1	3.0
14.50	26.5	24.7	19.1	17.1	17.0	17.3	13.8	14.4	13.8	17.9	10.8	3.4

Time	4	5	6	10	11	12	14	15	16	17	18	13
15.00	26.9	24.1	18.8	17.3	16.9	17.1	13.8	14.3	13.7	17.8	10.7	3.5
15.10	24.7	21.9	18.7	16.2	16.0	16.3	13.9	14.3	13.8	17.1	10.6	3.6
15.20	22.5	21.8	18.7	15.7	15.4	15.6	13.8	14.2	13.7	16.9	10.5	3.5
15.30	23.4	22.5	18.8	16.0	15.7	16.1	13.8	14.2	13.7	17.0	10.3	3.5
15.40	24.9	23.9	19.0	16.6	16.3	16.9	13.7	14.2	13.7	17.5	10.5	3.2
15.50	27.2	25.0	19.1	17.3	17.0	17.5	13.8	14.2	13.7	18.2	10.6	3.2
16.00	26.2	23.7	18.8	17.0	16.7	17.0	13.8	14.3	13.7	17.7	10.6	3.4
16.10	24.1	21.7	18.6	16.0	16.0	16.1	13.7	14.2	13.7	17.0	10.4	3.4
16.20	22.5	21.8	18.7	15.7	15.5	15.8	13.7	14.1	13.6	16.7	10.5	3.4
16.30	23.4	22.5	18.8	16.0	15.8	16.2	13.7	14.1	13.6	17.0	10.5	3.4
16.40	24.8	23.8	19.0	16.5	16.2	16.5	13.7	14.1	13.6	17.4	10.3	3.4
16.50	27.2	25.0	19.0	17.3	17.1	17.4	13.7	14.1	13.6	18.2	10.5	3.4
17.00	26.1	23.4	18.7	17.0	16.7	16.9	13.7	14.1	13.6	17.6	10.4	3.5
17.10	23.0	21.4	18.6	15.8	15.6	15.8	13.6	14.1	13.5	16.7	10.5	3.5
17.20	22.9	22.1	18.8	15.8	15.6	16.0	13.6	14.1	13.6	16.9	10.5	3.4
17.30	23.8	23.0	18.8	16.2	15.8	16.4	13.6	14.1	13.6	17.1	10.6	3.2
17.40	25.2	24.1	19.0	16.7	16.5	17.0	13.6	14.0	13.5	17.5	10.5	3.4
17.50	27.5	24.8	18.9	17.5	17.2	17.5	13.6	14.0	13.5	18.2	10.5	3.4
18.00	25.2	22.5	18.7	16.5	16.3	16.7	13.5	14.0	13.5	17.4	10.7	2.9
18.10	22.2	21.4	18.6	15.7	15.4	16.0	13.5	14.0	13.5	16.7	10.9	3.0
18.20	23.4	22.6	18.8	16.0	15.8	16.5	13.5	14.0	13.5	17.1	11.0	3.0
18.30	24.9	23.8	19.0	16.6	16.3	17.0	13.5	14.0	13.5	17.5	11.1	3.0
18.40	27.1	24.9	19.0	17.3	17.1	17.6	13.5	14.0	13.5	18.2	10.9	3.1
18.50	26.2	23.4	18.7	17.0	16.7	17.0	13.4	14.0	13.4	17.7	10.9	3.0
19.00	23.3	21.4	18.6	15.8	15.7	16.2	13.4	14.0	13.4	17.0	10.9	2.9
19.10	22.9	22.2	18.8	15.8	15.6	16.3	13.4	14.0	13.4	17.1	11.0	2.7
19.20	24.3	23.4	19.0	16.4	16.1	16.9	13.3	14.0	13.3	17.4	11.0	2.7
19.30	26.8	24.9	19.0	17.1	16.9	17.7	13.3	14.0	13.3	18.1	11.0	2.7
19.40	26.9	24.0	18.8	17.2	17.0	17.4	13.3	14.0	13.3	18.0	11.0	2.4
19.50	24.9	22.0	18.6	16.2	16.1	16.6	13.3	14.0	13.3	17.2	11.1	2.4

Time	4	5	6	10	11	12	14	15	16	17	18	13
20.00	22.5	21.7	18.7	15.6	15.4	16.0	13.3	14.0	13.3	16.9	10.9	2.5
20.10	23.6	22.8	18.8	16.0	15.8	16.6	13.3	14.0	13.3	17.1	11.3	2.6
20.20	25.3	24.1	19.0	16.7	16.4	17.1	13.3	14.0	13.3	17.7	11.3	2.6
20.30	27.3	24.9	19.0	17.3	17.0	17.7	13.3	14.0	13.3	18.3	11.0	2.7
20.40	26.2	23.6	18.7	17.0	22.4	17.0	13.2	14.0	13.2	17.7	10.8	2.7
20.50	24.2	21.8	18.5	16.1	16.0	16.5	13.2	14.0	13.2	17.1	11.2	2.7
21.00	22.5	21.8	18.7	15.7	15.4	16.1	13.2	14.0	13.2	16.9	11.1	2.7
21.10	23.8	23.0	18.8	16.1	15.8	16.6	13.2	14.0	13.2	17.1	11.2	2.7
21.20	25.7	24.3	19.0	16.9	16.6	17.3	13.2	14.0	13.2	17.8	11.3	2.7
21.30	27.2	24.5	18.8	17.4	17.1	17.7	13.2	13.9	13.2	18.0	11.3	2.7
21.40	25.4	22.4	16.5	16.4	16.2	16.7	13.2	14.0	13.2	17.4	11.3	2.8
21.50	22.5	21.5	18.6	15.6	15.5	16.2	13.2	14.0	13.2	16.9	11.4	2.8
22.00	23.3	22.4	18.8	15.8	15.6	16.3	15.6	16.4	16.9	17.0	11.2	2.7
22.10	24.6	23.7	19.0	16.6	16.3	17.1	15.7	14.9	14.6	17.4	11.5	2.8
22.20	27.3	24.9	19.0	17.4	17.3	18.0	14.5	14.9	14.7	18.3	11.5	2.8
22.30	25.9	23.4	18.7	17.0	16.7	17.1	16.9	15.7	15.9	17.8	11.5	3.0
22.40	22.5	21.4	18.6	15.7	15.5	16.2	15.7	15.0	14.8	17.0	11.5	2.9
22.50	23.0	22.1	18.8	15.9	15.7	16.5	14.9	16.5	17.3	17.3	11.5	2.9
23.00	24.3	23.4	19.0	16.5	16.3	17.1	17.5	15.8	15.6	17.6	11.6	2.9
23.10	22.8	21.9	18.6	15.9	15.7	16.4	16.0	15.2	15.0	17.2	11.5	3.0
23.20	20.1	19.3	17.7	15.0	14.8	15.2	15.2	16.3	17.8	16.6	11.6	2.9
23.30	19.1	18.2	17.0	14.6	14.3	14.6	17.9	15.8	15.4	16.1	11.6	2.9
23.40	18.4	17.4	16.4	14.3	14.1	14.3	16.0	15.3	15.0	15.9	11.6	2.9
23.50	17.8	16.9	16.0	14.0	13.8	13.9	15.3	16.2	17.0	15.6	11.6	2.8
24.00	17.3	16.5	15.6	13.9	13.6	13.6	18.0	15.9	15.4	15.4	11.3	2.8

APPENDIX 4

INPUT DATA FOR TEST HOUSE MODEL

INPUT DATA

AIRNET.OPINDA

SPACES

ISP	ZON	ID	TYPE	OCCU	LN, AZ (Length, or azimuth)	BR, IN (breadth, or inclination)	FLHT (floor height)	CEHT (space height)	STRA (temperature stratification.)	
1	1	LR	1	0	5.14	3.56	0.38	2.29	6.00	Liv. room
2	1	KIT	1	0	2.74	3.56	0.38	2.29	6.00	kitchen
3	1	HALL	3	0	7.96	1.98	0.38	2.29	3.00	hall
4	1	LAND	3	0	2.90	1.98	2.90	2.29	3.00	landing
5	1	UFLO	1	0	7.96	5.66	0.00	0.33	0.00	under floor space
6	2	BEDA	1	0	5.14	3.56	2.90	2.29	5.00	bedroom A
7	3	BEDB	1	0	2.74	3.56	2.90	2.29	5.00	bedroom B
8	4	BEDC	1	0	3.12	1.98	2.90	2.29	5.00	bedroom C
9	5	LOFT	1	0	7.96	5.66	5.21	0.93	0.00	loft space
10	6	BATH	1	0	1.75	1.98	2.90	2.29	0.00	bathroom
11	7	FWAD	5	0	207.75	90.00	0.38	2.29	0.00	front wall downstairs
12	7	FWAU	5	0	207.75	90.00	3.56	2.29	0.00	" " upstairs
13	7	BWAD	5	0	27.75	90.00	0.38	2.29	0.00	back wall downstairs
14	7	BWAU	5	0	27.75	90.00	3.56	2.29	0.00	" " upstairs
15	7	FROF	5	0	207.75	22.50	5.21	0.93	0.00	front roof surface
16	7	BROF	5	0	27.75	22.50	5.21	0.93	0.00	back " "
17	7	FGWA	5	0	117.75	90.00	0.00	5.21	0.00	front gable wall
18	7	BGWA	5	0	297.75	90.00	0.00	5.21	0.00	back " "
19	7	GRO	5	0	0.00	0.00	0.00	0.00	0.00	ground surface
20	7	FWAB	5	0	207.75	90.00	0.00	0.38	0.00	front } wall outside
21	7	BWAB	5	0	27.75	90.00	0.00	0.38	0.00	back } underfloor

INTERFACES

I/F	ID	TY	CLA	PUS (bounding spaces)	NEG (bounding spaces)	WDPS (widths and heights of pos., neg. surfaces.)	HTPS	WDNE	HTNE	PAP (surface orientation)	PAN (surface orientation)
1	LROS	1	3	1	11	3.56	2.29	3.56	2.29	3	0
2	LRWI	6	1	1	11	2.15	1.02	2.15	1.02	0	0
3	LRGW	1	1	1	17	2.74	2.29	2.74	2.29	5	0
4	LRKI	2	2	1	2	3.56	2.29	3.56	2.29	4	4
5	LRHA	2	2	1	3	5.14	2.29	7.96	2.29	6	6
6	LRUF	4	1	5	1	7.96	5.64	5.14	3.56	2	1
7	LRBA	4	2	1	6	5.14	3.56	5.14	3.56	2	1
8	KIOS	1	3	2	13	3.56	2.29	3.56	2.29	3	0
9	KIWI	6	2	2	13	1.62	0.76	1.62	0.76	0	0
10	NDKI	2	1	3	2	5.66	2.29	2.74	2.29	5	6
11	KIHA	2	2	2	3	2.74	2.29	2.00	2.29	5	0
12	KIUF	4	1	5	2	2.74	3.56	2.74	3.56	0	1
13	KIBB	4	2	2	7	2.74	3.56	2.74	3.56	2	1
14	HAFW	1	3	3	11	1.98	2.29	1.98	2.29	4	0
15	HAWI	6	3	3	11	0.68	1.00	0.68	1.00	0	0
16	HAFD	7	2	3	11	0.94	2.06	0.94	2.06	0	0
17	HABW	1	3	3	13	1.98	2.29	1.98	2.29	3	0
18	HABD	7	3	3	13	0.63	0.63	0.63	0.63	0	0
19	HAGW	1	1	3	18	2.74	2.29	2.74	2.29	0	0
20	HAUF	4	1	5	3	7.96	1.98	7.96	1.98	0	1
21	BAOS	1	2	6	12	3.56	2.29	3.56	2.29	3	0
22	BAWI	6	1	6	12	1.62	0.76	1.62	0.76	0	0
23	BAGH	1	1	6	17	2.74	2.29	2.74	2.29	5	0
24	BABD	2	3	6	7	3.56	2.29	3.56	2.29	4	4
25	BABC	2	3	6	8	5.14	2.29	3.12	2.29	6	5
26	BALO	4	4	6	9	5.14	3.56	7.96	5.64	2	1
27	BBOS	1	2	7	14	3.56	2.29	3.56	2.29	3	0
28	BBWI	6	1	7	14	1.62	0.76	1.62	0.76	0	0
29	LAND	2	1	4	7	2.90	2.29	2.74	2.29	5	6
30	BBBT	2	3	7	10	2.74	2.29	1.75	2.29	5	6
31	BBLO	4	4	7	9	2.74	3.56	2.74	3.56	2	0
32	BCOS	1	2	8	12	1.98	2.29	1.98	2.29	3	0
33	BCWI	6	1	8	12	1.07	0.76	1.07	0.76	0	0
34	BCLO	4	4	8	9	3.12	1.98	3.12	1.98	2	0
35	LALO	4	4	4	9	2.90	1.98	2.90	1.98	2	0
36	BTOS	1	2	10	14	1.98	2.29	1.98	2.29	3	0

37	BTWI	6	2	10	14	0.76	0.76	0.76	0.76	0	0
38	BTGW	1	1	10	18	1.75	2.29	1.75	2.29	5	0
39	BTLA	2	3	10	4	1.98	2.29	1.98	2.29	4	3
40	BTLO	4	4	10	9	1.75	1.98	1.75	1.98	2	0
41	HABT	4	2	3	10	7.96	1.93	1.75	1.98	2	1
42	HABC	4	2	3	8	3.12	1.98	3.12	1.98	0	1
43	HALA	4	2	3	4	2.90	1.07	2.90	1.07	0	1
44	LAGW	1	1	4	18	1.00	2.29	1.00	2.29	0	0
45	BCND	2	1	8	7	1.20	2.29	1.20	2.29	6	0
46	BALA	2	3	6	4	2.02	0.33	2.90	2.29	0	6
47	BBDO	7	4	7	4	0.74	1.96	0.74	1.96	0	0
48	BCLA	2	3	8	4	1.98	2.29	1.98	2.29	4	4
49	LUFR	5	1	9	15	9.40	5.64	4.70	5.64	2	0
50	LOBR	5	1	9	16	4.70	5.64	4.70	5.64	0	0
51	UFFW	1	1	5	20	5.64	0.50	5.64	0.50	3	0
52	UFBW	1	1	5	21	5.64	0.50	5.64	0.50	4	0
53	LRDO	7	4	1	3	0.81	1.96	0.81	1.96	0	0
54	KIDO	7	1	2	3	0.74	1.96	0.74	1.96	0	0
55	HADW	6	3	3	13	0.65	0.81	0.65	0.81	0	0
56	SW	8	1	3	4	2.90	0.91	2.90	0.91	0	0
57	BADO	7	4	6	4	0.74	1.96	0.74	1.96	0	0
58	BCDO	7	4	8	4	0.74	1.96	0.74	1.96	0	0
59	BTDO	7	1	10	4	0.66	1.96	0.66	1.96	0	0
60	HTLR	11	1	1	1	0.00	0.00	0.00	0.00	0	0
61	HTKI	11	1	2	2	0.00	0.00	0.00	0.00	0	0
62	HTHA	11	1	3	3	0.00	0.00	0.00	0.00	0	0
63	HTBA	11	1	6	6	0.00	0.00	0.00	0.00	0	0
64	HTBB	11	1	7	7	0.00	0.00	0.00	0.00	0	0
65	HTBC	11	1	8	8	0.00	0.00	0.00	0.00	0	0
66	GROS	3	1	5	19	7.96	5.64	7.96	5.64	1	0

	(coplanar partitions)		surface origin co-ordinates.					heat input	air supply	flow areas, cracks. window recess		
I/F	CPP	CPN	COXP	COYP	COXN	COYN	COZN	HTEF	SUPV	CFAR	OFAR	RECE
1	0	0	0.00	0.00	0.00	0.00	0.00	0.0	0.00	0.00	0.00	0.00
2	1	1	0.56	1.04	0.56	1.04	0.00	0.0	0.00	10.00	0.10	0.05
3	0	0	0.00	0.00	0.00	0.00	0.00	0.0	0.00	0.00	0.00	0.00
4	0	0	0.00	0.00	0.00	0.00	0.00	0.0	0.00	0.00	0.00	0.00
5	0	0	0.00	0.00	0.00	0.00	0.00	0.0	0.00	0.00	0.00	0.00
6	0	0	0.00	0.00	0.00	0.00	0.00	0.0	0.00	100.00	0.10	0.00
7	0	0	0.00	0.00	0.00	0.00	0.00	0.0	0.00	18.00	0.00	0.00
8	0	0	0.00	0.00	0.00	0.00	0.00	0.0	0.00	0.00	0.00	0.00
9	8	8	1.01	0.97	1.01	0.97	0.00	0.0	0.00	10.00	0.10	0.05
10	0	0	0.00	0.00	0.00	0.00	0.00	0.0	0.00	0.00	0.00	0.00
11	0	5	0.00	0.00	0.00	0.00	0.00	0.0	0.00	0.00	0.00	0.00
12	6	0	5.14	0.00	0.00	0.00	0.00	0.0	0.00	60.00	0.00	0.00
13	0	0	0.00	0.00	0.00	0.00	0.00	0.0	0.00	10.00	0.00	0.00
14	0	0	0.00	0.00	0.00	0.00	0.00	0.0	0.00	0.00	0.00	0.00
15	14	14	0.10	1.14	0.10	1.14	0.00	0.0	0.00	0.00	0.00	0.05
16	14	14	0.78	0.00	0.78	0.00	0.00	0.0	0.00	8.00	1.94	0.00
17	0	0	0.00	0.00	0.00	0.00	0.00	0.0	0.00	0.00	0.00	0.00
18	17	17	1.00	0.23	1.00	0.23	0.00	0.0	0.00	8.00	1.94	0.00
19	10	0	0.00	0.00	0.00	0.00	0.00	0.0	0.00	0.00	0.00	0.00
20	6	0	0.00	3.56	0.00	0.00	0.00	0.0	0.00	75.00	0.00	0.00
21	0	0	0.00	0.00	0.00	0.00	0.00	0.0	0.00	0.00	0.00	0.00
22	21	21	0.53	1.11	0.53	1.11	0.00	0.0	0.00	15.00	0.10	0.05
23	0	0	0.00	0.00	0.00	0.00	0.00	0.0	0.00	0.00	0.00	0.00
24	0	0	0.00	0.00	0.00	0.00	0.00	0.0	0.00	0.00	0.00	0.00
25	0	0	0.00	0.00	0.00	0.00	0.00	0.0	0.00	0.00	0.00	0.00
26	0	0	0.00	0.00	0.00	0.00	0.00	0.0	0.00	0.00	0.00	0.00
27	0	0	0.00	0.00	0.00	0.00	0.00	0.0	0.00	0.00	0.00	0.00
28	27	27	0.86	1.11	0.86	1.11	0.00	0.0	0.00	15.00	0.10	0.05
29	0	0	0.00	0.00	0.00	0.00	0.00	0.0	0.00	0.00	0.00	0.00
30	0	0	0.00	0.00	0.00	0.00	0.00	0.0	0.00	0.00	0.00	0.00
31	0	26	0.00	0.00	5.14	0.00	0.00	0.0	0.00	0.00	0.00	0.00
32	0	0	0.00	0.00	0.00	0.00	0.00	0.0	0.00	0.00	0.00	0.00
33	32	32	0.84	1.11	0.84	1.11	0.00	0.0	0.00	15.00	0.10	0.05
34	0	26	0.00	0.00	0.00	3.56	0.00	0.0	0.00	0.00	0.00	0.00

35	0	26	0.00	0.00	3.12	3.56	0.00	0.0	0.00	2.60	0.30	0.00
36	0	0	0.00	0.00	0.00	0.00	0.00	0.0	0.00	0.00	0.00	0.00
37	36	36	0.81	1.11	0.81	1.11	0.00	0.0	0.00	2.00	0.10	0.05
38	0	0	0.00	0.00	0.00	0.00	0.00	0.0	0.00	0.00	0.00	0.00
39	0	0	0.00	0.00	0.00	0.00	0.00	0.0	0.00	0.00	0.00	0.00
40	0	26	0.00	0.00	6.20	3.56	0.00	0.0	0.00	0.00	0.00	0.00
41	0	0	0.00	0.00	0.00	0.00	0.00	0.0	0.00	4.00	0.00	0.00
42	41	0	4.65	0.00	0.00	0.00	0.00	0.0	0.00	4.00	0.00	0.00
43	41	0	1.75	0.91	0.00	0.91	0.00	0.0	0.00	0.00	0.00	0.00
44	29	0	0.00	0.00	0.00	0.00	0.00	0.0	0.00	0.00	0.00	0.00
45	0	29	0.00	0.00	1.90	0.00	0.00	0.0	0.00	0.00	0.00	0.00
46	25	0	3.12	1.96	0.00	0.00	0.00	0.0	0.00	0.00	0.00	0.00
47	30	46	2.00	0.00	0.30	0.00	0.00	0.0	0.00	0.66	1.45	0.00
48	0	0	0.00	0.00	0.00	0.00	0.00	0.0	0.00	0.00	0.00	0.00
49	0	0	0.00	0.00	0.00	0.00	0.00	0.0	0.00	5.64	0.00	0.00
50	49	0	4.70	0.00	0.00	0.00	0.00	0.0	0.00	5.64	0.00	0.00
51	0	0	0.00	0.00	0.00	0.00	0.00	0.0	0.00	1.02	0.00	0.00
52	0	0	0.00	0.00	0.00	0.00	0.00	0.0	0.00	1.02	0.00	0.00
53	5	5	2.94	0.00	4.20	0.00	0.00	0.0	0.00	0.74	1.59	0.00
54	11	5	1.92	0.00	1.92	0.00	0.00	0.0	0.00	5.38	1.45	0.00
55	17	17	1.00	1.07	1.00	1.07	0.00	0.0	0.00	0.00	0.00	0.00
56	41	43	1.75	0.00	0.00	0.00	0.00	0.0	0.00	0.00	1.59	0.00
57	25	46	3.12	0.00	2.13	0.00	0.00	0.0	0.00	0.66	1.45	0.00
58	48	48	0.00	0.00	1.07	0.00	0.00	0.0	0.00	0.66	1.45	0.00
59	39	39	1.22	0.00	1.22	0.00	0.00	0.0	0.00	5.23	1.29	0.00
60	0	0	0.00	0.00	0.00	0.00	0.00	1246.0	0.20	0.00	0.00	0.00
61	0	0	0.00	0.00	0.00	0.00	0.00	497.0	0.10	0.00	0.00	0.00
62	0	0	0.00	0.00	0.00	0.00	0.00	990.0	0.10	0.00	0.00	0.00
63	0	0	0.00	0.00	0.00	0.00	0.00	598.0	0.10	0.00	0.00	0.00
64	0	0	0.00	0.00	0.00	0.00	0.00	598.0	0.10	0.00	0.00	0.00
65	0	0	0.00	0.00	0.00	0.00	0.00	598.0	0.10	0.00	0.00	0.00
66	0	0	0.00	0.00	0.00	0.00	0.00	0.0	0.00	0.00	0.00	0.00

IZON	KOSP	TUPC	TLRC
1	1	296.86	296.86
2	6	290.06	288.16
3	7	290.06	288.16
4	8	290.06	288.16
5	9	273.16	273.16
6	10	290.06	288.16
7	11	273.16	273.16

↑
space controlling zone.

Zone heating control thermostat set points. (°K)

DERIVED DATA (from Files, etc.)

AIRNET.OPDEDA

I/F	NOLA (number of layers)	EMSP (ε ros.)	SABS (solar abs. coeff.)	EMSN (ε neg.)	FCOF (air flow coefficients)	FEXP	AREA (surface)
1	4	0.90	0.40	0.90	8.40	0.50	5.96
2	1	0.90	0.00	0.90	0.10	0.95	2.19
3	10	0.90	0.70	0.90	8.40	0.50	6.27
4	7	0.90	0.40	0.90	8.40	0.50	8.15
5	7	0.90	0.40	0.90	8.40	0.50	10.18
6	4	0.90	0.90	0.95	0.10	0.95	19.38
7	8	0.90	0.90	0.95	0.10	0.95	18.30
8	4	0.90	0.40	0.90	8.40	0.50	6.92
9	1	0.90	0.00	0.90	1.00	0.72	1.23
10	9	0.90	0.40	0.90	8.40	0.50	6.69
11	7	0.90	0.40	0.90	8.40	0.50	4.82
12	4	0.90	0.90	0.95	0.10	0.95	9.75
13	8	0.90	0.90	0.95	0.10	0.95	9.75
14	4	0.90	0.40	0.90	8.40	0.50	1.92
15	1	0.90	0.00	0.90	0.10	0.95	0.60
16	6	0.90	0.40	0.90	2.00	0.61	1.94
17	4	0.90	0.40	0.90	8.40	0.50	3.61
18	3	0.90	0.40	0.90	1.00	0.72	0.40
19	10	0.90	0.70	0.90	8.40	0.50	6.27
20	4	0.90	0.90	0.95	0.10	0.95	15.76
21	6	0.90	0.60	0.90	8.40	0.50	6.92
22	1	0.90	0.00	0.90	0.10	0.95	1.23
23	10	0.90	0.70	0.90	8.40	0.50	6.27
24	5	0.90	0.40	0.90	8.40	0.50	8.15
25	5	0.90	0.40	0.90	8.40	0.50	9.65
26	6	0.90	0.90	0.95	0.10	0.95	18.30
27	6	0.90	0.60	0.90	8.40	0.50	6.92
28	1	0.90	0.00	0.90	0.10	0.95	1.23
29	9	0.90	0.40	0.90	8.40	0.50	4.35
30	5	0.90	0.40	0.90	8.40	0.50	4.82
31	6	0.90	0.90	0.95	0.10	0.95	9.75
32	6	0.90	0.60	0.90	8.40	0.50	3.72
33	1	0.90	0.00	0.90	0.10	0.95	0.81
34	6	0.90	0.90	0.95	0.10	0.95	6.18
35	6	0.90	0.90	0.95	0.10	0.95	5.74
36	6	0.90	0.60	0.90	8.40	0.50	3.96
37	1	0.90	0.00	0.90	1.00	0.72	0.58
38	10	0.90	0.70	0.90	8.40	0.50	4.01
39	5	0.90	0.40	0.90	8.40	0.50	3.24
40	6	0.90	0.90	0.95	0.10	0.95	3.46
41	8	0.90	0.90	0.95	0.10	0.95	3.44
42	8	0.90	0.90	0.95	0.10	0.95	6.18
43	8	0.90	0.90	0.95	0.10	0.95	3.10
44	10	0.90	0.70	0.90	8.40	0.50	2.29
45	9	0.90	0.40	0.90	8.40	0.50	2.75
46	5	0.90	0.40	0.90	8.40	0.50	0.67
47	5	0.90	0.40	0.90	8.40	0.50	1.45
48	5	0.90	0.40	0.90	8.40	0.50	3.08
49	9	0.90	0.70	0.90	1.00	0.72	26.51
50	9	0.90	0.70	0.90	1.00	0.72	26.51
51	10	0.90	0.70	0.90	8.40	0.50	2.82
52	10	0.90	0.70	0.90	8.40	0.50	2.82
53	5	0.90	0.40	0.90	8.40	0.50	1.59
54	5	0.90	0.40	0.90	2.00	0.61	1.45
55	1	0.90	0.00	0.90	0.10	0.95	0.53
56	1	1.00	0.00	1.00	8.40	0.50	2.64
57	5	0.90	0.40	0.90	8.40	0.50	1.45
58	5	0.90	0.40	0.90	8.40	0.50	1.45
59	5	0.90	0.40	0.90	2.00	0.61	1.29

60	1	1.00	0.00	1.00	8.40	0.50	0.00
61	1	1.00	0.00	1.00	8.40	0.50	0.00
62	1	1.00	0.00	1.00	8.40	0.50	0.00
63	1	1.00	0.00	1.00	8.40	0.50	0.00
64	1	1.00	0.00	1.00	8.40	0.50	0.00
65	1	1.00	0.00	1.00	8.40	0.50	0.00
66	10	0.95	0.70	0.90	8.40	0.50	44.89

THERMAL PROPERTIES

I/F	LA	TYpe of layer	COND W/m²C	RETC – 1/thermal diffusivity secs.
1				
	1	0	19.00	528.00
	2	4	5.30	1680.00
	3	0	2.00	2675.00
	4	0	26.70	612.00
2				
	1	5	350.00	16.10
3				
	1	0	19.00	528.00
	2	4	10.90	217.20
	3	4	10.10	355.30
	4	0	27.20	1136.00
	5	0	13.10	4544.00
	6	0	13.10	4544.00
	7	4	5.60	4.10
	8	0	16.00	6300.00
	9	0	32.00	1575.00
	10	0	40.00	1008.00
4				
	1	0	19.00	528.00
	2	4	25.90	116.00
	3	4	25.90	116.00
	4	4	25.90	116.00
	5	4	25.90	116.00
	6	4	25.90	116.00
	7	0	19.00	528.00
5				
	1	0	19.00	528.00
	2	4	25.90	116.00
	3	4	25.90	116.00
	4	4	25.90	116.00
	5	4	25.90	116.00
	6	4	25.90	116.00
	7	0	19.00	528.00
6				
	1	0	23.40	516.00
	2	0	23.40	516.00
	3	0	15.60	1161.00
	4	0	1.73	1620.00
7				
	1	0	19.00	528.00
	2	2	15.30	500.00
	3	2	15.30	500.00
	4	2	15.30	500.00
	5	0	15.60	1161.00
	6	0	23.40	516.00
	7	0	23.40	516.00
	8	0	1.73	1620.00
8				
	1	0	19.00	528.00
	2	4	5.30	1680.00
	3	0	2.00	2675.00
	4	0	26.70	612.00
9				
	1	5	350.00	16.10

10			
	1	0	19.00 528.00
	2	4	10.90 217.20
	3	4	10.10 355.60
	4	0	5.50 28416.00
	5	4	5.60 4.10
	6	0	5.50 28416.00
	7	4	10.10 355.60
	8	4	10.90 217.20
	9	0	19.00 528.00
11			
	1	0	19.00 528.00
	2	4	25.90 116.00
	3	4	25.90 116.00
	4	4	25.90 116.00
	5	4	25.90 116.00
	6	4	25.90 116.00
	7	0	19.00 528.00
12			
	1	0	23.40 516.00
	2	0	23.40 516.00
	3	0	15.60 1161.00
	4	0	1.73 1620.00
13			
	1	0	19.00 528.00
	2	2	15.30 500.00
	3	2	15.30 500.00
	4	2	15.30 500.00
	5	0	15.60 1161.00
	6	0	23.40 516.00
	7	0	23.40 516.00
	8	0	1.73 1620.00
14			
	1	0	19.00 528.00
	2	4	5.30 1680.00
	3	0	2.00 2675.00
	4	0	26.70 612.00
15			
	1	5	175.00 64.30
16			
	1	0	50.00 129.00
	2	0	45.00 616.00
	3	0	11.30 9856.00
	4	0	11.30 9856.00
	5	0	45.00 616.00
	6	0	16.70 1161.00
17			
	1	0	19.00 528.00
	2	4	5.30 1680.00
	3	0	2.00 2675.00
	4	0	26.70 612.00
18			
	1	0	50.00 129.00
	2	0	16.70 1161.00
	3	0	50.00 129.00
19			
	1	0	19.00 528.00
	2	4	10.90 217.20
	3	4	10.10 355.30
	4	0	27.20 1136.00
	5	0	13.10 4544.00
	6	0	13.10 4544.00
	7	4	5.60 4.10
	8	0	16.00 6300.00
	9	0	32.00 1575.00
	10	0	40.00 1008.00

20			
1	0	23.40	516.00
2	0	23.40	516.00
3	0	15.60	1161.00
4	0	1.73	1620.00
21			
1	0	19.00	528.00
2	4	5.30	1680.00
3	0	2.00	2675.00
4	4	5.70	410.00
5	0	8.50	3690.00
6	0	25.50	430.00
22			
1	5	350.00	16.10
23			
1	0	19.00	528.00
2	4	10.90	217.20
3	4	10.10	355.30
4	0	27.20	1136.00
5	0	13.10	4544.00
6	0	13.10	4544.00
7	4	5.60	4.10
8	0	16.00	6300.00
9	0	32.00	1575.00
10	0	40.00	1008.00
24			
1	0	19.00	528.00
2	4	23.30	128.00
3	4	23.30	128.00
4	4	23.30	128.00
5	0	19.00	528.00
25			
1	0	19.00	528.00
2	4	23.30	128.00
3	4	23.30	128.00
4	4	23.30	128.00
5	0	19.00	528.00
26			
1	0	14.70	880.20
2	0	4.48	368.00
3	0	4.48	368.00
4	0	4.48	368.00
5	0	4.48	368.00
6	0	4.48	368.00
27			
1	0	19.00	528.00
2	4	5.30	1680.00
3	0	2.00	2675.00
4	4	5.70	410.00
5	0	8.50	3690.00
6	0	25.50	436.00
28			
1	5	350.00	16.10
29			
1	0	19.00	528.00
2	4	10.90	217.20
3	4	10.10	355.60
4	0	5.50	28416.00
5	4	5.60	4.10
6	0	5.50	28416.00
7	4	10.10	355.60
8	4	10.90	217.20
9	0	19.00	528.00

30			
1	0	19.00	528.00
2	4	23.30	128.00
3	4	23.30	128.00
4	4	23.30	128.00
5	0	19.00	528.00
31			
1	0	14.70	880.20
2	0	4.48	368.00
3	0	4.48	368.00
4	0	4.48	368.00
5	0	4.48	368.00
6	0	4.48	368.00
32			
1	0	19.00	528.00
2	4	5.30	1680.00
3	0	2.00	2675.00
4	4	5.70	410.00
5	0	8.50	3690.00
6	0	25.50	436.00
33			
1	5	350.00	16.10
34			
1	0	14.70	880.20
2	0	4.48	368.00
3	0	4.48	368.00
4	0	4.48	368.00
5	0	4.48	368.00
6	0	4.48	368.00
35			
1	0	14.70	880.20
2	0	4.48	368.00
3	0	4.48	368.00
4	0	4.48	368.00
5	0	4.48	368.00
6	0	4.48	368.00
36			
1	0	19.00	528.00
2	4	5.30	1680.00
3	0	2.00	2675.00
4	4	5.70	410.00
5	0	8.50	3690.00
6	0	25.50	436.00
37			
1	5	350.00	16.10
38			
1	0	19.00	528.00
2	4	10.90	217.20
3	4	10.10	355.30
4	0	27.20	1130.00
5	0	13.10	4544.00
6	0	13.10	4544.00
7	4	5.60	4.10
8	0	16.00	6300.00
9	0	32.00	1575.00
10	0	40.00	1008.00
39			
1	0	19.00	528.00
2	4	23.30	128.00
3	4	23.30	128.00
4	4	23.30	128.00
5	0	19.00	528.00

40				
	1	0	14.70	880.20
	2	0	4.48	368.00
	3	0	4.48	368.00
	4	0	4.48	368.00
	5	0	4.48	368.00
	6	0	4.48	368.00
41				
	1	0	19.00	528.00
	2	2	15.30	500.00
	3	2	15.30	500.00
	4	2	15.30	500.00
	5	0	15.60	1161.00
	6	0	23.40	516.00
	7	0	23.40	516.00
	8	0	1.73	1620.00
42				
	1	0	19.00	528.00
	2	2	15.30	500.00
	3	2	15.30	500.00
	4	2	15.30	500.00
	5	0	15.60	1161.00
	6	0	23.40	516.00
	7	0	23.40	516.00
	8	0	1.73	1620.00
43				
	1	0	19.00	528.00
	2	2	15.30	500.00
	3	2	15.30	500.00
	4	2	15.30	500.00
	5	0	15.60	1161.00
	6	0	23.40	516.00
	7	0	23.40	516.00
	8	0	1.73	1620.00
44				
	1	0	19.00	528.00
	2	4	10.90	217.20
	3	4	10.10	355.30
	4	0	27.20	1136.00
	5	0	13.10	4544.00
	6	0	13.10	4544.00
	7	4	5.60	4.10
	8	0	16.00	6300.00
	9	0	32.00	1575.00
	10	0	40.00	1008.00
45				
	1	0	19.00	528.00
	2	4	10.90	217.20
	3	4	10.10	355.60
	4	0	5.50	28416.00
	5	4	5.60	4.10
	6	0	5.50	28416.00
	7	4	10.10	355.60
	8	4	10.90	217.20
	9	0	19.00	528.00
46				
	1	0	19.00	528.00
	2	4	23.30	128.00
	3	4	23.30	128.00
	4	4	23.30	128.00
	5	0	19.00	528.00

PAGE
NUMBERS
CUT OFF
IN
ORIGINAL

47				
	1	0	50.00	129.00
	2	0	45.00	616.00
	3	0	9.00	15400.00
	4	0	45.00	616.00
	5	0	50.00	129.00
48				
	1	0	19.00	528.00
	2	4	23.30	128.00
	3	4	23.30	128.00
	4	4	23.30	128.00
	5	0	19.00	528.00
49				
	1	0	19.00	536.00
	2	0	380.00	1.30
	3	2	11.40	105.00
	4	2	11.40	105.00
	5	0	380.00	1.30
	6	2	23.30	128.00
	7	2	23.30	128.00
	8	2	23.30	128.00
	9	0	117.00	140.00
50				
	1	0	19.00	536.00
	2	0	380.00	1.30
	3	2	11.40	105.00
	4	2	11.40	105.00
	5	0	380.00	1.30
	6	2	23.30	128.00
	7	2	23.30	128.00
	8	2	23.30	128.00
	9	0	117.00	140.00
51				
	1	0	19.00	528.00
	2	4	10.90	217.20
	3	4	10.10	355.30
	4	0	27.20	1136.00
	5	0	13.10	4544.00
	6	0	13.10	4544.00
	7	4	5.60	4.10
	8	0	16.00	6300.00
	9	0	32.00	1575.00
	10	0	40.00	1008.00
52				
	1	0	19.00	528.00
	2	4	10.90	217.20
	3	4	10.10	355.30
	4	0	27.20	1136.00
	5	0	13.10	4544.00
	6	0	13.10	4544.00
	7	4	5.60	4.10
	8	0	16.00	6300.00
	9	0	32.00	1575.00
	10	0	40.00	1008.00
53				
	1	0	50.00	129.00
	2	0	45.00	616.00
	3	0	9.00	15400.00
	4	0	45.00	616.00
	5	0	50.00	129.00
54				
	1	0	50.00	129.00
	2	0	45.00	616.00
	3	0	9.00	15400.00
	4	0	45.00	616.00
	5	0	50.00	129.00

55			
	1	5	175.00 64.30
56			
	1	2	7.10 20.00
57			
	1	0	50.00 129.00
	2	0	45.00 616.00
	3	0	9.00 15400.00
	4	0	45.00 616.00
	5	0	50.00 129.00
58			
	1	0	50.00 129.00
	2	0	45.00 616.00
	3	0	9.00 15400.00
	4	0	45.00 616.00
	5	0	50.00 129.00
59			
	1	0	50.00 129.00
	2	0	45.00 616.00
	3	0	9.00 15400.00
	4	0	45.00 616.00
	5	0	50.00 129.00
60			
	1	6	0.00 0.00
61			
	1	6	0.00 0.00
62			
	1	6	0.00 0.00
63			
	1	6	0.00 0.00
64			
	1	6	0.00 0.00
65			
	1	6	0.00 0.00
66			
	1	0	38.70 954.00
	2	0	3.68 3025.00
	3	0	3.68 3025.00
	4	0	1.80 12125.00
	5	0	1.24 500000.00
	6	0	1.24 500000.00
	7	0	1.24 500000.00
	8	0	1.24 500000.00
	9	0	1.24 500000.00
	10	0	17.50 2496.00

Angle Factors

A.F.s for negative side

orientation number of viewed surface.

	FYIIP for positive side						FYIIN					
I/F	1	2	3	4	5	6	1	2	3	4	5	6
1	1.75	1.49	0.00	0.47	0.94	1.10	0.30	0.00	0.00	0.00	0.00	0.00
2	0.51	0.77	0.00	0.19	0.32	0.31	0.00	0.00	0.00	0.00	0.00	0.00
3	1.80	1.80	0.94	0.29	0.00	0.99	0.00	0.00	0.00	0.00	0.00	0.00
4	2.26	2.26	0.47	0.00	0.29	1.28	1.97	1.97	1.39	0.00	0.77	1.26
5	2.82	2.90	1.10	1.28	0.99	0.00	2.55	-0.02	0.10	0.47	1.91	0.00
6	17.52	0.00	0.26	0.03	0.00	0.00	0.00	7.08	1.75	2.26	1.80	2.82
7	7.08	0.00	1.49	2.26	1.80	2.90	0.00	7.08	1.96	2.26	1.80	2.77
8	1.71	1.62	0.00	1.39	0.99	1.39	0.00	0.00	0.00	0.00	0.00	0.00
9	0.27	0.35	0.00	0.29	0.13	0.17	0.00	0.00	0.00	0.00	0.00	0.00
10	1.77	0.04	0.08	0.06	0.00	1.91	1.50	1.50	1.39	1.26	0.58	0.00
11	1.14	1.22	0.99	0.77	0.00	0.58	1.93	0.70	0.71	0.01	0.26	0.00
12	8.92	0.00	0.00	0.23	0.00	0.00	0.00	2.81	1.71	1.97	1.14	1.53
13	2.81	0.00	1.62	1.97	1.22	1.50	0.00	2.81	1.73	1.97	1.16	0.97
14	0.44	0.11	0.03	0.00	0.06	0.47	0.00	0.00	0.00	0.00	0.00	0.00
15	0.11	0.02	0.01	0.00	0.01	0.11	0.00	0.00	0.00	0.00	0.00	0.00

16	0.50	0.02	0.03	0.00	0.08	0.54	0.00	0.00	0.00	0.00	0.00	0.00
17	0.81	0.63	0.00	0.03	0.08	0.10	0.00	0.00	0.00	0.00	0.00	0.00
18	0.13	0.03	0.00	0.00	0.01	0.01	0.00	0.00	0.00	0.00	0.00	0.00
19	1.48	0.81	0.89	0.01	0.00	0.55	0.00	0.00	0.00	0.00	0.00	0.00
20	14.32	0.00	0.14	0.14	0.00	0.00	0.00	0.86	0.81	0.44	1.77	2.55
21	1.96	1.84	0.00	0.56	1.04	1.25	0.00	0.00	0.00	0.00	0.00	0.00
22	0.29	0.41	0.00	0.11	0.22	0.14	0.00	0.00	0.00	0.00	0.00	0.00
23	1.80	1.80	1.04	0.29	0.00	0.97	0.00	0.00	0.00	0.00	0.00	0.00
24	2.26	2.26	0.56	0.00	0.29	1.14	1.97	1.97	1.39	0.00	0.73	0.94
25	2.77	2.65	1.25	1.14	0.97	0.00	1.49	1.49	0.93	0.55	0.00	0.75
26	7.08	0.00	1.84	2.26	1.80	2.65	6.00	12.98	0.00	0.00	0.00	0.00
27	1.73	1.59	0.00	1.39	0.98	0.93	0.00	0.00	0.00	0.00	0.00	0.00
28	0.24	0.38	0.00	0.29	0.14	0.10	0.00	0.00	0.00	0.00	0.00	0.00
29	0.07	0.91	0.25	0.76	0.00	0.70	0.97	0.97	0.93	0.94	0.37	0.00
30	1.16	1.23	0.98	0.73	0.00	0.37	0.69	0.69	0.78	0.50	0.81	0.00
31	2.81	0.00	1.59	1.97	1.23	0.97	0.00	0.59	0.00	0.00	0.00	0.00
32	0.82	0.74	0.00	0.28	0.93	0.56	0.00	0.00	0.00	0.00	0.00	0.00
33	0.11	0.20	0.00	0.07	0.14	0.21	0.00	0.00	0.00	0.00	0.00	0.00
34	1.34	0.00	0.74	0.69	1.49	0.55	0.00	4.44	0.00	0.00	0.00	0.00
35	0.10	0.00	0.70	0.67	0.91	0.89	0.00	2.54	0.00	0.00	0.00	0.00
36	0.72	0.65	0.00	0.70	0.82	0.78	0.00	0.00	0.00	0.00	0.00	0.00
37	0.06	0.13	0.00	0.12	0.09	0.13	0.00	0.00	0.00	0.00	0.00	0.00
38	0.69	0.69	0.82	0.78	0.00	0.81	0.00	0.00	0.00	0.00	0.00	0.00
39	0.53	0.61	0.70	0.00	0.78	0.50	0.06	0.70	0.00	0.28	0.25	0.38
40	0.52	0.00	0.65	0.61	0.69	0.69	0.00	0.07	0.00	0.00	0.00	0.00
41	0.86	0.00	0.63	0.11	0.04	-0.02	0.00	0.52	0.72	0.53	0.69	0.69
42	1.85	0.00	0.03	0.26	0.64	1.55	0.00	1.34	0.82	0.62	1.49	0.55
43	1.06	0.00	0.09	0.02	0.40	0.76	0.00	0.10	0.06	0.05	0.07	0.05
44	0.03	0.44	0.62	0.07	0.00	0.34	0.00	0.00	0.00	0.00	0.00	0.00
45	0.55	0.55	0.56	0.08	0.75	0.00	0.53	0.53	0.19	0.32	0.22	0.00
46	0.11	0.29	0.02	0.14	0.04	0.00	0.05	0.00	0.38	0.32	0.70	0.00
47	0.34	0.27	0.11	0.53	0.00	0.08	0.02	0.25	0.18	0.06	0.22	0.00
48	0.62	0.69	0.28	0.00	0.55	0.08	0.05	0.07	0.28	0.00	0.76	0.32
49	12.98	0.00	0.00	0.00	0.00	0.00	0.00	0.00	0.00	0.00	0.00	0.00
50	2.65	0.00	0.00	0.00	0.00	0.00	0.00	0.00	0.00	0.00	0.00	0.00
51	1.24	0.26	0.00	0.03	0.00	0.00	0.00	0.00	0.00	0.00	0.00	0.00
52	1.24	0.03	0.03	0.00	0.00	0.00	0.00	0.00	0.00	0.00	0.00	0.00
53	0.53	0.45	0.06	0.21	0.14	0.00	0.46	0.31	0.02	0.02	0.49	0.00
54	0.36	0.28	0.11	0.49	0.00	0.17	0.41	0.08	0.07	0.00	0.23	0.00
55	0.09	0.11	0.00	0.00	0.02	0.01	0.00	0.00	0.00	0.00	0.00	0.00
56	0.89	0.00	0.08	0.02	0.67	0.29	0.00	0.55	0.36	0.34	0.59	0.21
57	0.48	0.41	0.06	0.21	0.12	0.00	0.02	0.22	0.06	0.22	0.31	0.00
58	0.32	0.24	0.14	0.00	0.52	0.06	0.03	0.25	0.13	0.00	0.17	0.16
59	0.25	0.17	0.28	0.00	0.13	0.41	0.02	0.22	0.00	0.11	0.12	0.23
60	0.00	0.00	0.00	0.00	0.00	0.00	0.00	0.00	0.00	0.00	0.00	0.00
61	0.00	0.00	0.00	0.00	0.00	0.00	0.00	0.00	0.00	0.00	0.00	0.00
62	0.00	0.00	0.00	0.00	0.00	0.00	0.00	0.00	0.00	0.00	0.00	0.00
63	0.00	0.00	0.00	0.00	0.00	0.00	0.00	0.00	0.00	0.00	0.00	0.00
64	0.00	0.00	0.00	0.00	0.00	0.00	0.00	0.00	0.00	0.00	0.00	0.00
65	0.00	0.00	0.00	0.00	0.00	0.00	0.00	0.00	0.00	0.00	0.00	0.00
66	0.00	17.52	1.24	1.24	0.00	0.00	0.00	0.00	0.00	0.00	0.00	0.00

ISUB I/F	S1	S2	S3	S4	S5	S6	S7	S8	S9	S10
1	0	0	0	0	0	0	0	0	0	0
2	0	0	0	0	0	0	0	0	0	0
3	0	0	0	0	0	0	0	0	0	0
4	0	0	0	0	0	0	0	0	0	0
5	0	0	0	0	0	0	0	0	0	0
6	0	0	0	0	0	0	0	0	0	0
7	0	0	0	0	0	0	0	0	0	0
8	0	0	0	0	0	0	0	0	0	0
9	0	0	0	0	0	0	0	0	0	0
10	0	0	0	0	0	0	0	0	0	0
11	18	19	43	55	0	0	0	0	0	0
12	0	0	0	0	0	0	0	0	0	0
13	0	0	0	0	0	0	0	0	0	0
14	0	0	0	0	0	0	0	0	0	0
15	42	0	0	0	0	0	0	0	0	0
16	42	0	0	0	0	0	0	0	0	0
17	0	0	0	0	0	0	0	0	0	0
18	11	19	0	0	0	0	0	0	0	0
19	11	18	43	54	55	56	0	0	0	0
20	0	0	0	0	0	0	0	0	0	0
21	0	0	0	0	0	0	0	0	0	0
22	0	0	0	0	0	0	0	0	0	0
23	0	0	0	0	0	0	0	0	0	0
24	0	0	0	0	0	0	0	0	0	0
25	0	0	0	0	0	0	0	0	0	0
26	0	0	0	0	0	0	0	0	0	0
27	0	0	0	0	0	0	0	0	0	0
28	0	0	0	0	0	0	0	0	0	0
29	0	0	0	0	0	0	0	0	0	0
30	0	0	0	0	0	0	0	0	0	0
31	50	0	0	0	0	0	0	0	0	0
32	0	0	0	0	0	0	0	0	0	0
33	0	0	0	0	0	0	0	0	0	0
34	0	0	0	0	0	0	0	0	0	0
35	50	0	0	0	0	0	0	0	0	0
36	0	0	0	0	0	0	0	0	0	0
37	59	0	0	0	0	0	0	0	0	0
38	0	0	0	0	0	0	0	0	0	0
39	0	0	0	0	0	0	0	0	0	0
40	50	0	0	0	0	0	0	0	0	0
41	0	0	0	0	0	0	0	0	0	0
42	15	16	53	0	0	0	0	0	0	0
43	11	19	53	54	0	0	0	0	0	0
44	47	56	59	0	0	0	0	0	0	0
45	47	0	0	0	0	0	0	0	0	0
46	0	0	0	0	0	0	0	0	0	0
47	44	45	56	59	0	0	0	0	0	0
48	0	0	0	0	0	0	0	0	0	0
49	0	0	0	0	0	0	0	0	0	0
50	31	35	40	0	0	0	0	0	0	0
51	0	0	0	0	0	0	0	0	0	0
52	0	0	0	0	0	0	0	0	0	0
53	42	43	0	0	0	0	0	0	0	0
54	19	43	56	0	0	0	0	0	0	0
55	11	19	0	0	0	0	0	0	0	0
56	19	44	47	54	57	58	0	0	0	0
57	56	58	0	0	0	0	0	0	0	0
58	56	57	0	0	0	0	0	0	0	0
59	37	44	47	0	0	0	0	0	0	0
60	0	0	0	0	0	0	0	0	0	0
61	0	0	0	0	0	0	0	0	0	0
62	0	0	0	0	0	0	0	0	0	0
63	0	0	0	0	0	0	0	0	0	0
64	0	0	0	0	0	0	0	0	0	0
65	0	0	0	0	0	0	0	0	0	0
66	0	0	0	0	0	0	0	0	0	0

Viewed sub-surfaces.

PTSS Sub-surface angle factors.

I/F	S1	S2	S3	S4	S5	S6	S7	S8	S9	S10
1	0.00	0.00	0.00	0.00	0.00	0.00	0.00	0.00	0.00	0.00
2	0.00	0.00	0.00	0.00	0.00	0.00	0.00	0.00	0.00	0.00
3	0.00	0.00	0.00	0.00	0.00	0.00	0.00	0.00	0.00	0.00
4	0.00	0.00	0.00	0.00	0.00	0.00	0.00	0.00	0.00	0.00
5	0.00	0.00	0.00	0.00	0.00	0.00	0.00	0.00	0.00	0.00
6	0.00	0.00	0.00	0.00	0.00	0.00	0.00	0.00	0.00	0.00
7	0.00	0.00	0.00	0.00	0.00	0.00	0.00	0.00	0.00	0.00
8	0.00	0.00	0.00	0.00	0.00	0.00	0.00	0.00	0.00	0.00
9	0.00	0.00	0.00	0.00	0.00	0.00	0.00	0.00	0.00	0.00
10	0.00	0.00	0.00	0.00	0.00	0.00	0.00	0.00	0.00	0.00
11	0.10	1.26	0.16	0.15	0.00	0.00	0.00	0.00	0.00	0.00
12	0.00	0.00	0.00	0.00	0.00	0.00	0.00	0.00	0.00	0.00
13	0.00	0.00	0.00	0.00	0.00	0.00	0.00	0.00	0.00	0.00
14	0.00	0.00	0.00	0.00	0.00	0.00	0.00	0.00	0.00	0.00
15	0.16	0.00	0.00	0.00	0.00	0.00	0.00	0.00	0.00	0.00
16	0.36	0.00	0.00	0.00	0.00	0.00	0.00	0.00	0.00	0.00
17	0.00	0.00	0.00	0.00	0.00	0.00	0.00	0.00	0.00	0.00
18	0.10	0.06	0.00	0.00	0.00	0.00	0.00	0.00	0.00	0.00
19	1.26	0.06	0.25	0.37	0.09	0.37	0.00	0.00	0.00	0.00
20	0.00	0.00	0.00	0.00	0.00	0.00	0.00	0.00	0.00	0.00
21	0.00	0.00	0.00	0.00	0.00	0.00	0.00	0.00	0.00	0.00
22	0.00	0.00	0.00	0.00	0.00	0.00	0.00	0.00	0.00	0.00
23	0.00	0.00	0.00	0.00	0.00	0.00	0.00	0.00	0.00	0.00
24	0.00	0.00	0.00	0.00	0.00	0.00	0.00	0.00	0.00	0.00
25	0.00	0.00	0.00	0.00	0.00	0.00	0.00	0.00	0.00	0.00
26	0.00	0.00	0.00	0.00	0.00	0.00	0.00	0.00	0.00	0.00
27	0.00	0.00	0.00	0.00	0.00	0.00	0.00	0.00	0.00	0.00
28	0.00	0.00	0.00	0.00	0.00	0.00	0.00	0.00	0.00	0.00
29	0.00	0.00	0.00	0.00	0.00	0.00	0.00	0.00	0.00	0.00
30	0.00	0.00	0.00	0.00	0.00	0.00	0.00	0.00	0.00	0.00
31	7.70	0.00	0.00	0.00	0.00	0.00	0.00	0.00	0.00	0.00
32	0.00	0.00	0.00	0.00	0.00	0.00	0.00	0.00	0.00	0.00
33	0.00	0.00	0.00	0.00	0.00	0.00	0.00	0.00	0.00	0.00
34	0.00	0.00	0.00	0.00	0.00	0.00	0.00	0.00	0.00	0.00
35	2.17	0.00	0.00	0.00	0.00	0.00	0.00	0.00	0.00	0.00
36	0.00	0.00	0.00	0.00	0.00	0.00	0.00	0.00	0.00	0.00
37	0.05	0.00	0.00	0.00	0.00	0.00	0.00	0.00	0.00	0.00
38	0.00	0.00	0.00	0.00	0.00	0.00	0.00	0.00	0.00	0.00
39	0.00	0.00	0.00	0.00	0.00	0.00	0.00	0.00	0.00	0.00
40	2.71	0.00	0.00	0.00	0.00	0.00	0.00	0.00	0.00	0.00
41	0.00	0.00	0.00	0.00	0.00	0.00	0.00	0.00	0.00	0.00
42	0.16	0.36	0.17	0.00	0.00	0.00	0.00	0.00	0.00	0.00
43	0.16	0.25	0.11	0.15	0.00	0.00	0.00	0.00	0.00	0.00
44	0.19	0.29	0.07	0.00	0.00	0.00	0.00	0.00	0.00	0.00
45	0.09	0.00	0.00	0.00	0.00	0.00	0.00	0.00	0.00	0.00
46	0.00	0.00	0.00	0.00	0.00	0.00	0.00	0.00	0.00	0.00
47	0.19	0.09	0.08	0.19	0.00	0.00	0.00	0.00	0.00	0.00
48	0.00	0.00	0.00	0.00	0.00	0.00	0.00	0.00	0.00	0.00
49	0.00	0.00	0.00	0.00	0.00	0.00	0.00	0.00	0.00	0.00
50	7.70	2.17	2.71	0.00	0.00	0.00	0.00	0.00	0.00	0.00
51	0.00	0.00	0.00	0.00	0.00	0.00	0.00	0.00	0.00	0.00
52	0.00	0.00	0.00	0.00	0.00	0.00	0.00	0.00	0.00	0.00
53	0.17	0.11	0.00	0.00	0.00	0.00	0.00	0.00	0.00	0.00
54	0.37	0.15	0.09	0.00	0.00	0.00	0.00	0.00	0.00	0.00
55	0.15	0.09	0.00	0.00	0.00	0.00	0.00	0.00	0.00	0.00
56	0.37	0.29	0.08	0.00	0.08	0.08	0.00	0.00	0.00	0.00
57	0.08	0.26	0.00	0.00	0.00	0.00	0.00	0.00	0.00	0.00
58	0.08	0.26	0.00	0.00	0.00	0.00	0.00	0.00	0.00	0.00
59	0.05	0.07	0.19	0.00	0.00	0.00	0.00	0.00	0.00	0.00
60	0.00	0.00	0.00	0.00	0.00	0.00	0.00	0.00	0.00	0.00
61	0.00	0.00	0.00	0.00	0.00	0.00	0.00	0.00	0.00	0.00
62	0.00	0.00	0.00	0.00	0.00	0.00	0.00	0.00	0.00	0.00
63	0.00	0.00	0.00	0.00	0.00	0.00	0.00	0.00	0.00	0.00
64	0.00	0.00	0.00	0.00	0.00	0.00	0.00	0.00	0.00	0.00
65	0.00	0.00	0.00	0.00	0.00	0.00	0.00	0.00	0.00	0.00
66	0.00	0.00	0.00	0.00	0.00	0.00	0.00	0.00	0.00	0.00

APPENDIX 5

COMFORT EQUATION FOR PREDICTED MEAN VOTE - AS DEVELOPED BY P.O. FANGER(49)

$$P.M.V. = \left\{0.352\exp\left(-0.042\frac{M}{A_{Du}}\right) + 0.032\right\}$$

$$\times\left\{\frac{M}{A_{Du}}(1-\eta)\right.$$

$$- 0.35\left[43 - 0.061\frac{M}{A_{Du}}(1-\eta) - p_a\right]$$

$$- 0.42\left[\frac{M}{A_{Du}}(1-\eta) - 50\right]$$

$$- 0.0023\frac{M}{A_{Du}}(44 - p_a)$$

$$- 0.0014\frac{M}{A_{Du}}(34 - t_a)$$

$$- 3.4\times10^{-8} f_{cl}\left[(t_{cl}+273)^4 - (t_{mrt}+273)^4\right]$$

$$\left. - f_{cl} h_c (t_{cl} - t_a)\right\} \qquad \text{A2.1}$$

where

$$t_{cl} = 35.7 - 0.032\frac{M}{A_{Du}}(1-\eta)$$

$$- 0.18\, I_{cl}\times\left\{3.4\times10^{-8} f_{cl}\left[(t_{cl}+273)^4 - (t_{mrt}+273)^4\right]\right.$$

$$\left. + f_{cl} h_c (t_{cl} - t_a)\right\} \qquad \text{A2.2}$$

and $$h_c = 2.05\,(t_{cl} - t_a)^{0.25} \qquad \text{A2.3a}$$

<u>or</u> $$h_c = 10.4\sqrt{v} \qquad \text{A2.3b}$$

whichever is the larger.

and P.M.V. = predicted mean vote on scale -

-3 = cold
-2 = cool
-1 = slightly cool
0 = neutral
1 = slightly warm
2 = warm
3 = hot.

M = metabolic rate (.kcal/h)

A_{Du} = body surface area (m^2)

η = external mechanical efficiency (usually η = 0)

p_a = atmospheric water vapour pressure (mm Hg)

t_a = air temperature (C)

f_{cl} = ratio $\frac{\text{clothed body surface area}}{\text{nude body surface area}}$

t_{cl} = surface temperature of outer clothing (C)

t_{mrt} = mean radiant temperature (C)

h_c = convective heat transfer coefficient (kcal/m^2 hr C)

I_{cl} = "clo" value representative of thermal resistance of clothing (typical business suit = 1)

v = air velocity (m/s)

t_{cl} is obtained from equation A2.2 by successive approximation, and then substituted into A2.1 to obtain PMV.

The following values are those normally assumed by the program

	Windows open	Windows closed	
air velocity	0.3	0	m/s
metabolic rate	60	50	kcal/hr m^2
clothing	1.0	0.7	clo
f_{cl}	1.15	1.1	-

REFERENCES

1. LEACH, S.J. and DESSON, R.A. Energy consumption in buildings in the UK and possibilities for energy conservation. *Proc. Int. Sym. of CIB on Energy Conservation in the Built Environment, 1976.*

2. I.H.V.E. Guide, 1970.

3. DANTER, E. Heat exchanges in a room and the definition of room temperature. *Building Services Engineer, 41 pp 232-245, 1974.*

4. DANTER, E. Periodic heat flow characteristics of simple walls and roofs. *J.I.H.V.E., 28 pp 136-146, 1960.*

5. MILBANK, N.O. and HARRINGTON - LYNN, J. Thermal response and the admittance procedure. *Building Services Engineer, 42 pp 38-42, 1974.*

6. STEPHENSON, D.G. and MITALAS, G.P. Cooling load calculations by thermal response factor method. *ASHRAE Trans., 73 pt.I, 1967.*

7. ASHRAE. Procedure for determining heating and cooling loads for computerised energy calculations - algorithms for building heat transfer subroutines. 1971.

8. KUSUDA, T. NBSLD, Computer program for heating and cooling loads in buildings. *National Bureau of Standards, 1974.*

9. BROWN, G. A method of calculating heating and cooling loads with the aid of a digital computer (in Swedish). *VVS 34 11, pp 401-410, 1963.*

10. BASNETT, P. Modelling real houses. *J. Arch. Research 3 3, pp 63-69, 1974.*

11. DICK, J.B. The fundamentals of natural ventilation of houses. *J.I.H.V.E. 18 pp 123-134, 1950.*

12. TAMURA, G.T. and WILSON, A.G. Building pressures caused by chimney action and mechanical ventilation. *Trans. ASHRAE 73, pt II, 1967.*

13. BARRETT, R.E. and LOCKLIN, D.W. Computer analysis of stack effect in high-rise buildings. *Trans. ASHRAE 74, pt. II, 1968.*

14. JACKMAN, P.J. A study of the natural ventilation of tall office buildings. *HVRA Lab. Report 53, 1969.*

15. DEN OUDEN, H Ph L. The use of an electrical analogue for studying the ventilation of buildings. *Publication 200, Res. Inst. for Public Health Engineering, 1963.*

16. BILSBORROW, R.E. Digital analogue for natural ventilation calculations. University of Sheffield, 1973.

17. TAMURA, G.T. Computer analysis of smoke control with building air handling systems. *ASHRAE Journal, August 1972, pp 46-54.*

18. WAKAMATSU, T. Calculation of smoke movement in buildings. *Research Paper 46, Building Research Institute, Japan, 1971.*

19. BILSBORROW, R.E. A comparison of computed infiltration rates with results obtained from a set of full-scale measurements, Sheffield University, 1972.

20. SHAW, C.Y., SANDER, D.M. and TAMURA, G.T. Air leakage measurements of the exterior walls of tall buildings. *Trans. ASHRAE 79, pt. II, 1973.*

21. TAMURA, G.T. Measurement of air leakage characteristics of house enclosures. *Trans. ASHRAE, 81 pt. I, 1975.*

22. SASAKI, J.R. and WILSON, A.G. Air leakage values for residential windows. *Trans. ASHRAE 71, pt. II, 1965.*

23. HOPKINS, L. and HANSFORD, B. Air flow through cracks. *Proc. Symp. on Ventilation of Housing, British Gas, 1974.*

24. HONMA, H. Ventilation of dwellings, and its disturbances. *Royal Institute of Technology, Stockholm, 1975.*

25. IRMINGER, I. Experiments on wind pressure. *Engineering Dec. 27, 1895, pp 787-788.*

26. DRYDEN, H.L. and HILL, G.C. Wind pressure on a model of the Empire State building. *National Bureau of Standards J. of Research 10, pp 493-523, 1933.*

27. JENSEN, M. The model-low for phenomena in natural wind. *Ingerioren 2 (4), pp 121-128, 1958.*

28. JENSEN, M. and FRANCK, N. Model-scale tests in turbulent wind. *Danish Technical Press, pt. I 1963, pt. II 1965.*

29. BAINES, W.D. Effects of velocity distribution on wind loads and flow patterns on buildings. *Proc. NPL Symp. no. 16 on Wind Effects on Buildings and Structures, pp.198-225, 1963.*

30. NING, C., YIN, F., HUNG-JU, W. and TIEN-TO, S. Wind tunnel studies of pressure distribution on elementary building forms. State University of Iowa, 1951.

31. DAVENPORT, A.G. The Spectrum of horizontal gustiness near the ground in strong winds. *Quart. J. Roy. Met. Soc. 87, pp 194-211, 1961.*

32. ARMITT, J. and COUNIHAN, J. The simulation of the atmospheric boundary layer in a wind tunnel. *Atmospheric Environment, 2, pp 49-71, 1968.*

33. LLOYD, A. The generation of shear flow in a wind tunnel. *Quart. J. Roy. Met. Soc. 93, pp 79-96, 1967.*

34. JACKMAN, P.J. and POTTER, I.N. Natural ventilation of large hospital buildings. *Hospital Engineering, Oct. 1975, pp 11-17.*

35. H.M. NAUTICAL ALMANAC OFFICE. The astronomical ephemeris. HMSO, London, 1972.

36. ROBINSON, N. (ed.) Solar radiation. *Elsevier, 1966.*

37. BENOY, M.B. The determination of solar heating. *The J. Roy. Aero. Soc.* 74, *pp 52-54. 1970.*

38. BAXTER, A.J. The effect of dust on solar radiation. *Build International* 6, *pp. 245-255, 1973.*

39. MOON, P. Proposed standard solar-radiation curves for engineering use. *J. Franklin Institute,* 230 *pp.583-617, 1940.*

40. OZISIK, M.N. Radiative transfer. *Wiley, 1973.*

41. ÅNGSTRÖM, A. Über die gegenstrahlung der atmosphäre. *Meteorol. Z.* 33, *pp.529-538, 1916.*

42. GEIGER, R. Das Klima der bodennahen Luftschicht. *Friedr. Vieweg & Sohn, Braunschweig, 1961. (Eng. trans. Scripta Technica Inc. 1965. The climate near the ground. Harvard Univ. Press., Cambridge, Mass.)*

43. ITO, N., KIMURA, K. and OKA, J. A field experiment study on the convective heat transfer coefficient on exterior surface of a building. *Trans. ASHRAE, no. 2225, 1972. pp.184-191* .

44. SPARROW, E.M. and CESS, R.D. Radiation heat transfer. *Brooks/Cole Pub. Co. 1966.*

45. MIN, T.C. SCHUTRUM, L.F., PARMELEE, G.V. and VOURIS, J.D. Natural convection and radiation in a panel-heated room. *Trans. ASHRAE,* 62 *pp.337-358, 1956.*

46. MACEY, H.H. Heat loss through a solid floor. *J. Institute of Fuel.* 22 *pp.369-371, 1949.*

47. SHAW, B.H. Heat and mass transfer by natural convection and combined natural convection and forced air flow through large rectangular openings in a vertical partition. *Proc. I. Mech. E. Conf. C117/71, pp 31-39.*

48. BAXTER, A.J. and LONGWORTH, A.L. The thermal response of room thermostats. *Heat. and Vent. Engineer, Sept. 1974, pp.103-106.*

49. FANGER, P.O. Thermal comfort. *Danish Technical Press, Copenhagen, 1970.*

50. MALINOWSKI, H.K. Wind effect on the air movement inside buildings. *Proc. 3rd Int. Conf. on Wind Effects on Buildings and Structures, Tokyo. pp 125-134, 1971.*

51. HARRIS-BASS, J., LAWRENCE, P. and KAVARANA, B. Adventitious ventilation of houses. *Proc. Symp. on Ventilation of Housing. British Gas, 1974.*

52. BLACKMAN, R.B. and TUKEY, J.W. The measurement of power spectra from the point of view of communications engineering. *Bell System Technical J., Jan, March 1958.*